NASA TECHNICAL MEMORANDUM

NASA TM X-1816

NASA TM X-1816

TRANSONIC AERODYNAMIC CHARACTERISTICS OF TWO HYPERSONIC CRUISE CONFIGURATIONS

by Richard A. Langhans

Langley Research Center

Langley Station, Hampton, Va.

NATIONAL AERONAUTICS AND SPACE ADMINISTRATION • WASHINGTON, D. C. • JUNE 1969

NASA TM X-1816

TRANSONIC AERODYNAMIC CHARACTERISTICS OF TWO HYPERSONIC CRUISE CONFIGURATIONS

By Richard A. Langhans

Langley Research Center
Langley Station, Hampton, Va.

NATIONAL AERONAUTICS AND SPACE ADMINISTRATION

For sale by the Clearinghouse for Federal Scientific and Technical Information
Springfield, Virginia 22151 – CFSTI price $3.00

TRANSONIC AERODYNAMIC CHARACTERISTICS OF TWO HYPERSONIC CRUISE CONFIGURATIONS

By Richard A. Langhans
Langley Research Center

SUMMARY

An investigation has been conducted in the Langley 8-foot transonic pressure tunnel to determine the aerodynamic characteristics of two hypersonic cruise airplane configurations. The investigation was conducted at Mach numbers ranging from 0.80 to 1.20, angles of attack from approximately -5° to 15°, and a constant Reynolds number per meter of 13.12×10^6. The results of the investigation show the distinct wing-body configuration is longitudinally unstable for the chosen center-of-gravity location and has a pitch-up tendency. This configuration is directionally stable and has positive effective dihedral. The blended wing-body configuration is longitudinally stable at Mach numbers greater than 0.90 and unstable at Mach numbers from 0.80 to 0.90. This configuration is directionally stable and has positive effective dihedral.

INTRODUCTION

The National Aeronautics and Space Administration has been conducting studies directed toward the development of a hypersonic cruise airplane. As part of these studies, two promising configurations were selected for a wind-tunnel investigation to define their aerodynamic characteristics. A comparative study of these configurations is presented in references 1 and 2. As part of this investigation, the two configurations were tested at the Langley 8-foot transonic pressure tunnel to determine their transonic aerodynamic characteristics. The purpose of this paper is to present the results obtained during this investigation at Mach numbers ranging from 0.80 to 1.20, angles of attack from approximately -5° to 15°, and angles of sideslip of approximately 5°. The data are presented without analysis to expedite publication.

SYMBOLS

The results presented herein are referred to the body-axis system with the exception of the lift and drag coefficients which are referred to the stability-axis system. The moment reference center, chosen to be within the bounds of possible center-of-gravity

locations based on weight distribution and fuel transfer, is located at 46 percent $\bar{c}$ for the distinct wing-body configuration (fig. 1(a)) and at 38.5 percent $\bar{c}$ for the blended wing-body configuration (fig. 1(b)). The units used for physical quantities presented herein are given in the International System of Units (SI). Details concerning the use of SI, together with physical constants and conversion factors, may be found in reference 3. The coefficients and symbols used herein are defined as follows:

b	wing span (configuration DWB, 32.7025 cm; configuration BWB, 35.0266 cm)
$\bar{c}$	wing mean aerodynamic chord (configuration DWB, 23.937 cm; configuration BWB, 26.619 cm)
C_D	drag coefficient, $\frac{\text{Drag}}{qS}$
$C_{D,b}$	base-drag coefficient, $\frac{\text{Base drag}}{qS}$
C_l	rolling-moment coefficient, $\frac{\text{Rolling moment}}{qSb}$
C_L	lift coefficient, $\frac{\text{Lift}}{qS}$
C_m	pitching-moment coefficient, $\frac{\text{Pitching moment}}{qS\bar{c}}$
C_n	yawing-moment coefficient, $\frac{\text{Yawing moment}}{qSb}$
C_Y	side-force coefficient, $\frac{\text{Side force}}{qS}$
C_{l_β}	effective-dihedral parameter, $\Delta C_l/\Delta\beta$, per deg
C_{L_α}	lift-curve slope, $\partial C_L/\partial\alpha$, per deg
$C_{m_{C_L}}$	longitudinal-stability parameter, $\partial C_m/\partial C_L$, per deg
C_{n_β}	directional-stability parameter, $\Delta C_n/\Delta\beta$, per deg
C_{Y_β}	side-force parameter, $\Delta C_Y/\Delta\beta$, per deg
L/D	lift-drag ratio

M	free-stream Mach number
q	free-stream dynamic pressure, N/m^2
S	wing area (configuration DWB, 0.060343 m^2; configuration BWB, 0.074438 m^2)
α	angle of attack, deg
β	angle of sideslip (positive when nose is left), deg
δ_h	horizontal-tail deflection (positive when trailing edge is down), deg
δ_e	elevon deflection (positive when trailing edge is down), deg

Subscripts:

$(L/D)_{max}$	at maximum lift-drag ratio
max	maximum
min	minimum
o	at $C_L = 0$

Symbols used to designate the two configurations are given below:

BWB	blended wing-body
DWB	distinct wing-body

APPARATUS AND PROCEDURES

Models

Details of the two configurations investigated are presented in figure 1. The distinct wing-body configuration (DWB) has a low delta wing and a high body-mounted horizontal tail for pitch control. The blended wing-body configuration (BWB) has a double-delta planform wing mounted close to the body center line and utilizes elevons for longitudinal control. Photographs of the models are presented in figure 2.

Tunnel

The investigation was made in the Langley 8-foot transonic pressure tunnel. This facility is rectangular in cross section; the upper and lower walls are slotted longitudinally to allow continuous operation through the transonic speed range with negligible effects of choking and blockage. The stagnation temperature and dewpoint were maintained at values to preclude condensation shock effects. The tunnel was operated at a constant Reynolds number per meter of approximately 13.12×10^6. The average dynamic pressures for the investigation are presented in figure 3.

Measurements

Six-component force and moment measurements were determined by means of an electrical strain-gage balance located inside the fuselage. The measurements were taken over an angle-of-attack range from -5° to 15° for Mach numbers varying from 0.8 to 1.20. Additional measurements were taken over the angle-of-attack range and Mach number range for a sideslip angle of approximately 5°.

In order to insure a turbulent boundary layer, 0.127-cm-wide strips of No. 180 carborundum grains were applied approximately 1.02 cm aft of the leading edges of the wings, tail surfaces, and inlets; and a 0.127-cm-wide strip of No. 120 carborundum grains was applied to the nose at model station 5.08.

CORRECTIONS AND ACCURACY

No corrections to the free-stream Mach number and dynamic pressure for the effects of model and wake blockage are necessary for tests in the slotted test section. Also, no results are presented for supersonic Mach numbers at which boundary-reflected disturbances would be expected to affect the results.

The drag data have been adjusted to the condition of free-stream static pressure acting over the fuselage cavity and base. No correction was made to the drag data for flow through the ducts.

The angles of attack and sideslip have been corrected for the deflection of the balance and sting under load. The angles of attack, sideslip, and control deflections are estimated to be accurate to within $\pm 0.1^\circ$. Based upon unpublished tunnel calibrations, local deviations from the quoted free-stream Mach number did not exceed ± 0.003.

Accuracies of the measured coefficients, based upon instrument calibration and data repeatability, are estimated to be within the following limits:

C_L	±0.005
C_D	±0.0005
C_m	±0.0009
C_l	±0.0004
C_n	±0.0005
C_Y	±0.002

PRESENTATION OF RESULTS

The figures presenting the results of this investigation are listed in the following table:

Data presented in the summary figures for the distinct wing-body with the horizontal tail at 0^o were interpolated from cross plots of the presented data.

CONCLUDING REMARKS

An investigation has been conducted in the Langley 8-foot transonic pressure tunnel to determine the aerodynamic characteristics of two hypersonic cruise airplane configurations. The investigation was conducted at Mach numbers ranging from 0.80 to 1.20, angles of attack from approximately -5^o to 15^o, and a constant Reynolds number per meter of 13.12×10^6.

The results of the investigation show the distinct wing-body configuration is longitudinally unstable for the chosen center-of-gravity location and has a pitch-up tendency. This configuration is directionally stable and has positive effective dihedral. The blended wing-body configuration is longitudinally stable at Mach numbers from 0.90 to 1.20 and unstable at Mach numbers from 0.80 to 0.90. The configuration is directionally stable for the chosen center-of-gravity location and has positive effective dihedral.

Langley Research Center,
National Aeronautics and Space Administration,
Langley Station, Hampton, Va., April 4, 1969,
722-01-00-07-23.

REFERENCES

1. Penland, Jim A.; Edwards, Clyde L. W.; Witcofski, Robert D.; and Marcum, Don C., Jr.: Comparative Aerodynamic Study of Two Hypersonic Cruise Aircraft Configurations Derived From Trade-Off Studies. NASA TM X-1436, 1967.

2. Jarlett, F. E.: Performance Potential of Hydrogen Fueled, Airbreathing Cruise Aircraft. Vols. 1-4, Rep. No. GD/C-DCB66-004/1-4 (Contract NAS 2-3180), Gen. Dyn., Sept. 30, 1966.

3. Mechtly, E. A.: The International System of Units – Physical Constants and Conversion Factors. NASA SP-7012, 1964.

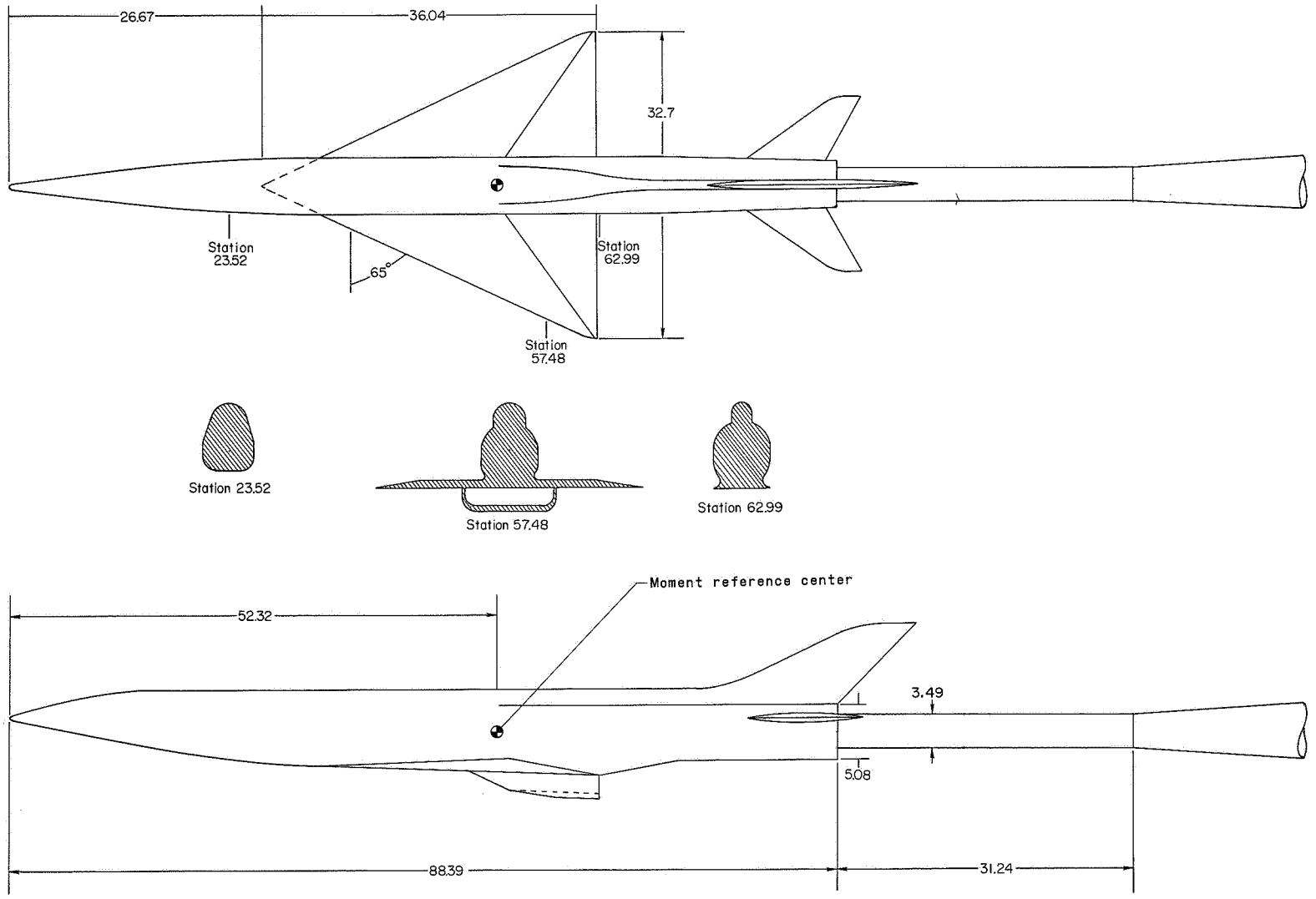

(a) Configuration DWB.

Figure 1.- Details of the model. Dimensions are in centimeters unless otherwise specified.

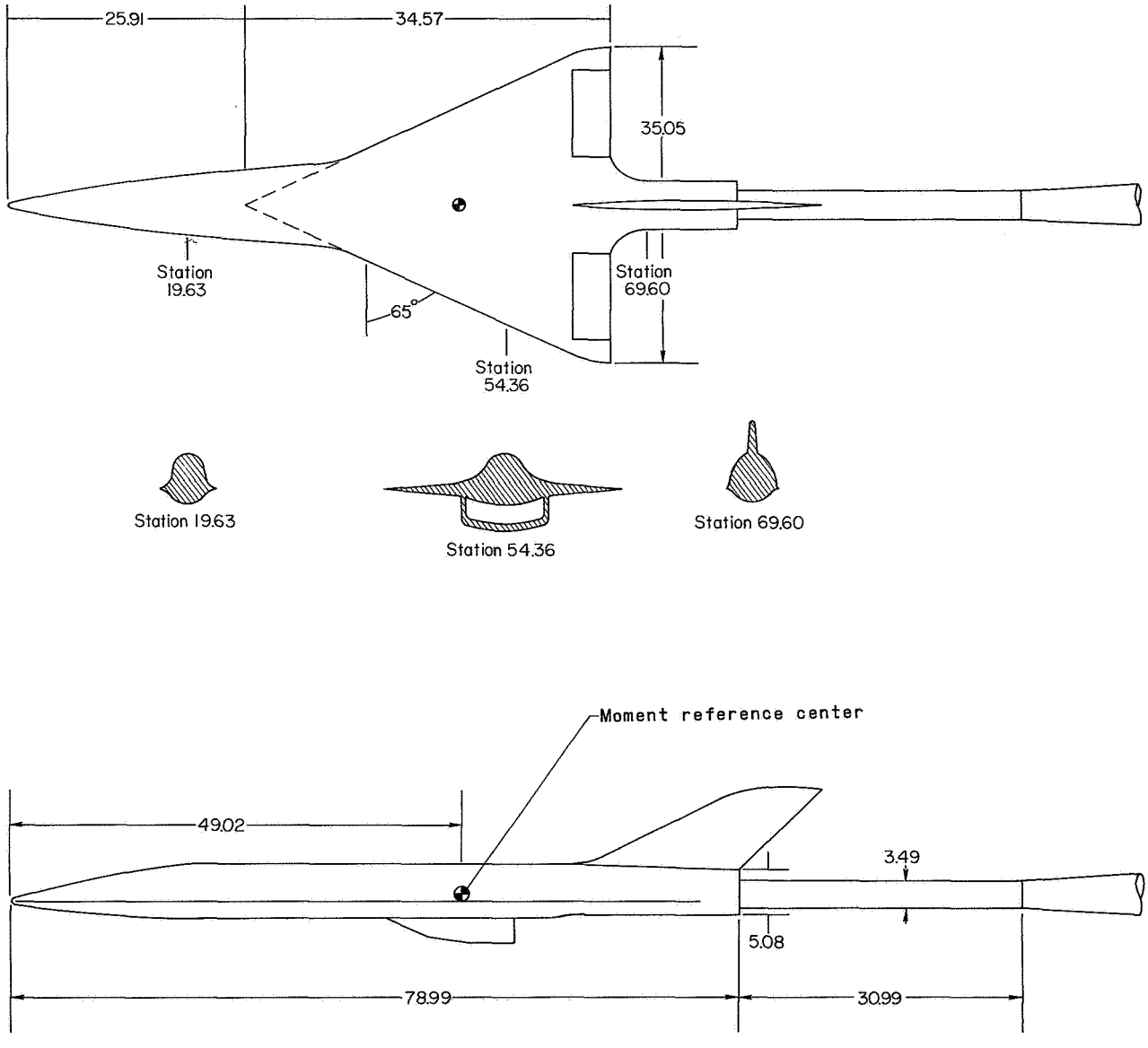

(b) Configuration BWB.

Figure 1.- Concluded.

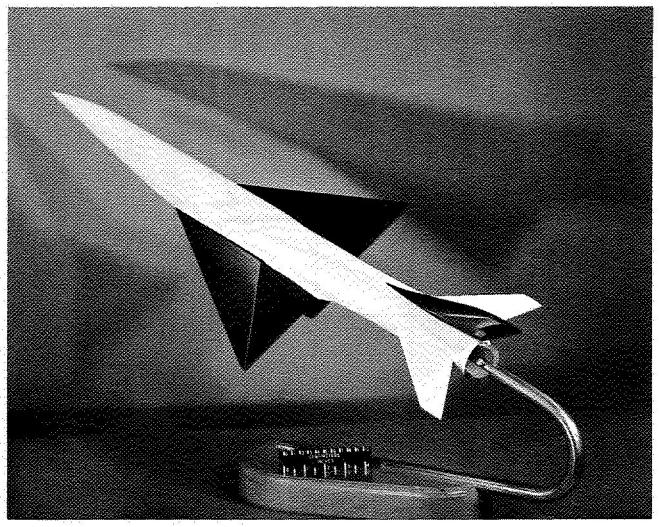

L-67-7270

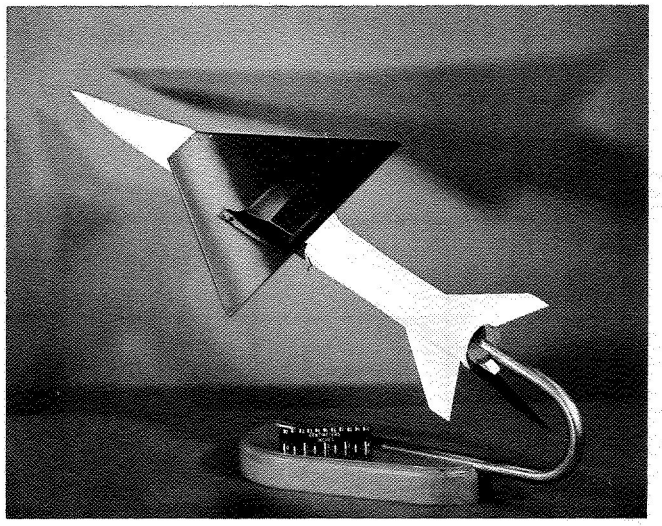

L-67-7268

Configuration DWB

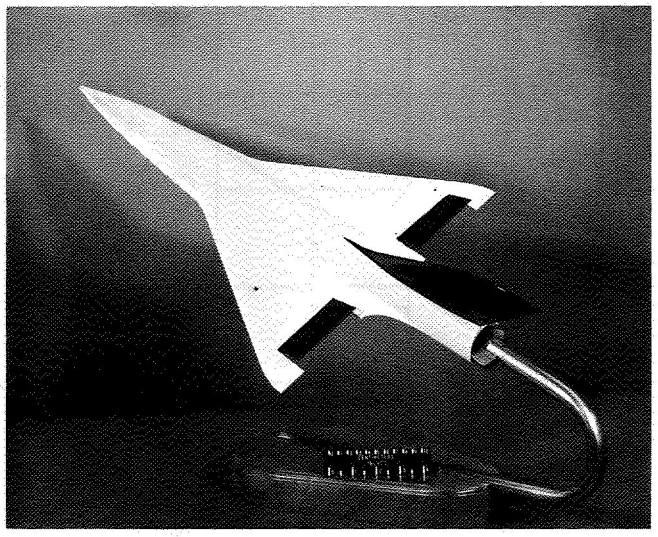

L-67-7274

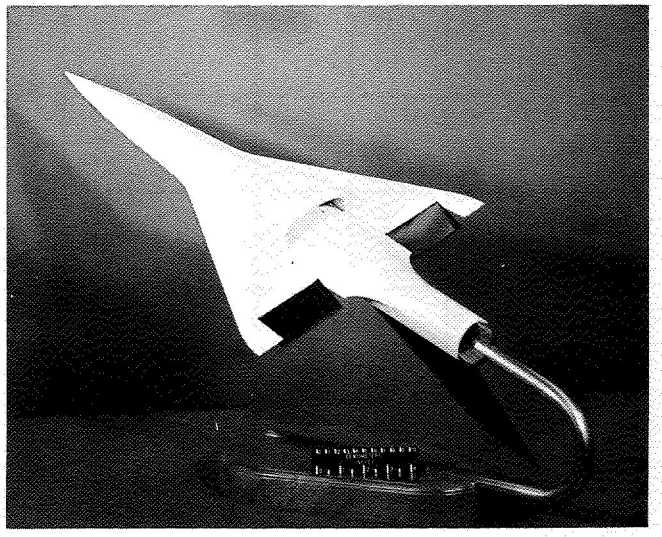

L-67-7269

Configuration BWB

Figure 2.- Model photographs.

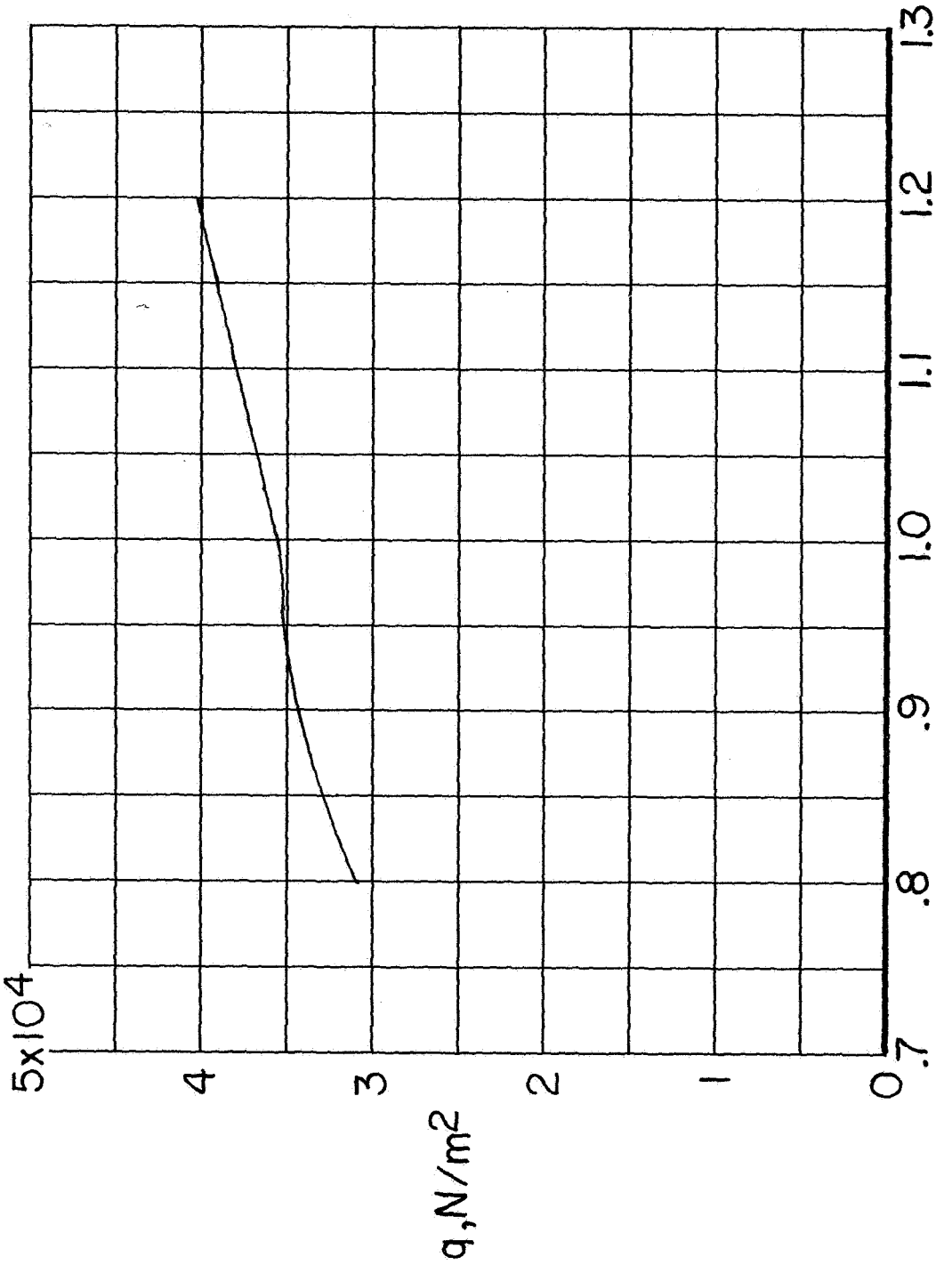

Figure 3.- Variation of dynamic pressure with Mach number.

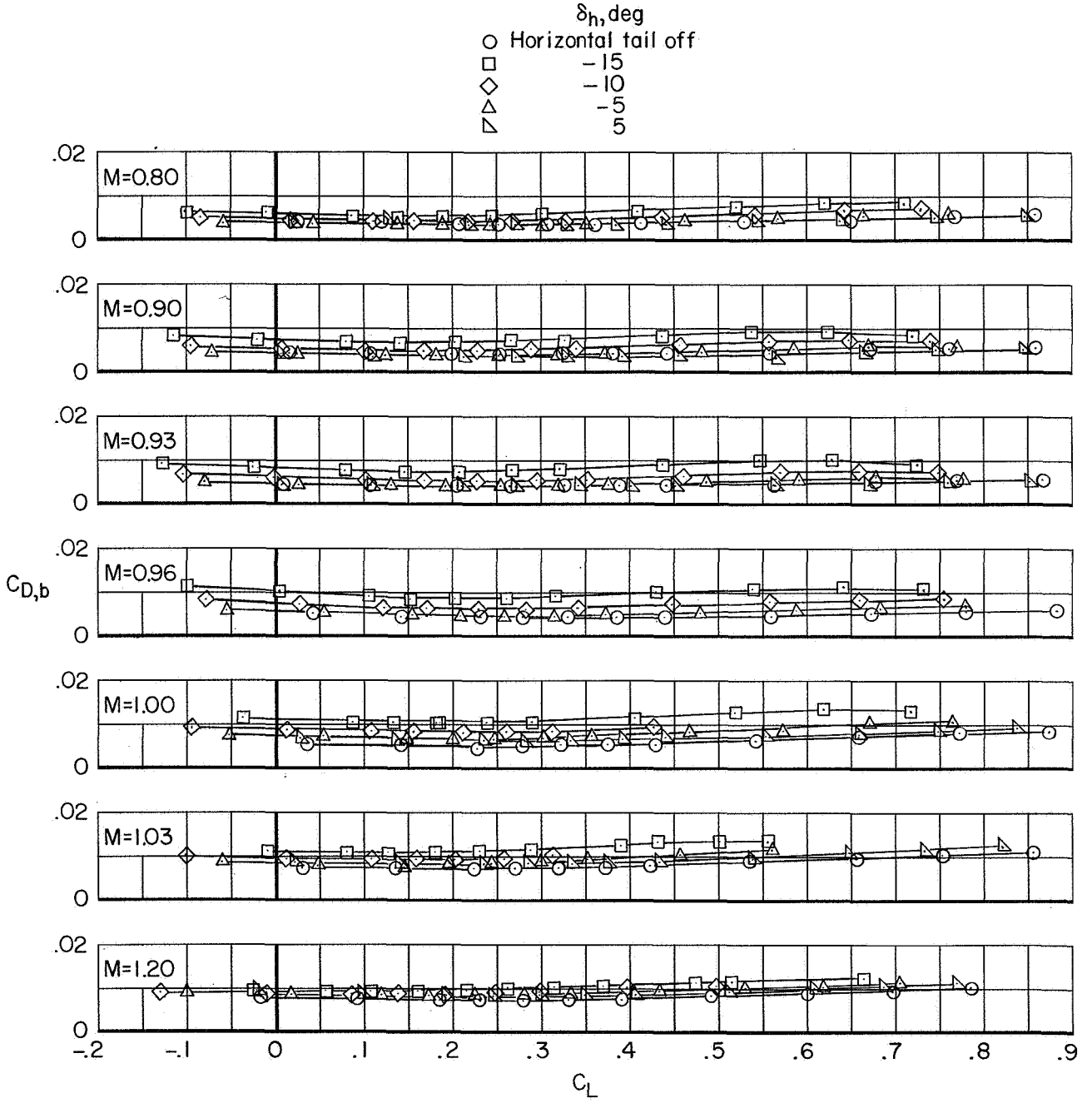

(a) Horizontal-tail effects; inlet on.

Figure 4.- Variation of base-drag coefficient with lift coefficient for configuration DWB.

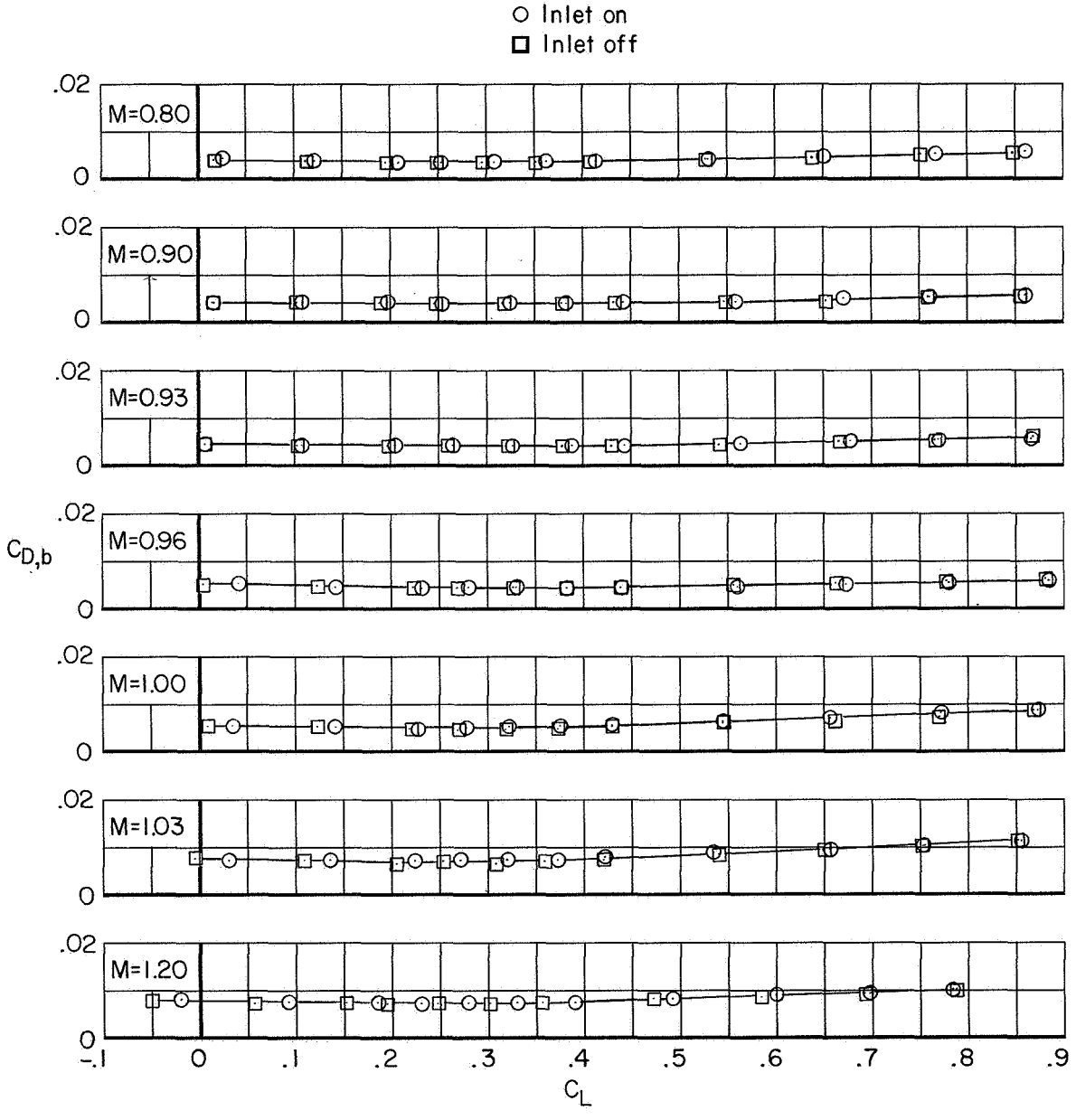

(b) Inlet effects; horizontal tail off.

Figure 4.- Concluded.

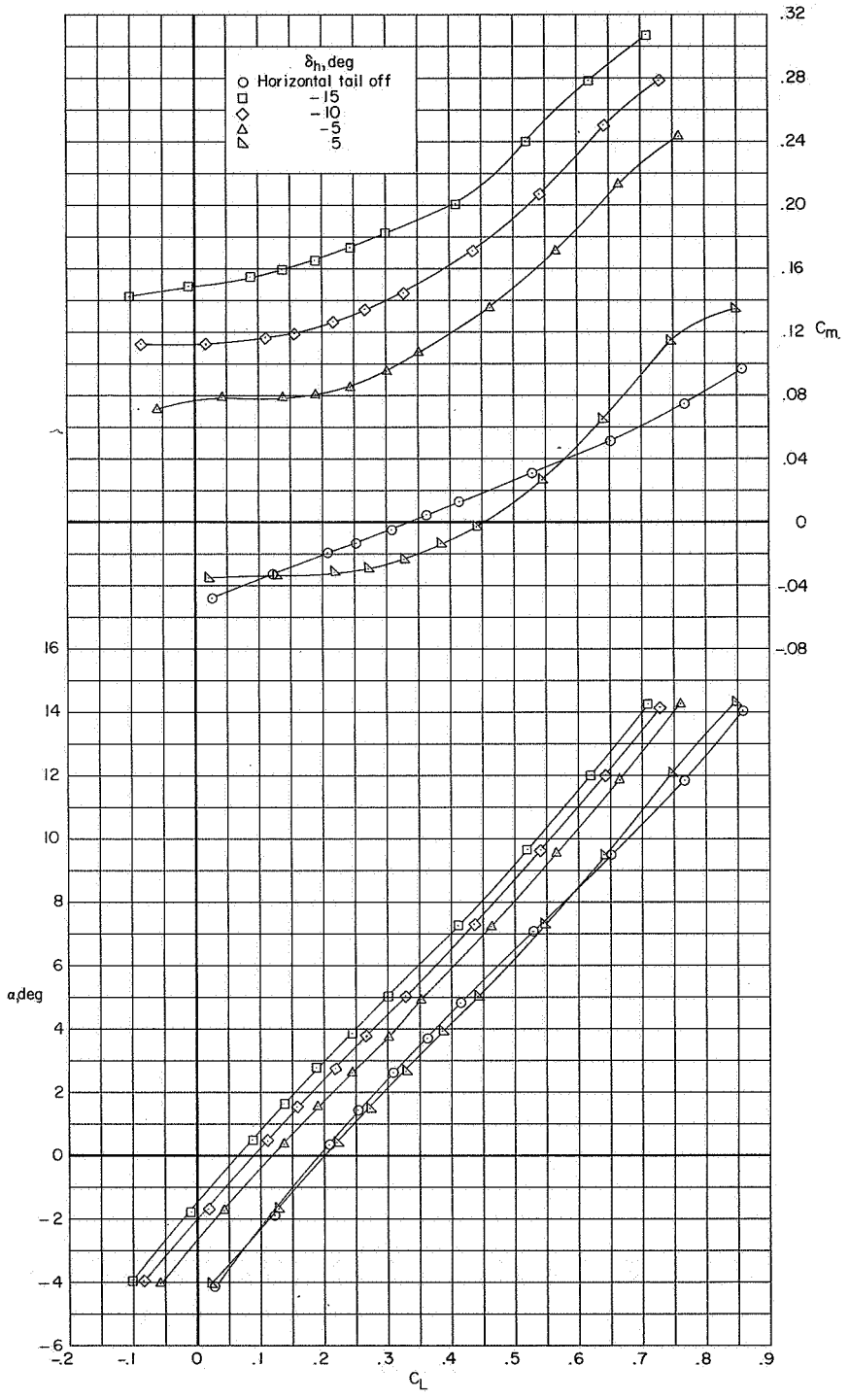

(a) M = 0.80.

Figure 5.- Horizontal-tail effects on the longitudinal aerodynamic characteristics of configuration DWB. Inlet on.

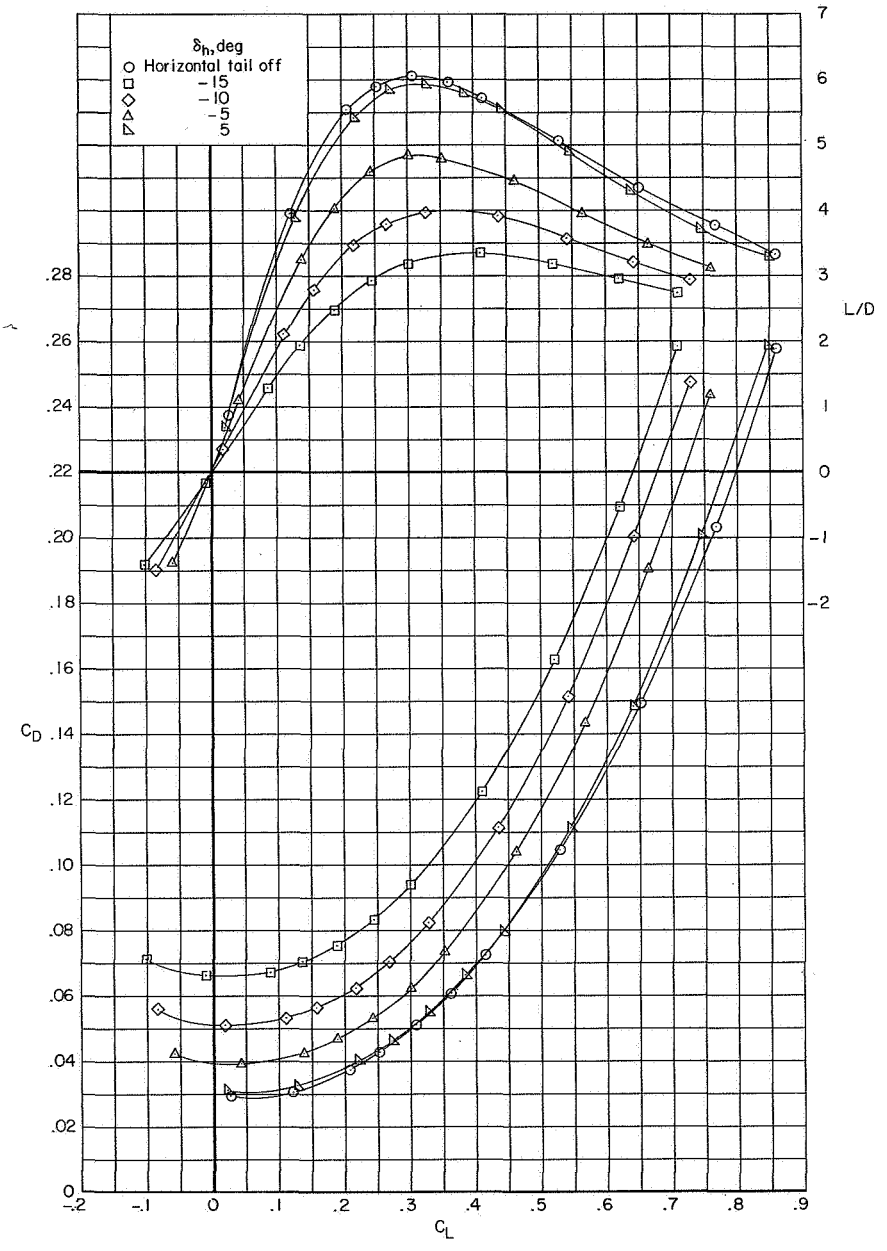

(a) Concluded.

Figure 5.- Continued.

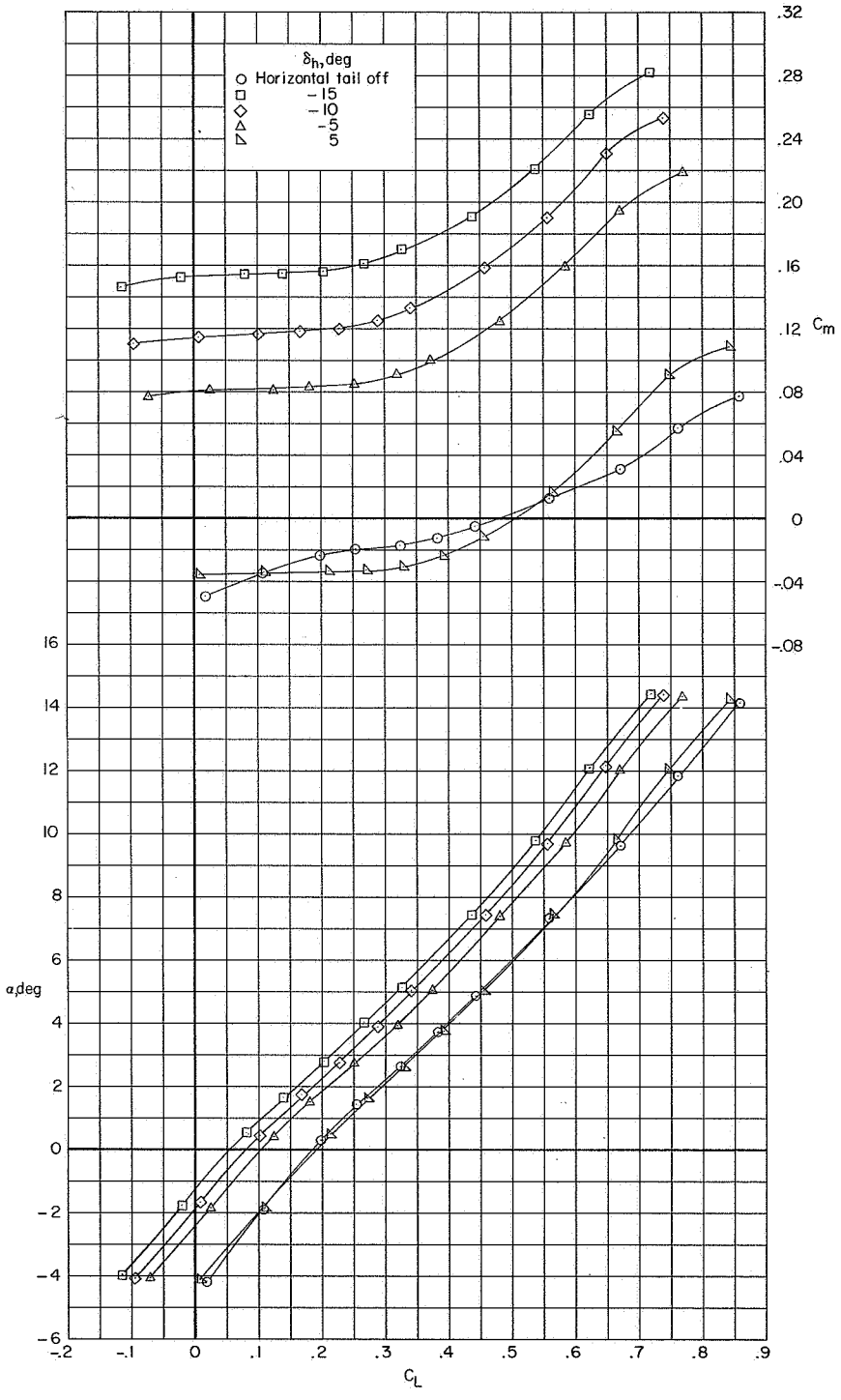

(b) M = 0.90.

Figure 5.- Continued.

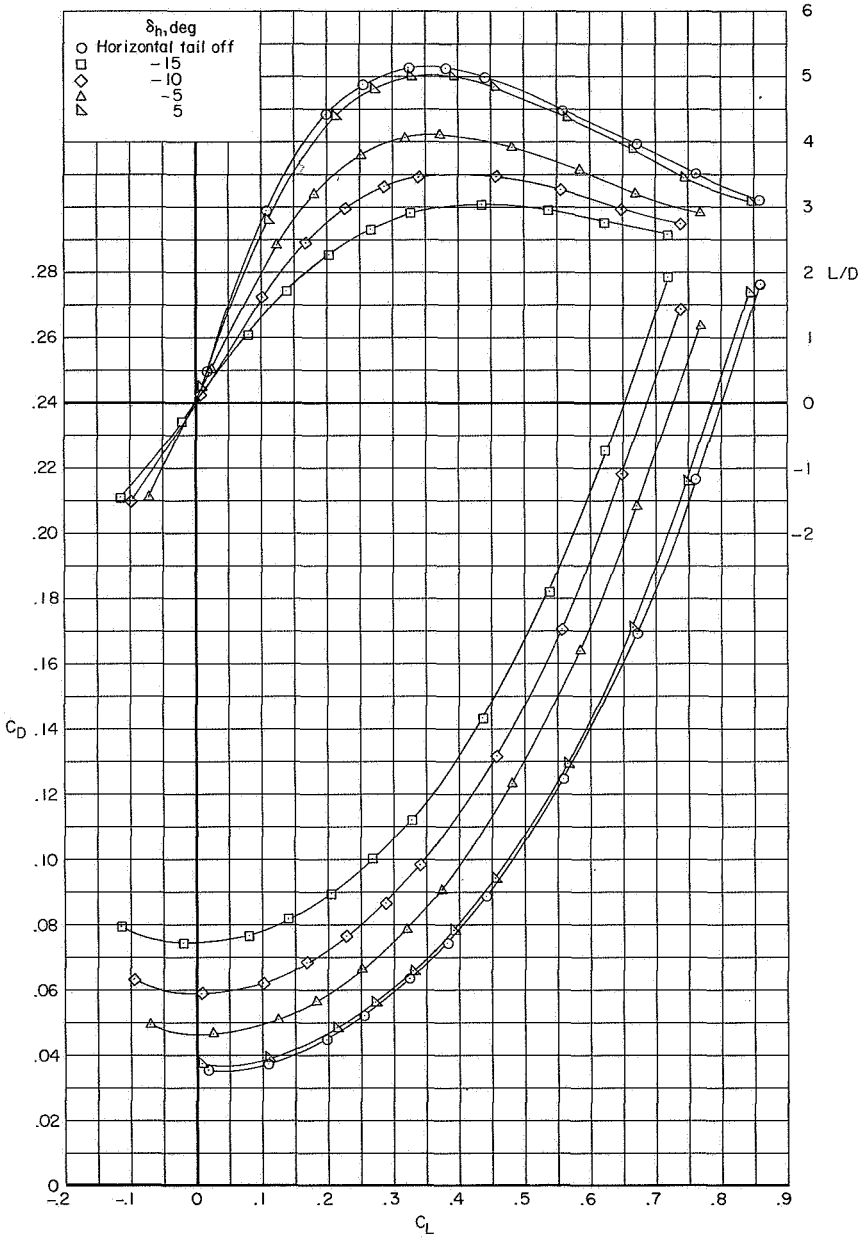

(b) Concluded.

Figure 5.- Continued.

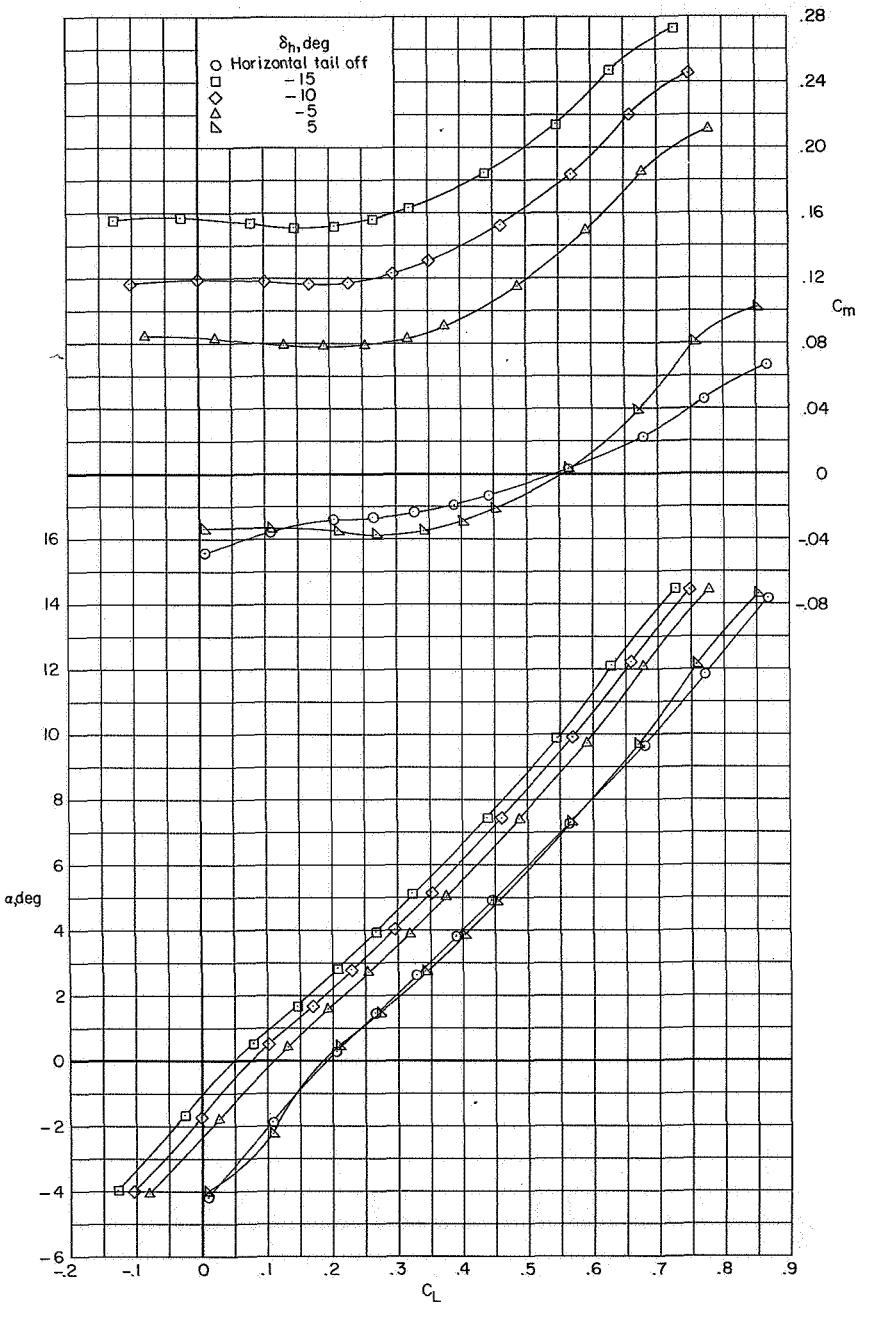

(c) M = 0.93.

Figure 5.- Continued.

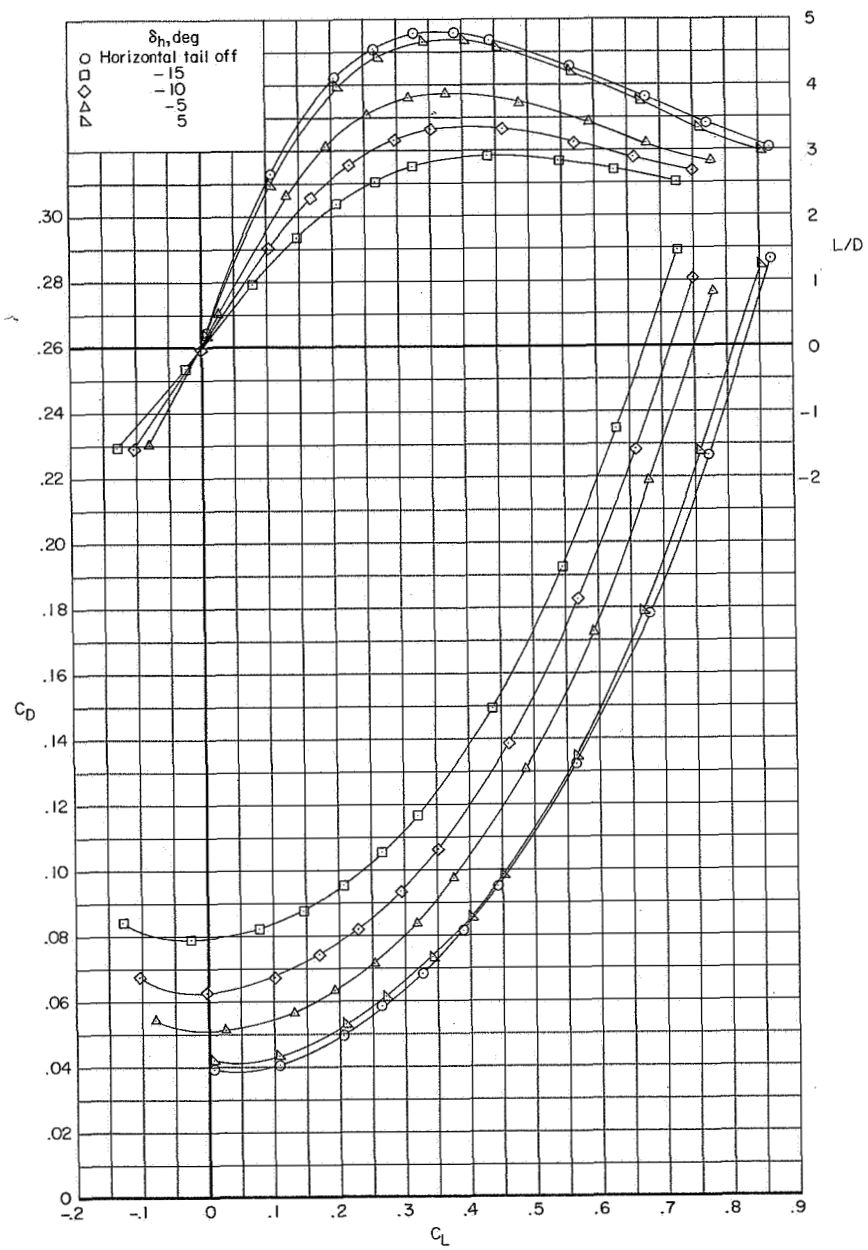

(c) Concluded.

Figure 5.- Continued.

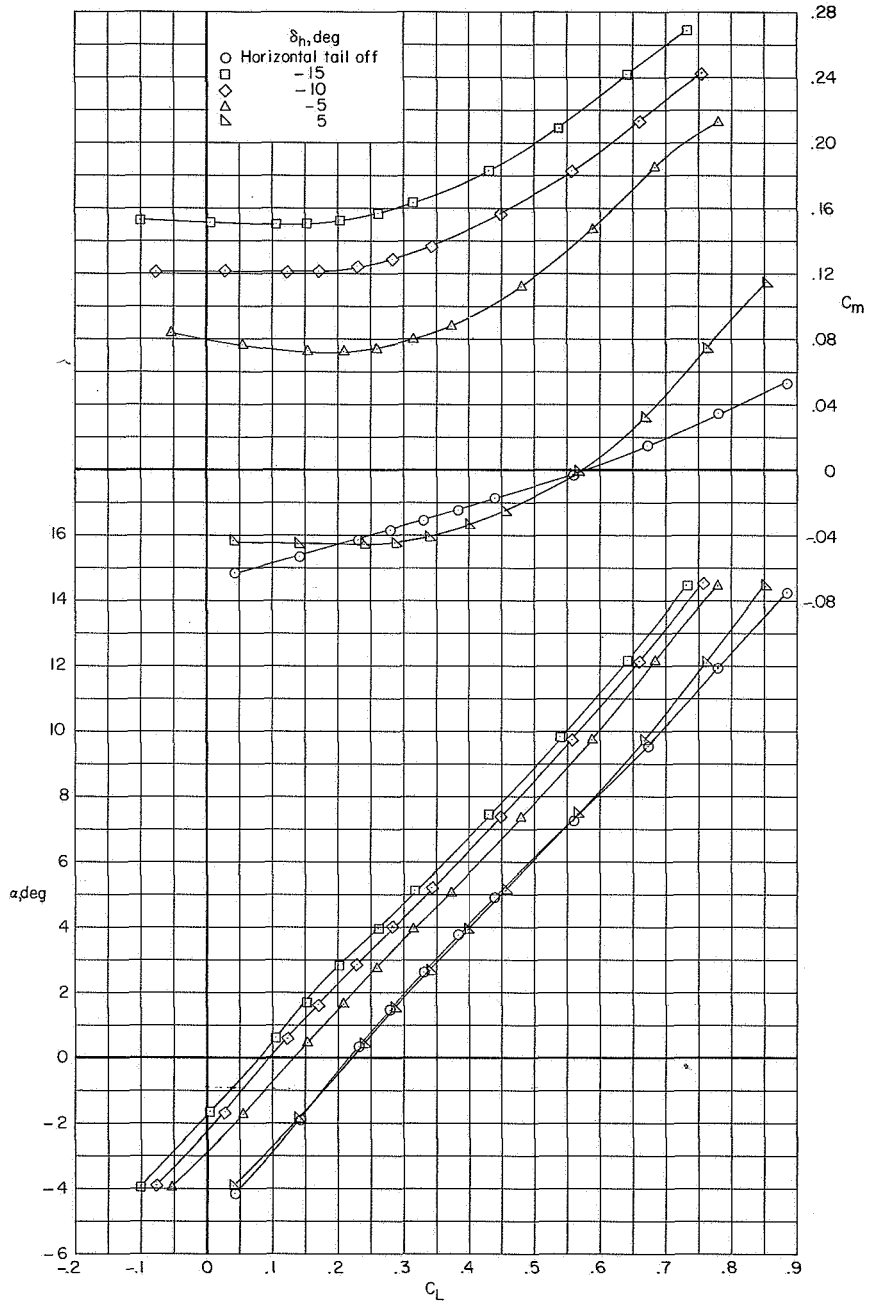

(d) M = 0.96.

Figure 5.- Continued.

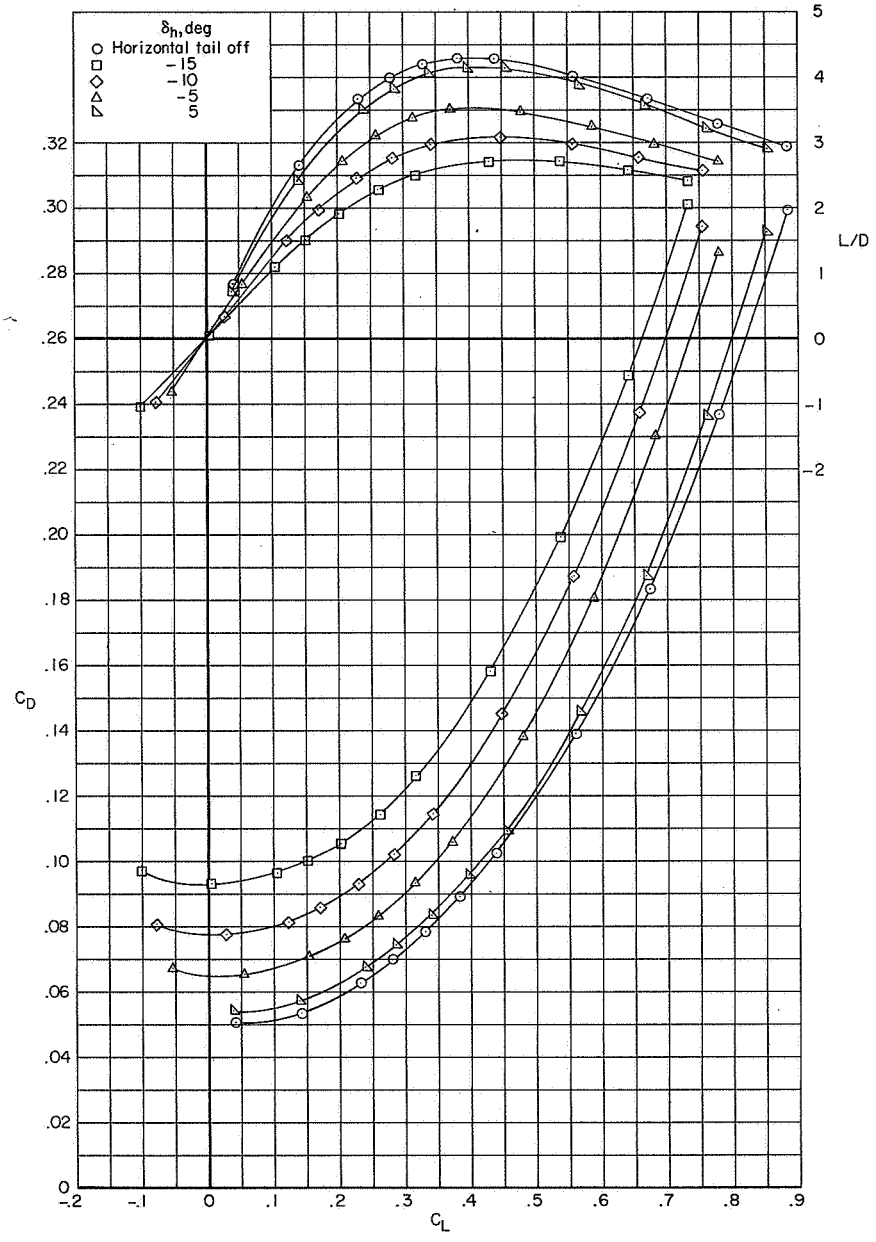

(d) Concluded.

Figure 5.- Continued.

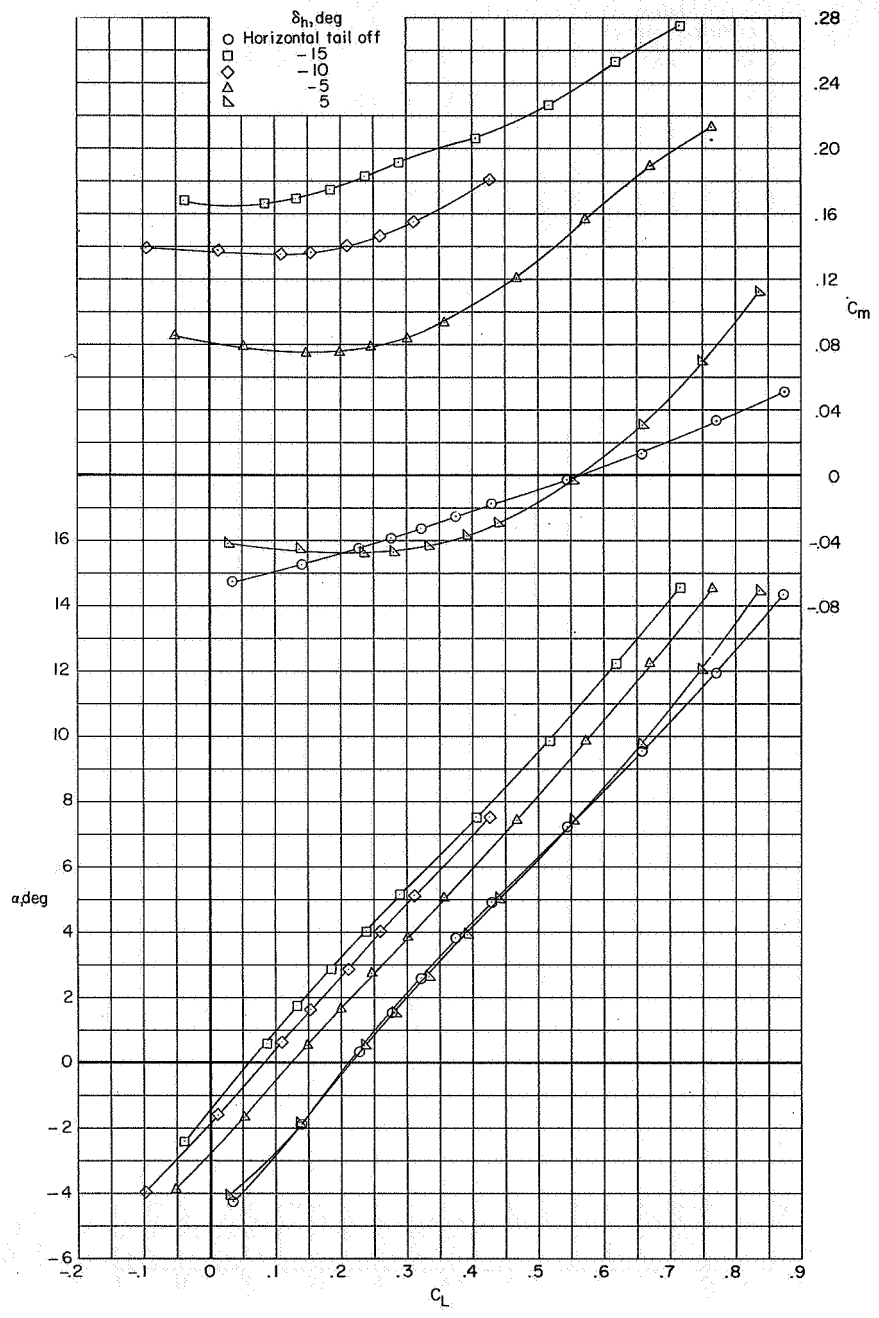

(e) M = 1.00.

Figure 5.- Continued.

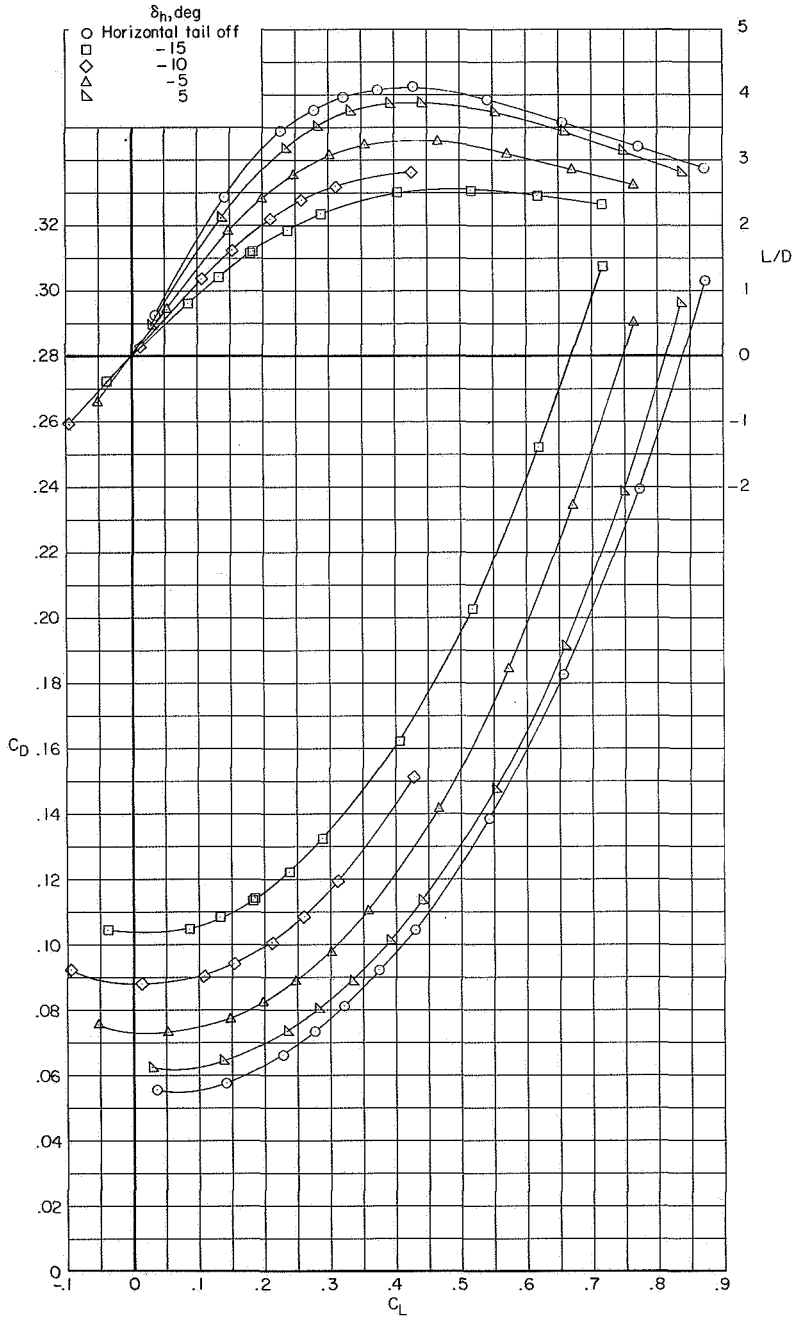

(e) Concluded.

Figure 5.- Continued.

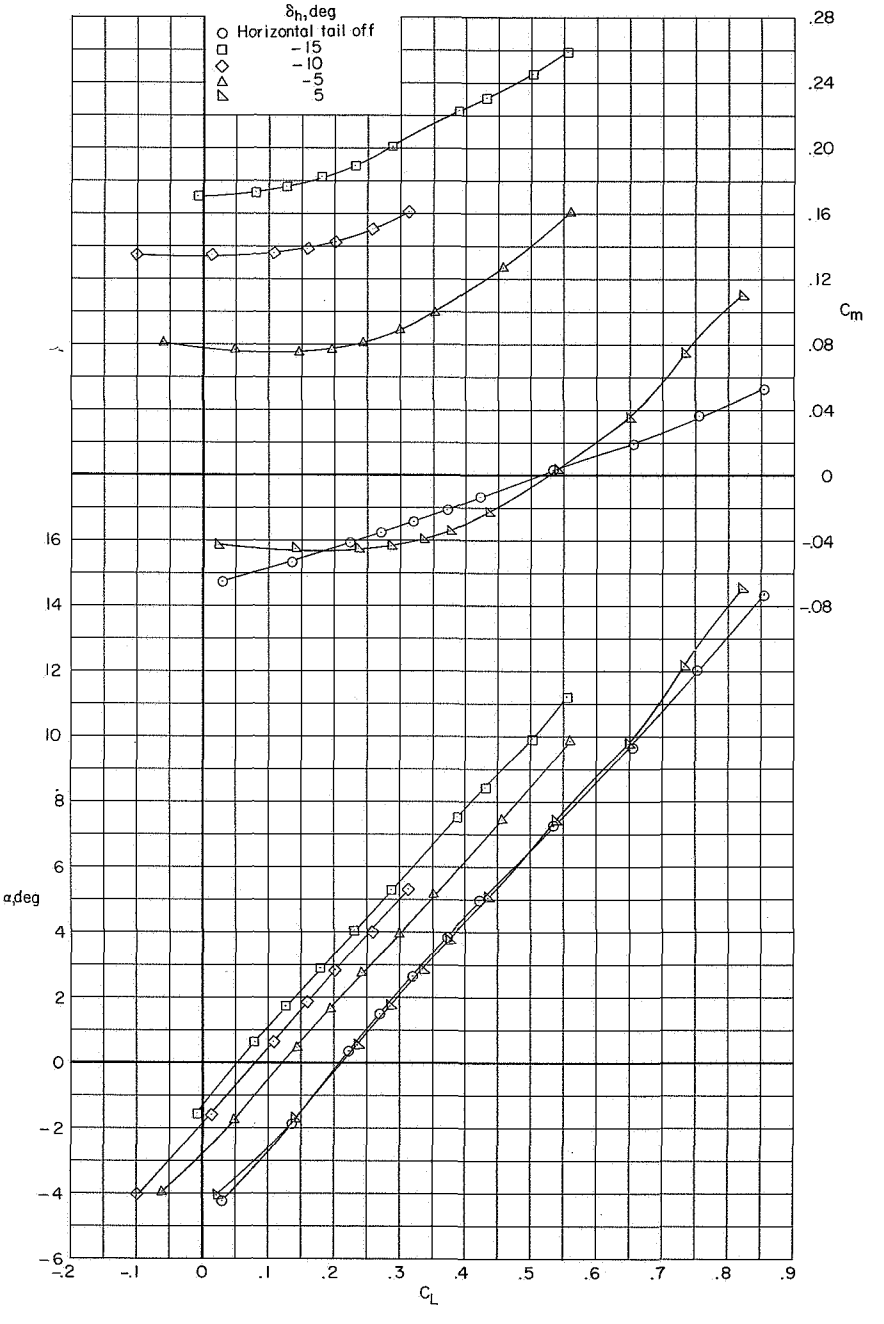

(f) M = 1.03.

Figure 5.- Continued.

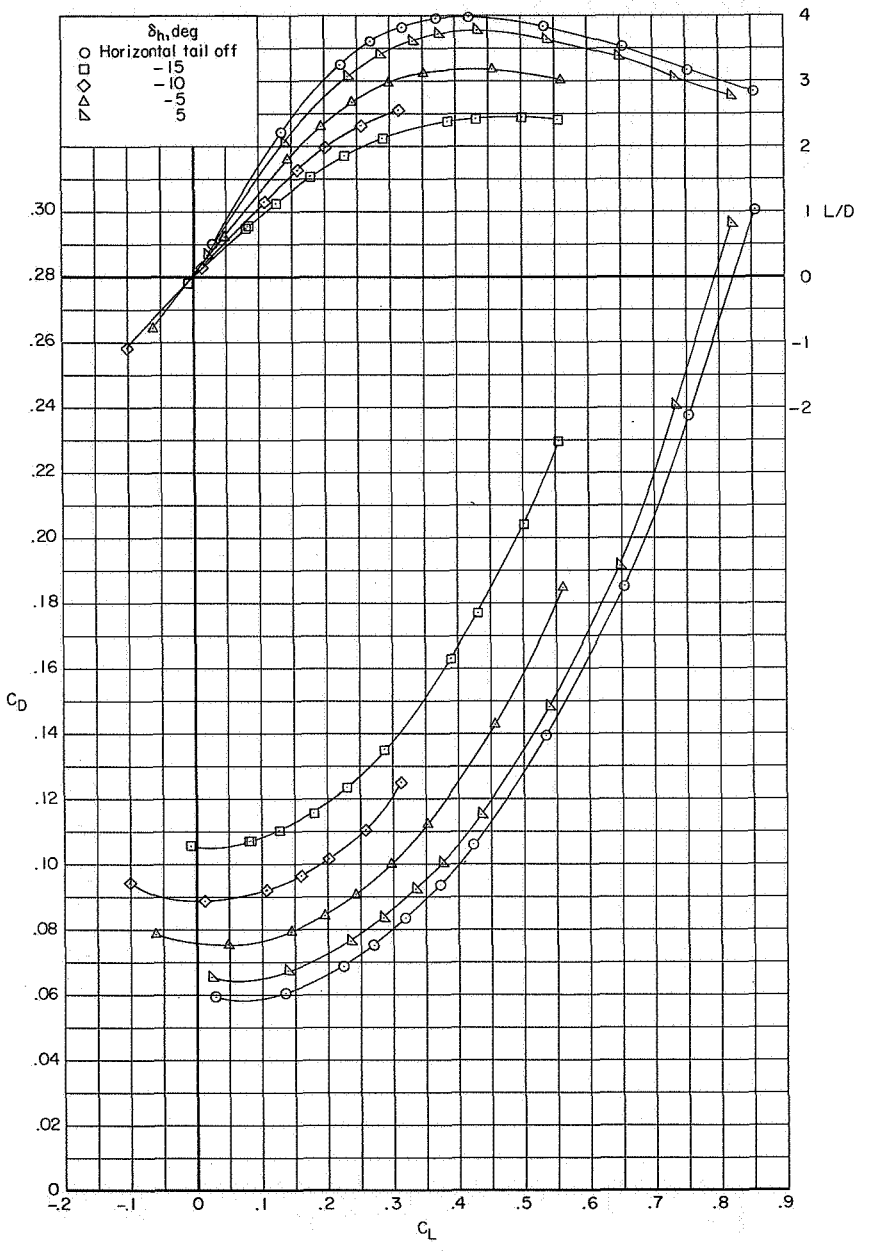

(f) Concluded.

Figure 5.- Continued.

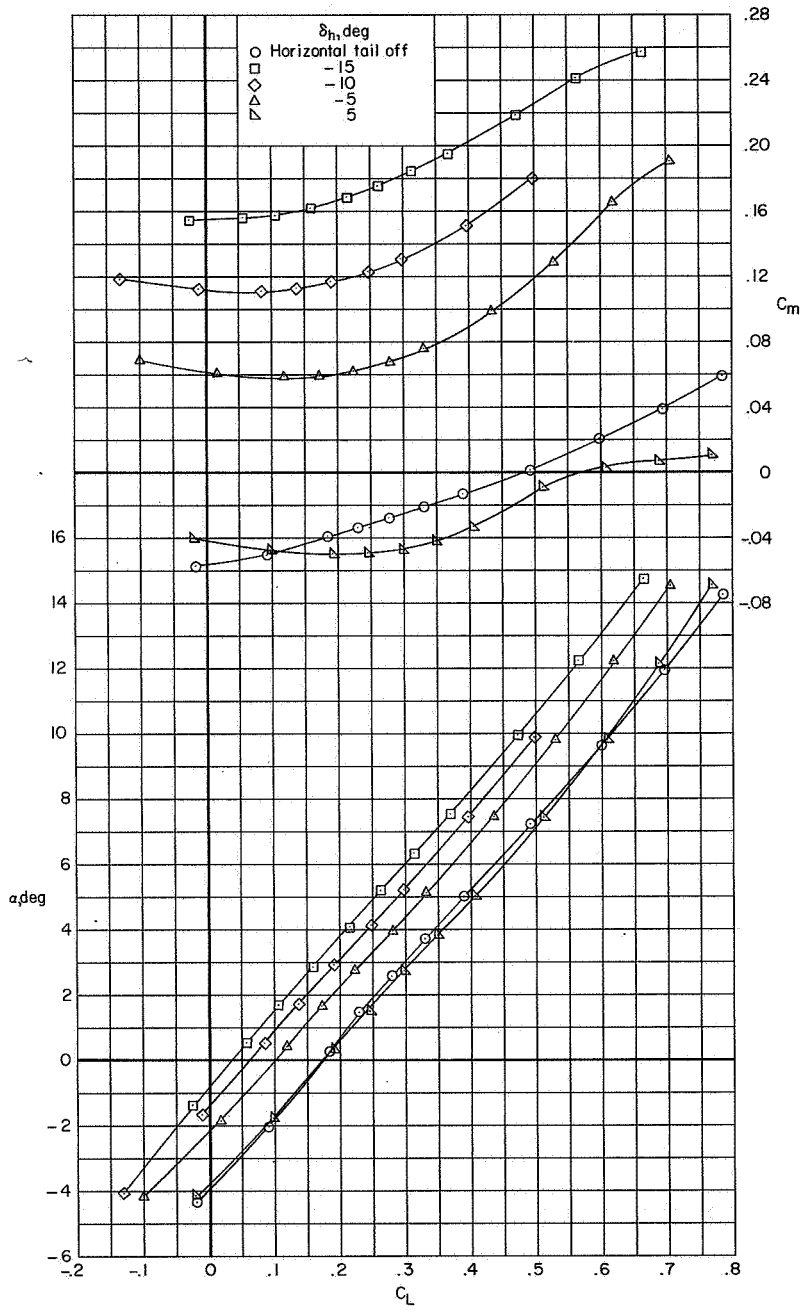

(g) M = 1.20.

Figure 5.- Continued.

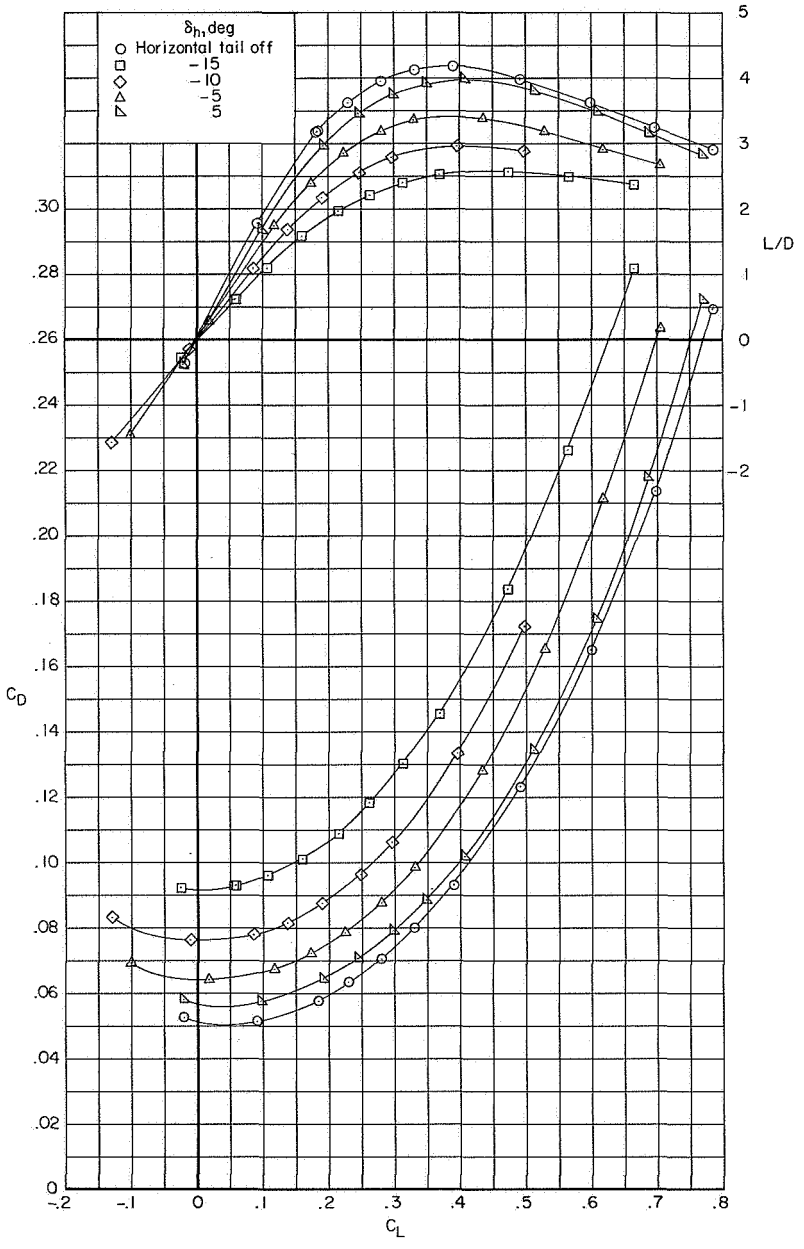

(g) Concluded.

Figure 5.- Concluded.

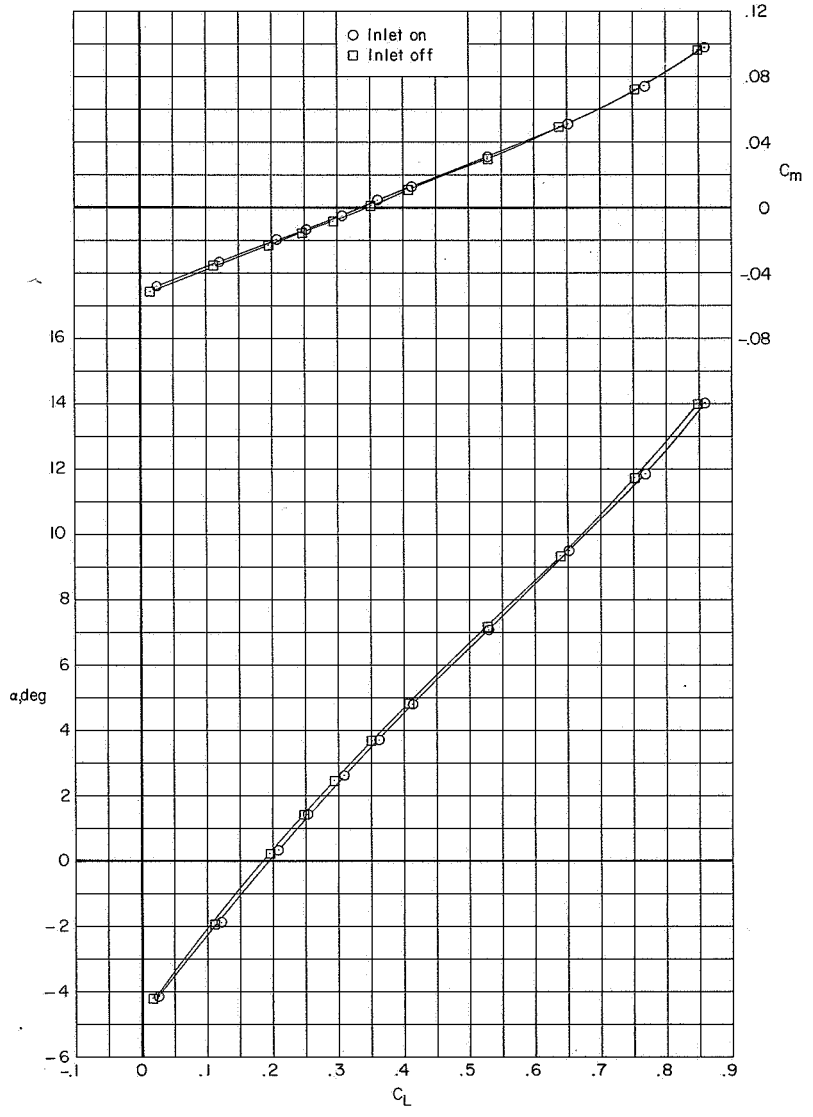

(a) M = 0.80.

Figure 6.- Inlet effects on the longitudinal aerodynamic characteristics of configuration DWB. Horizontal tail off.

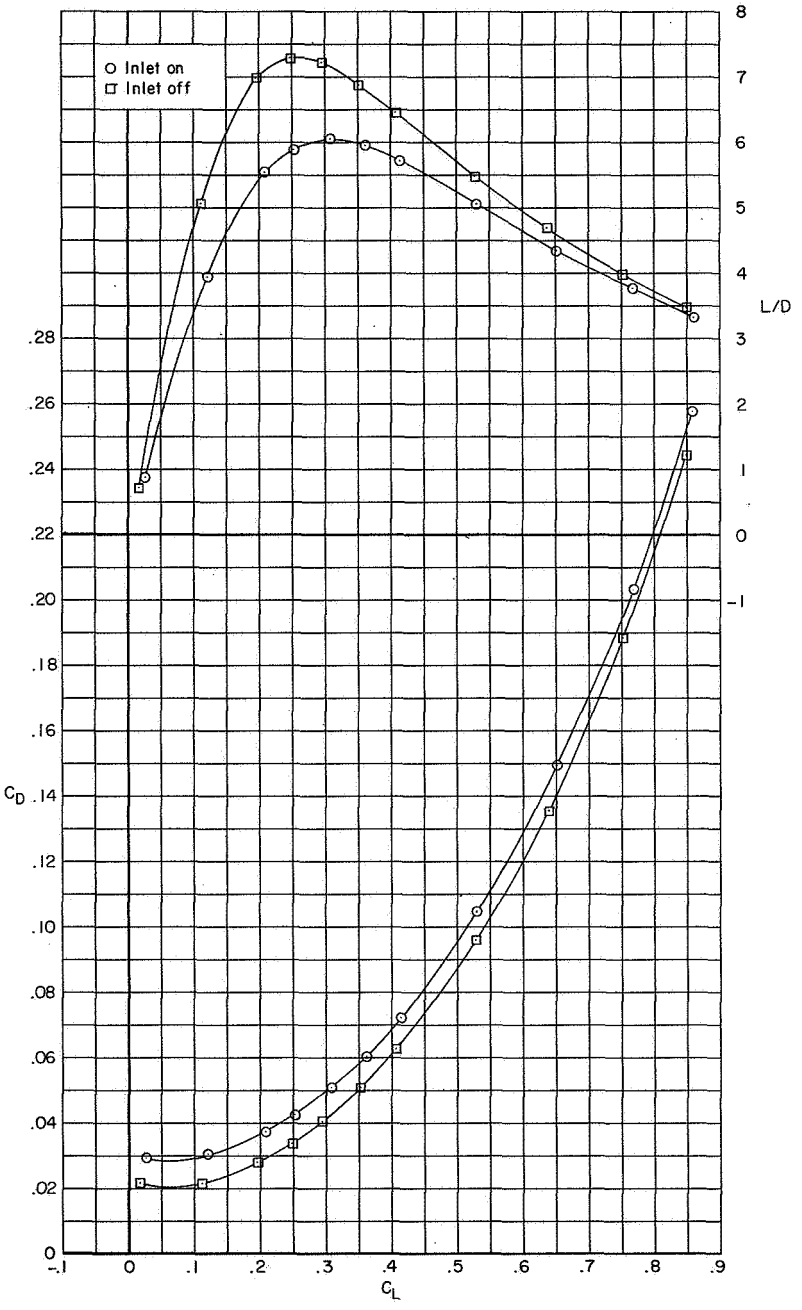

(a) Concluded.

Figure 6.- Continued.

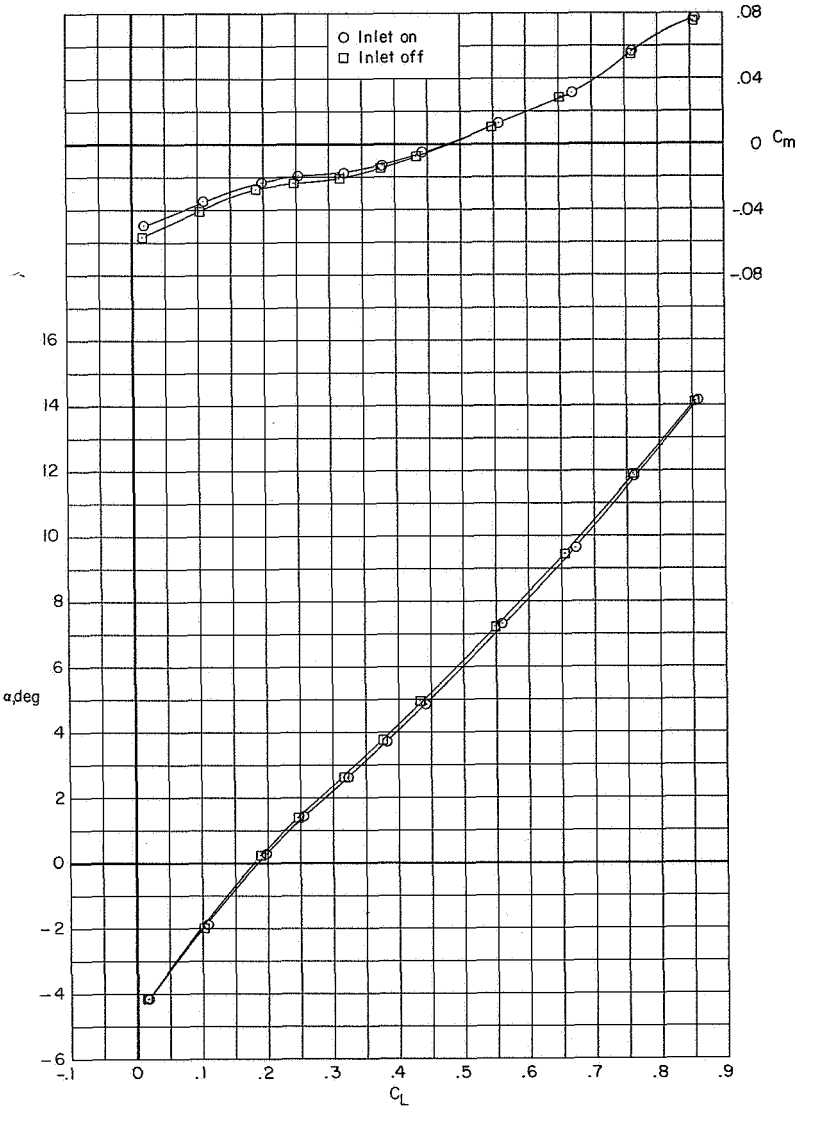

(b) M = 0.90.

Figure 6.- Continued.

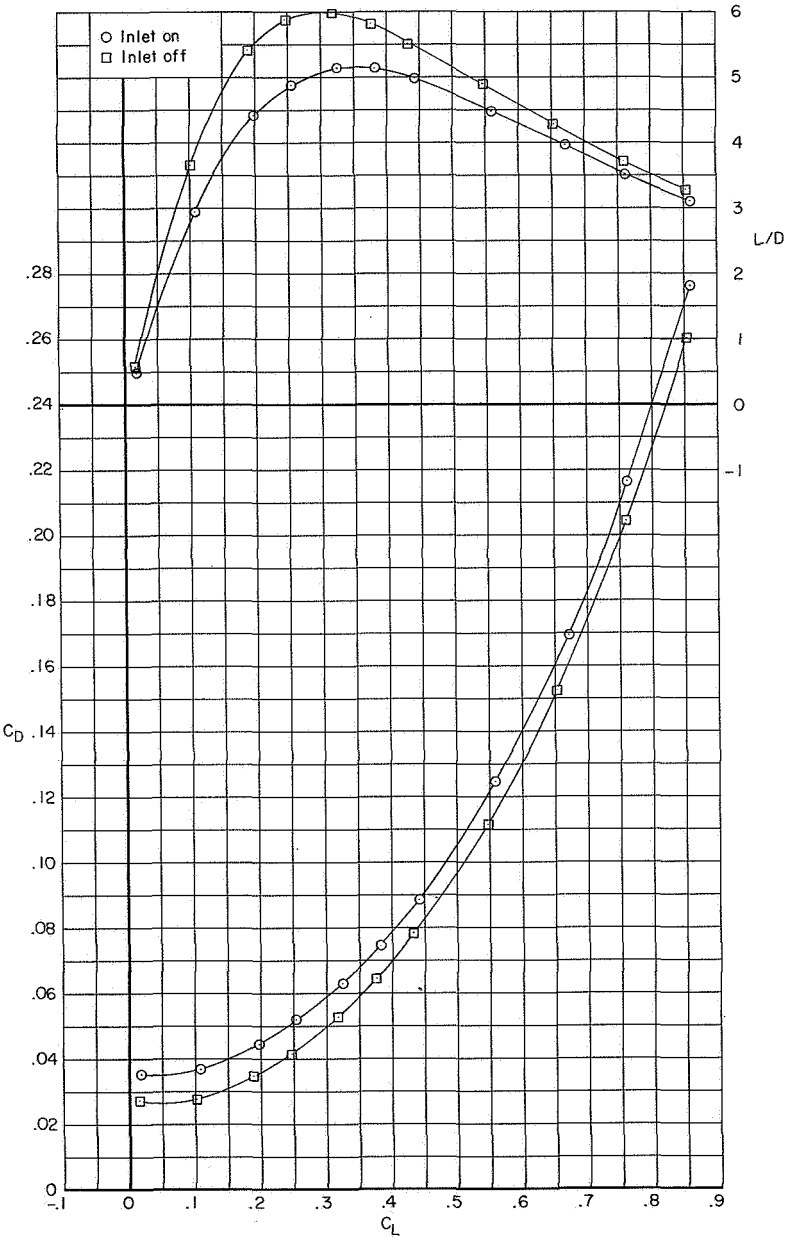

(b) Concluded.

Figure 6.- Continued.

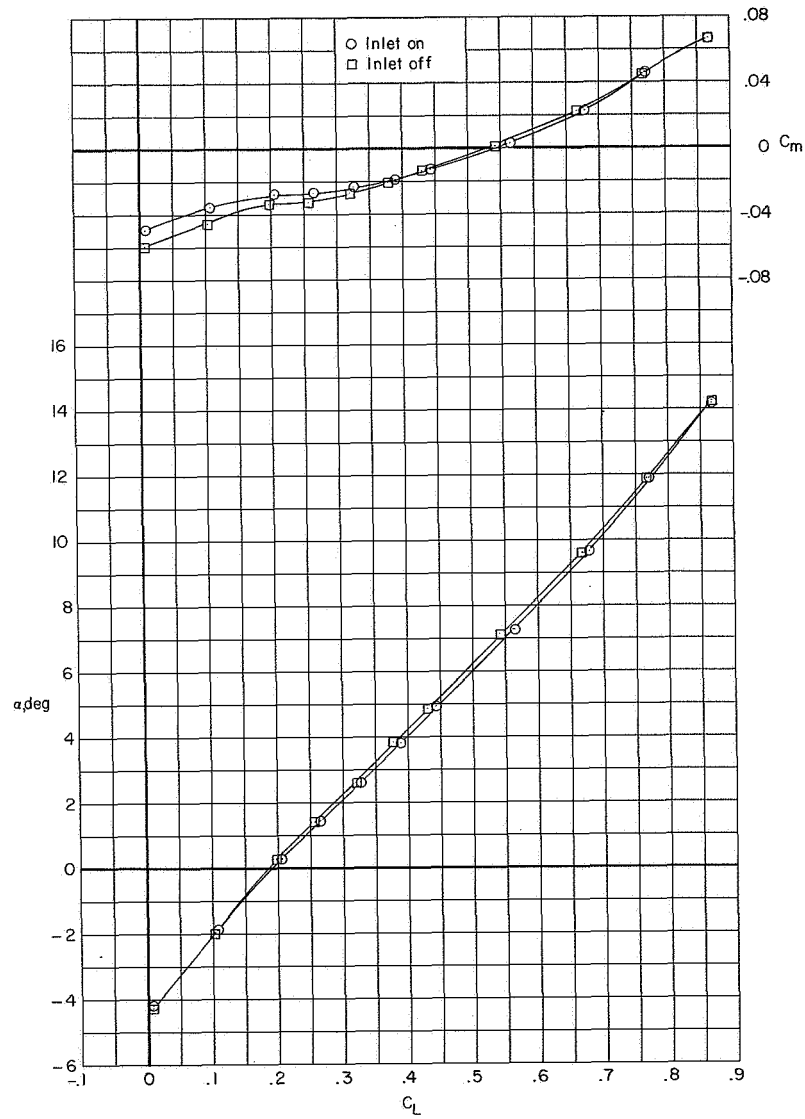

(c) M = 0.93.

Figure 6.- Continued.

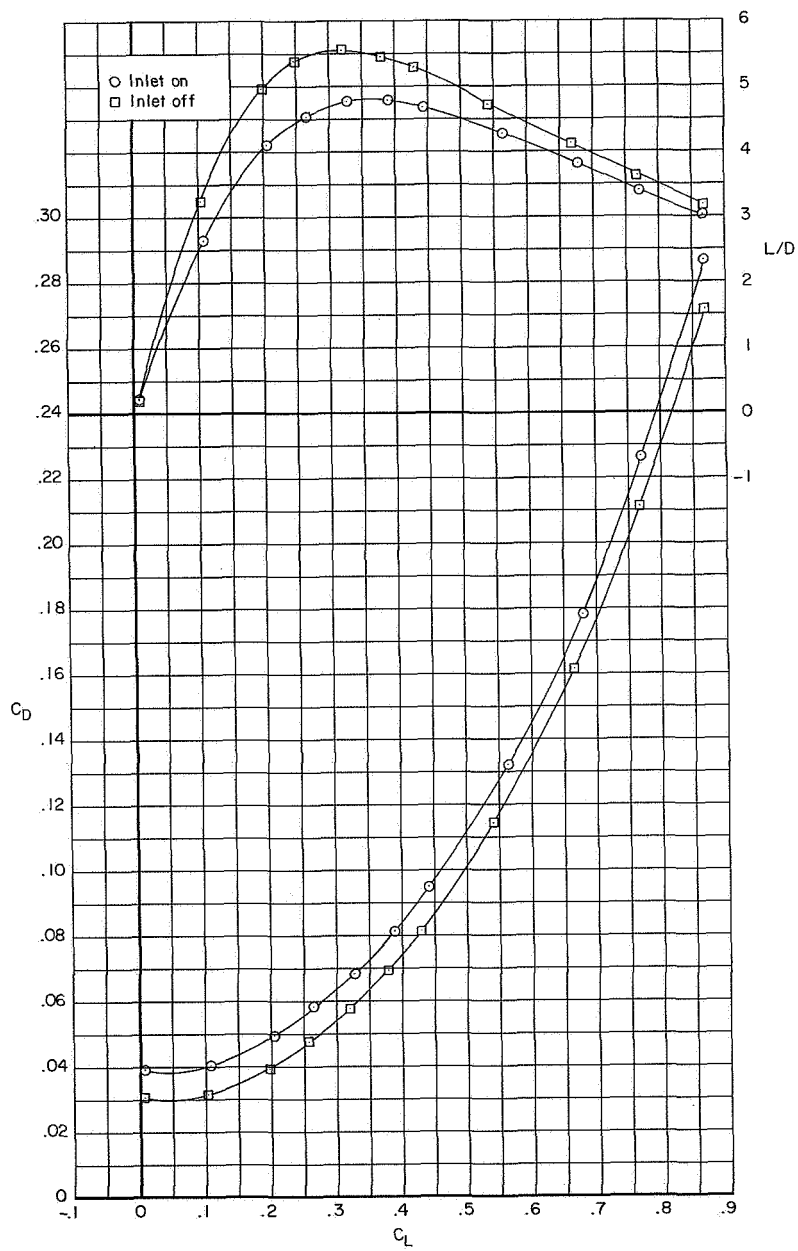

(c) Concluded.

Figure 6.- Continued.

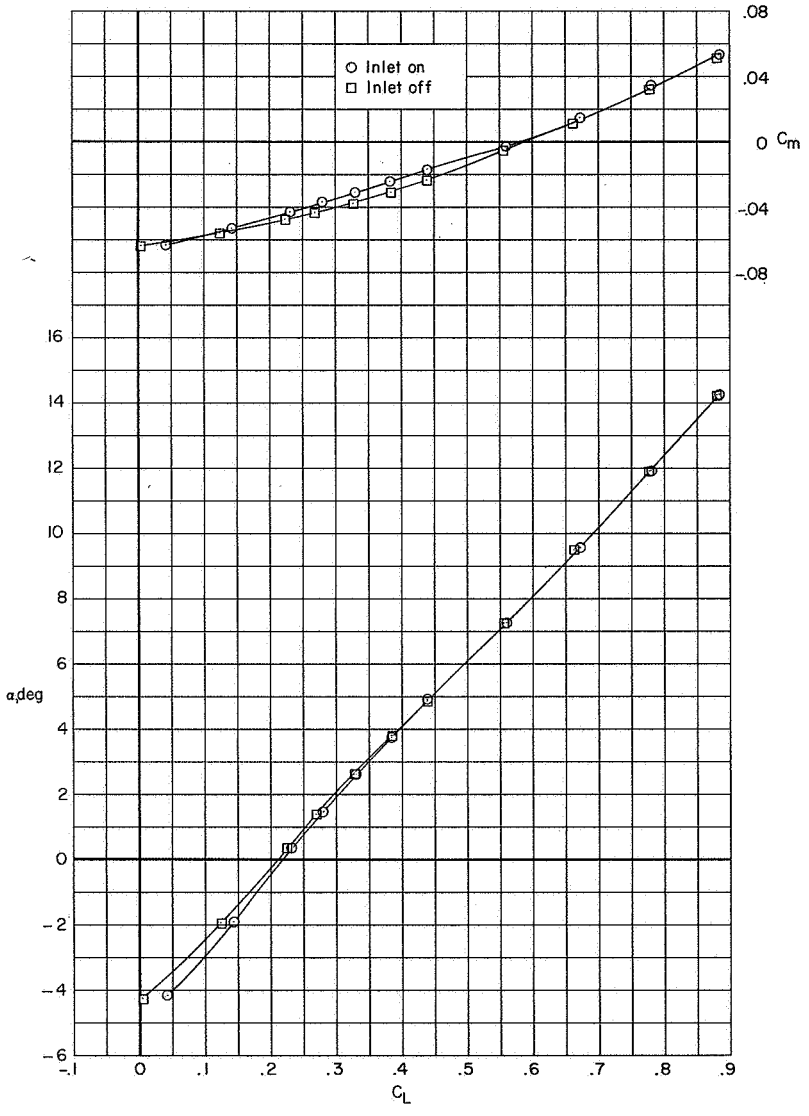

(d) M = 0.96.

Figure 6.- Continued.

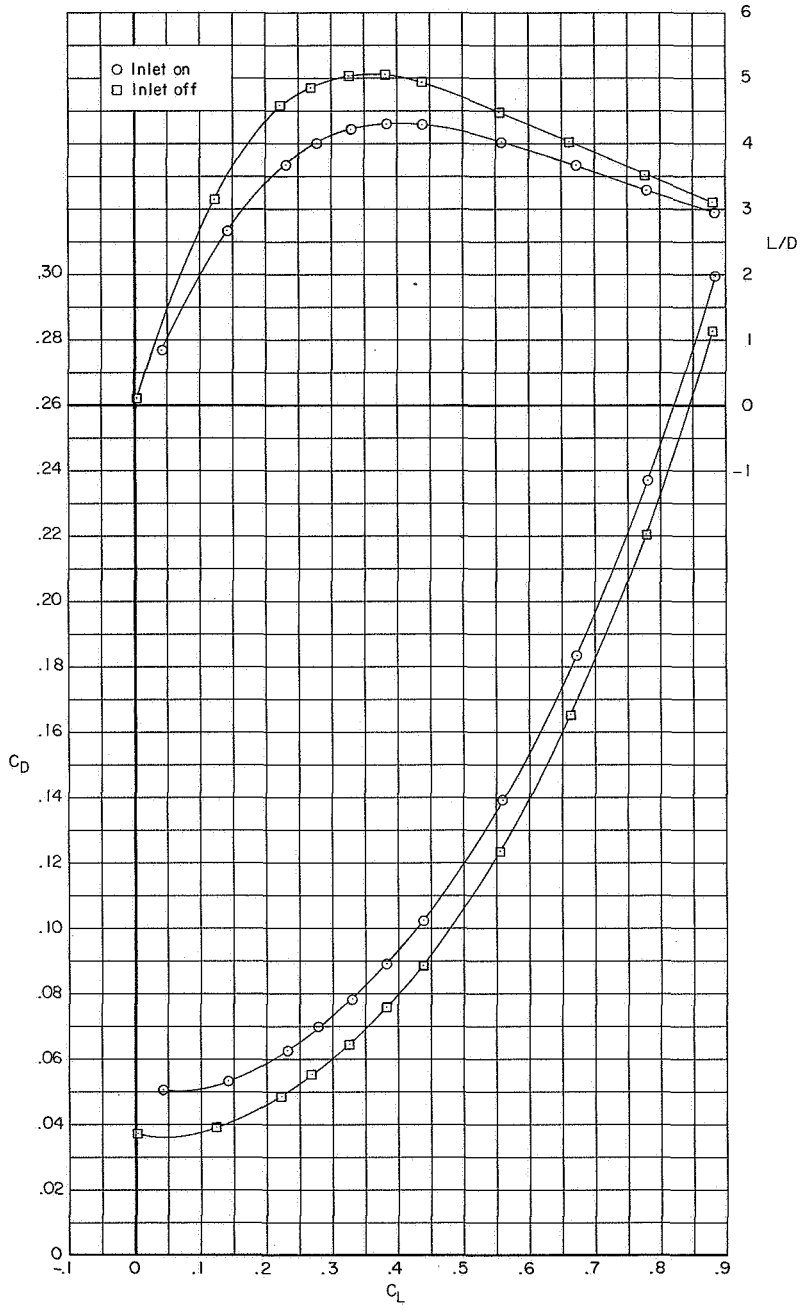

(d) Concluded.

Figure 6.- Continued.

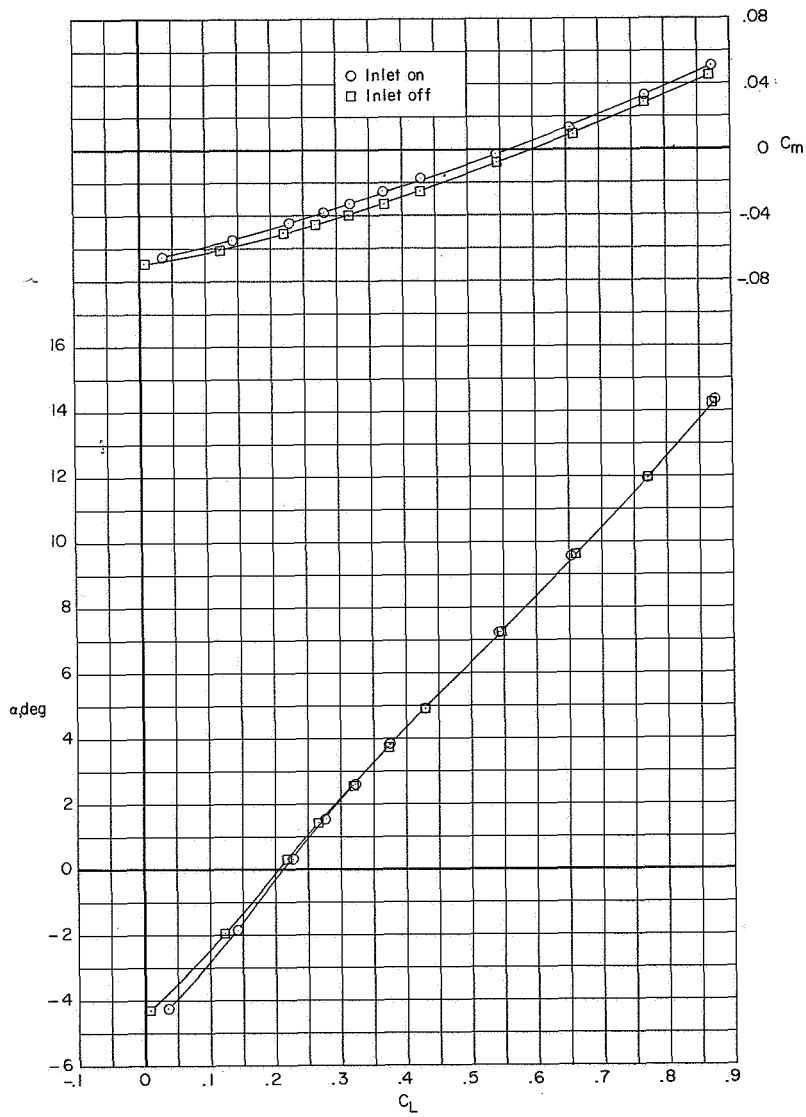

(e) M = 1.00.

Figure 6.- Continued.

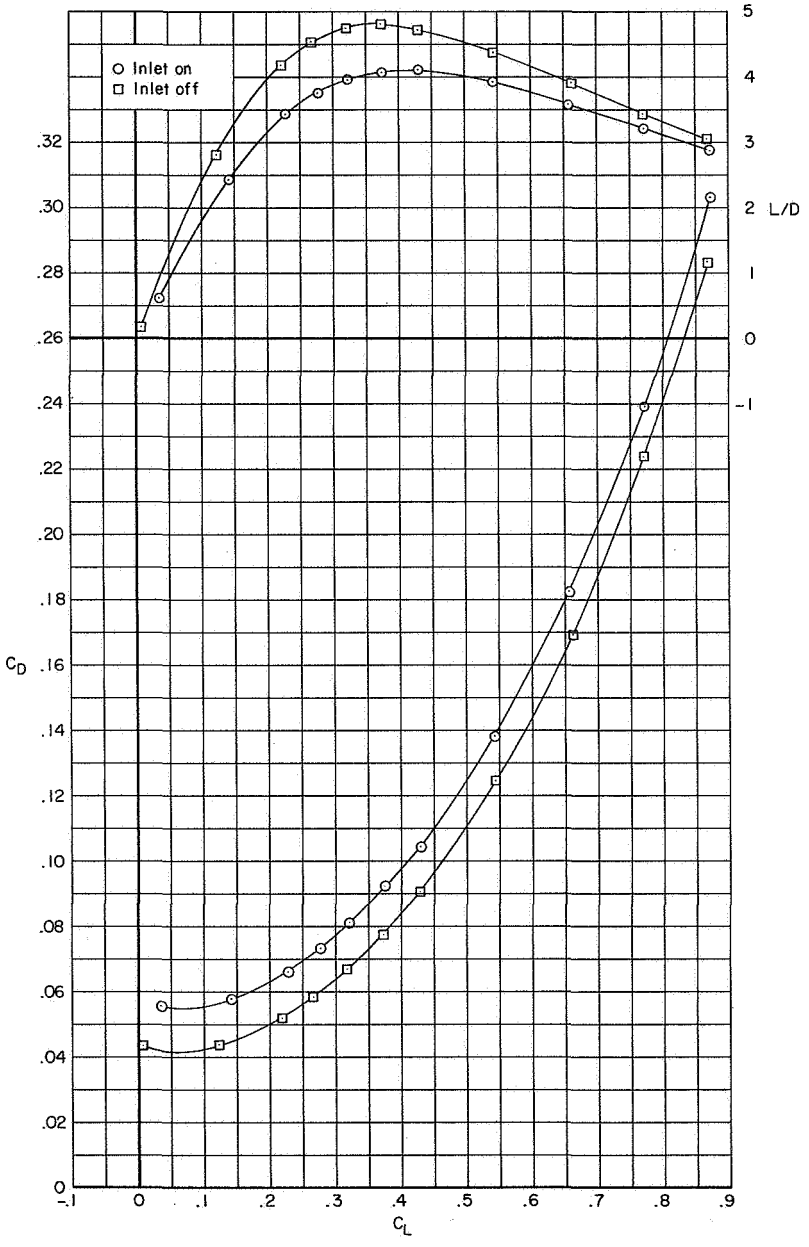

(e) Concluded.

Figure 6.- Continued.

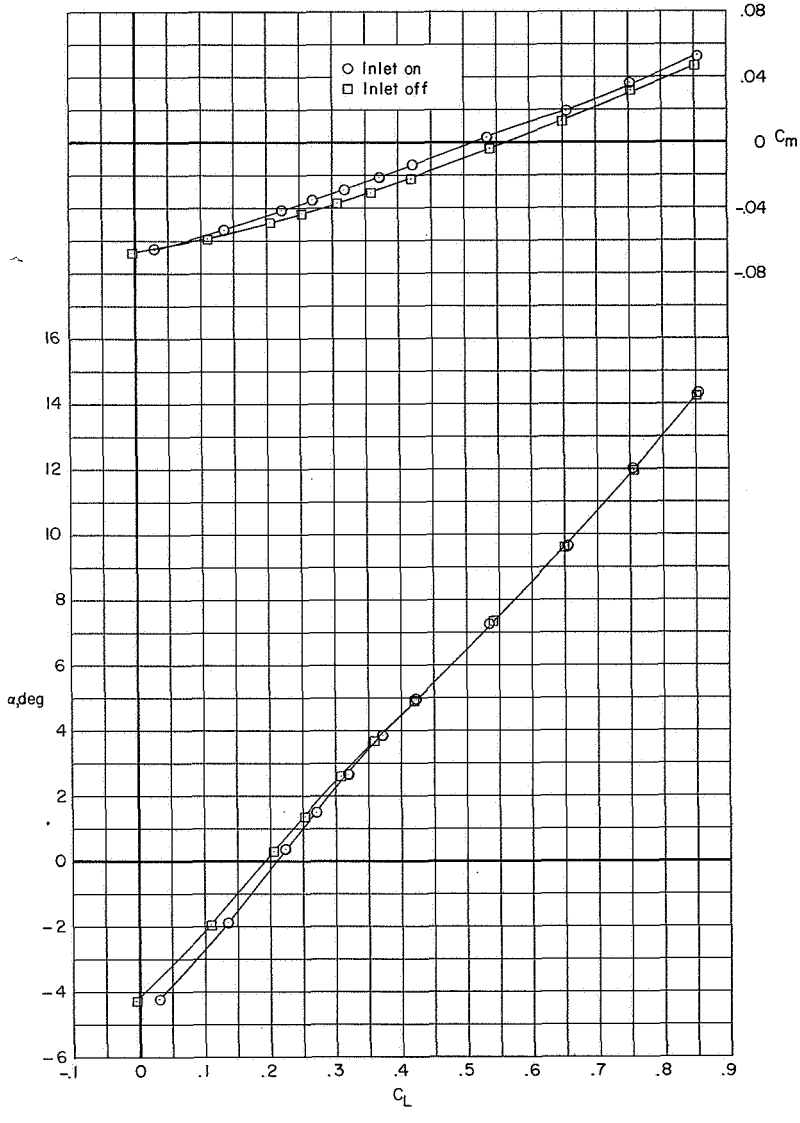

(f) M = 1.03.

Figure 6.- Continued.

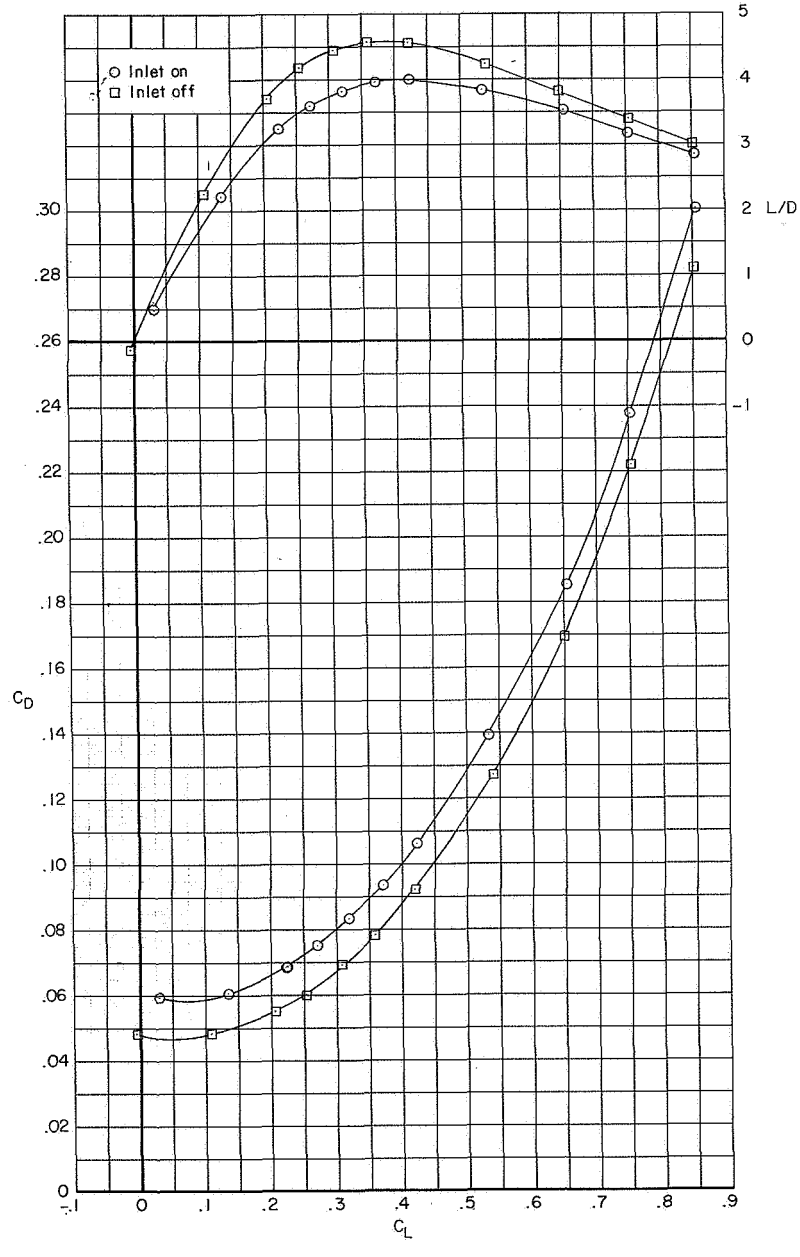

(f) Concluded.

Figure 6.- Continued.

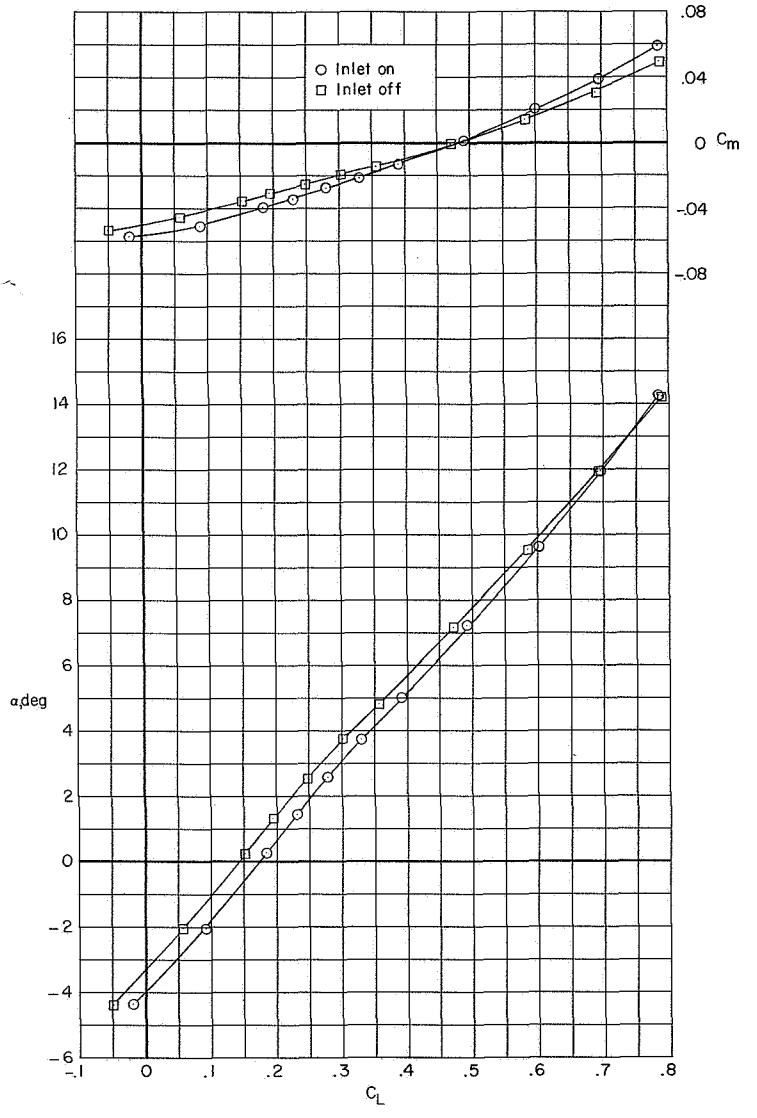

(g) M = 1.20.

Figure 6.- Continued.

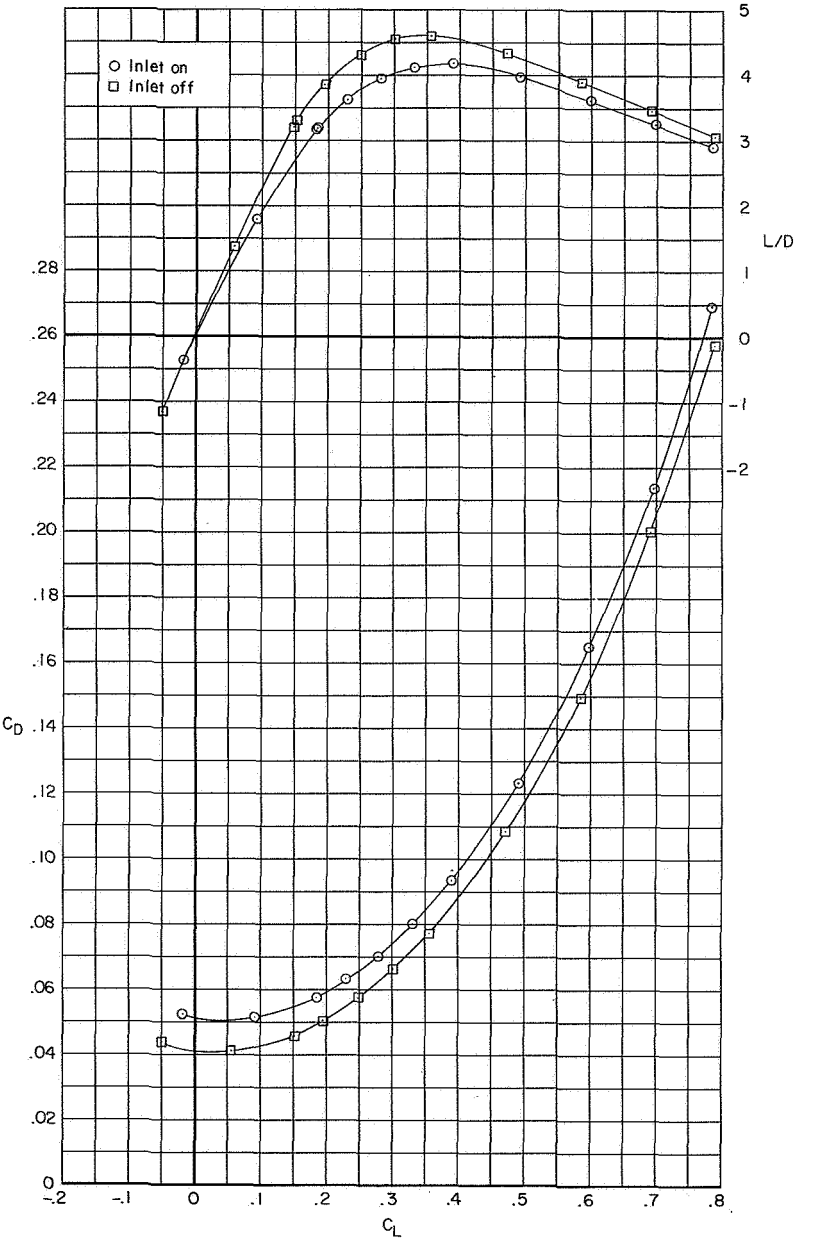

(g) Concluded.

Figure 6.- Concluded.

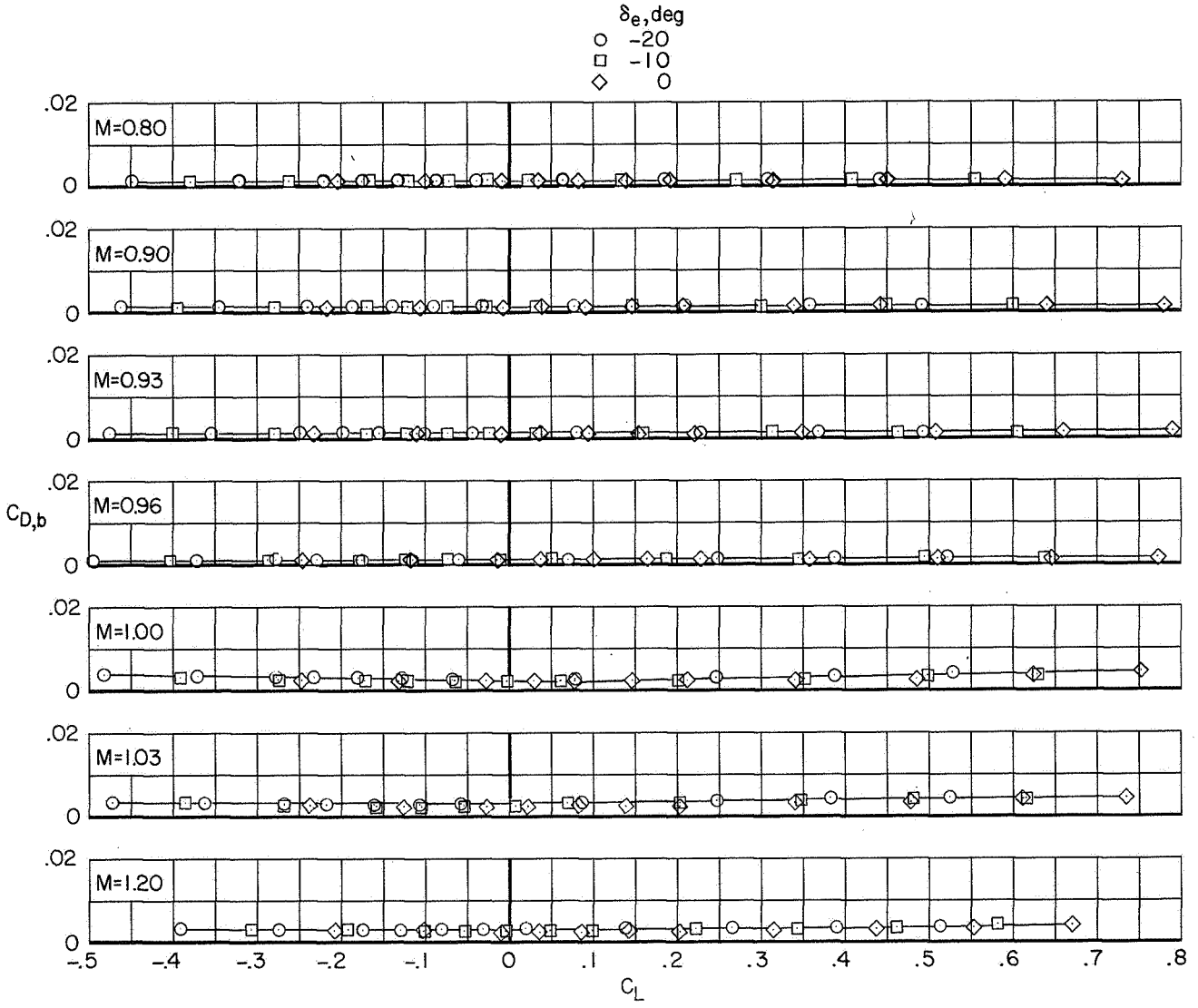

(a) Elevon effects; inlet on.

Figure 7.- Variation of base-drag coefficient with lift coefficient for configuration BWB.

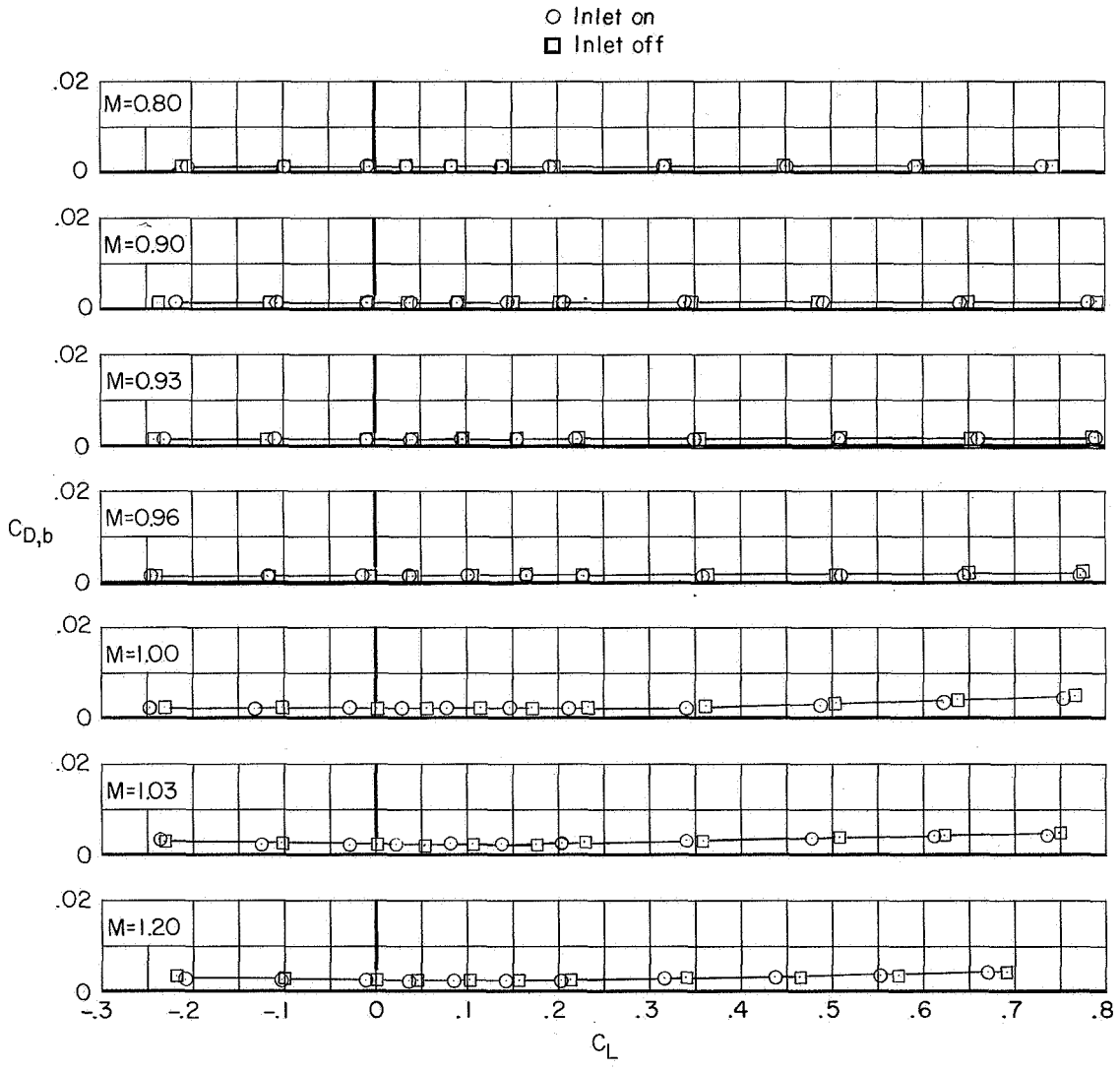

(b) Inlet effects; $\delta_e = 0^0$.

Figure 7.- Concluded.

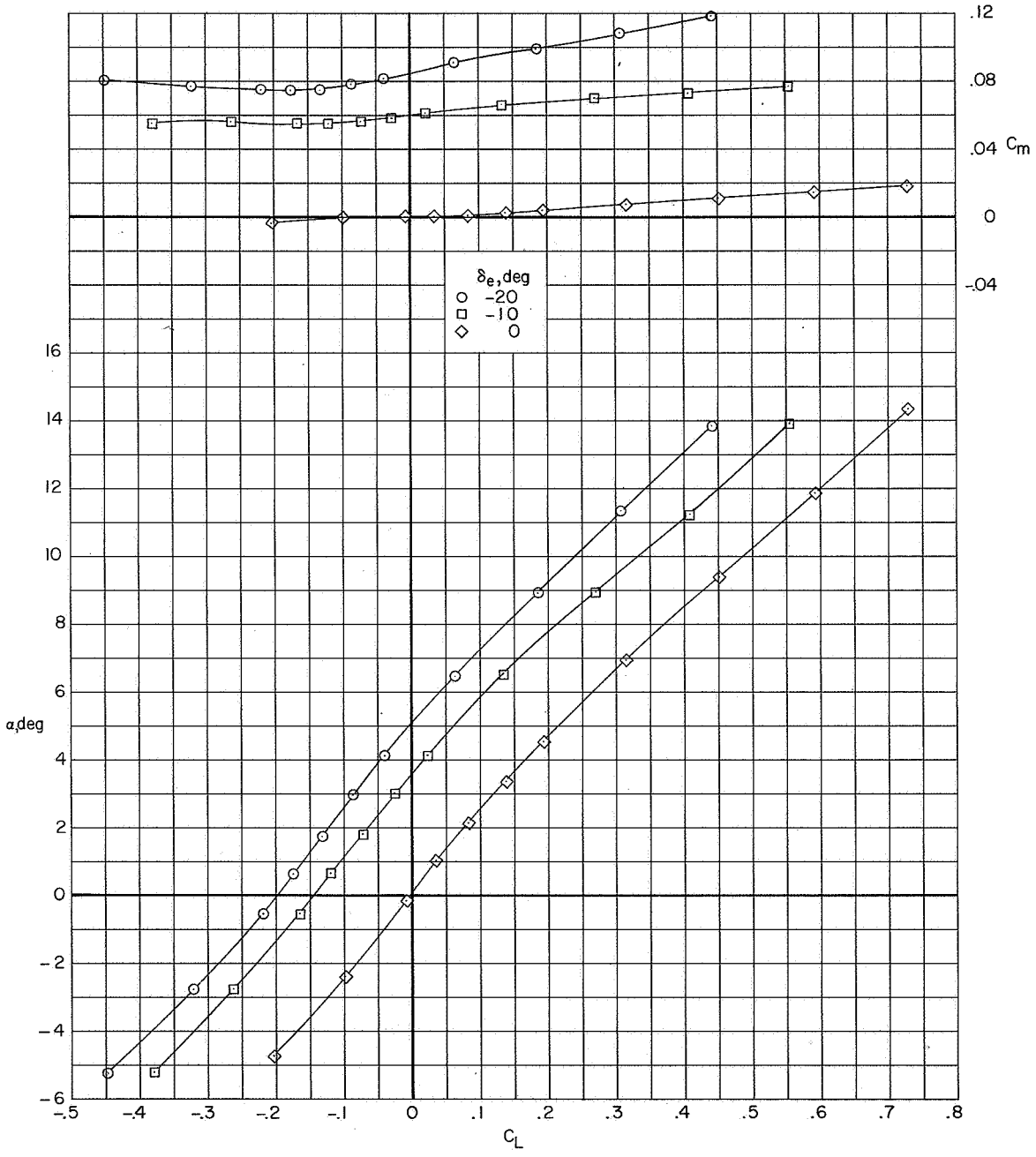

(a) M = 0.80.

Figure 8.- Elevon effects on the longitudinal aerodynamic characteristics of configuration BWB. Inlet on.

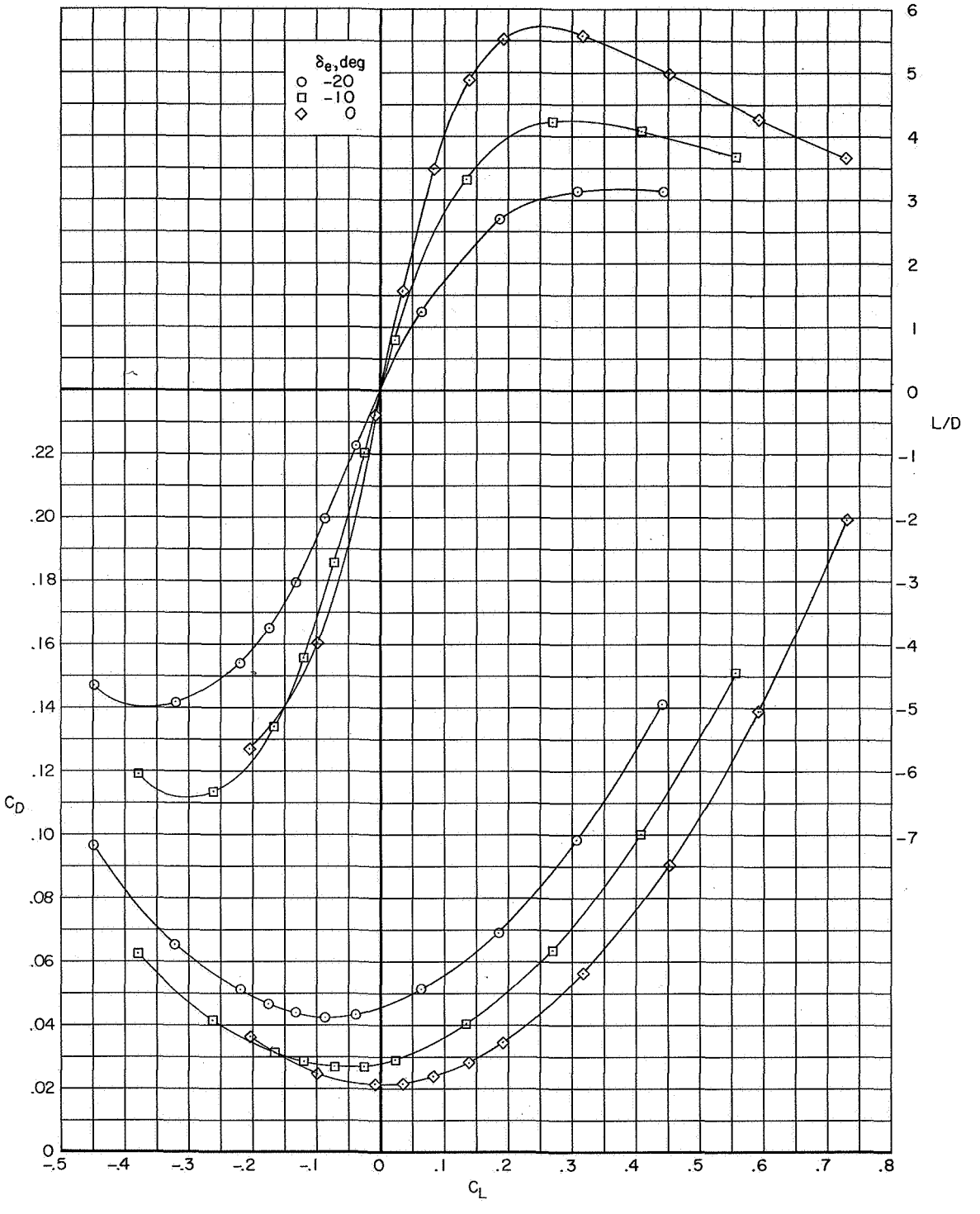

(a) Concluded.

Figure 8.- Continued.

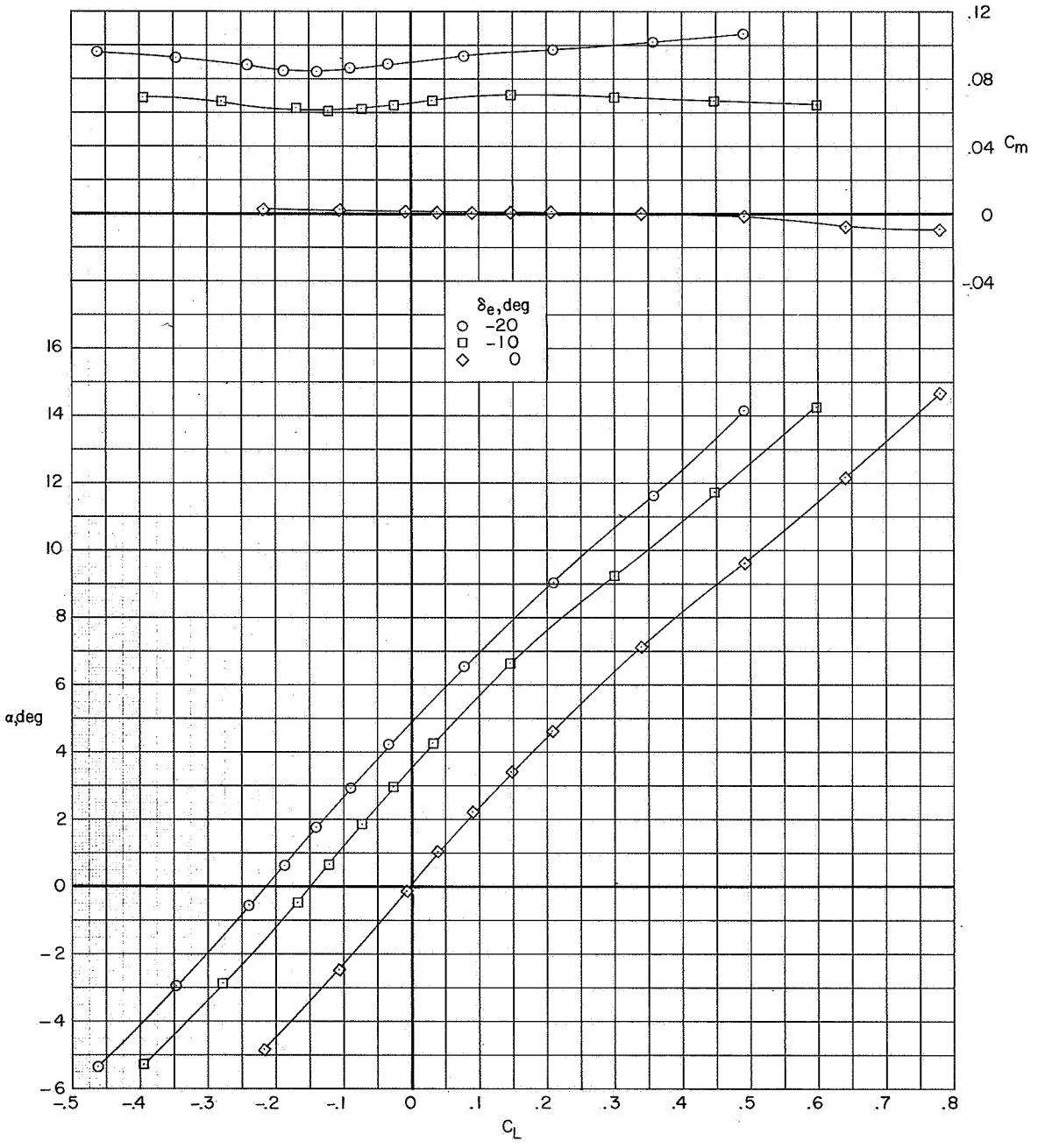

(b) M = 0.90.

Figure 8.- Continued.

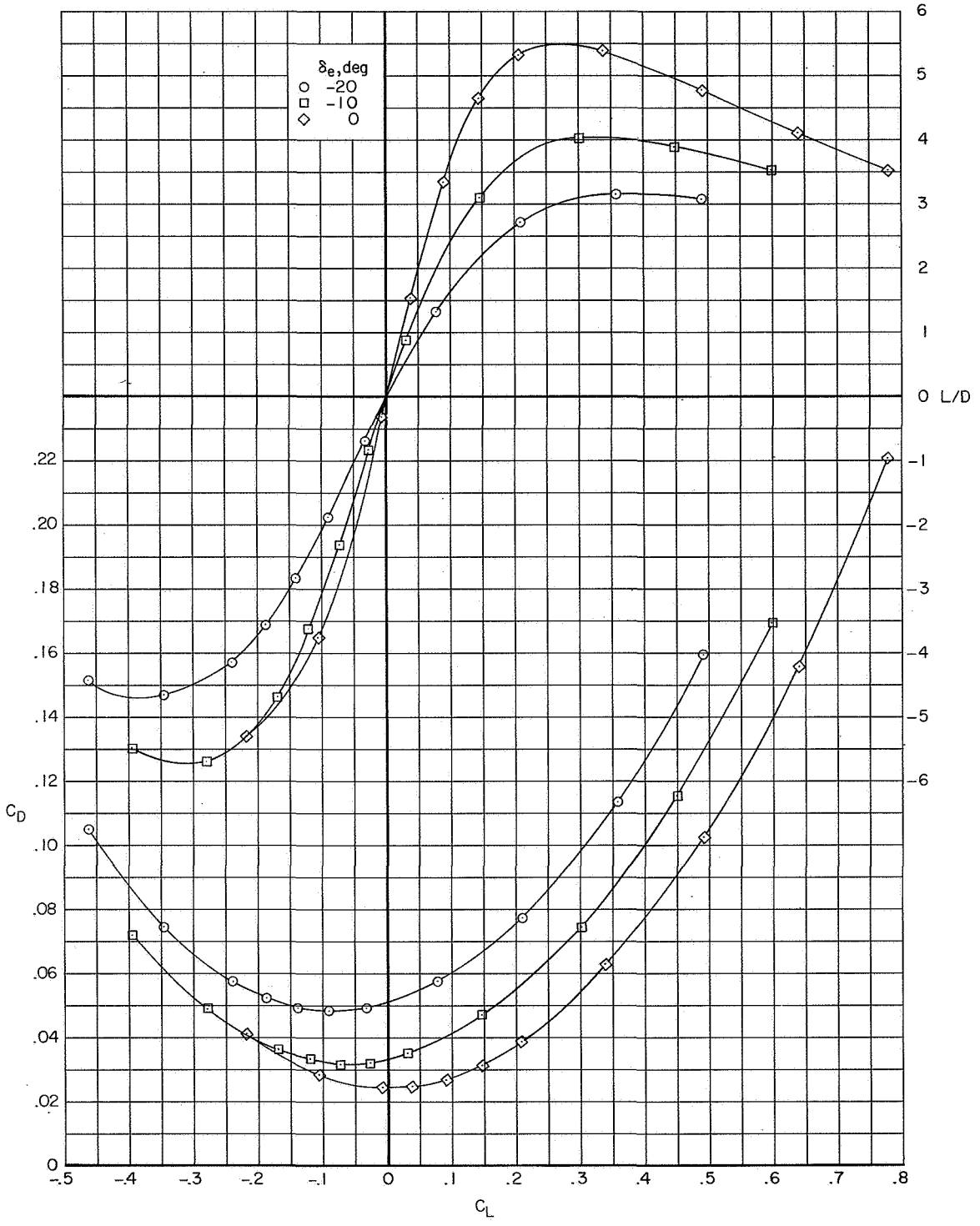

(b) Concluded.

Figure 8.- Continued.

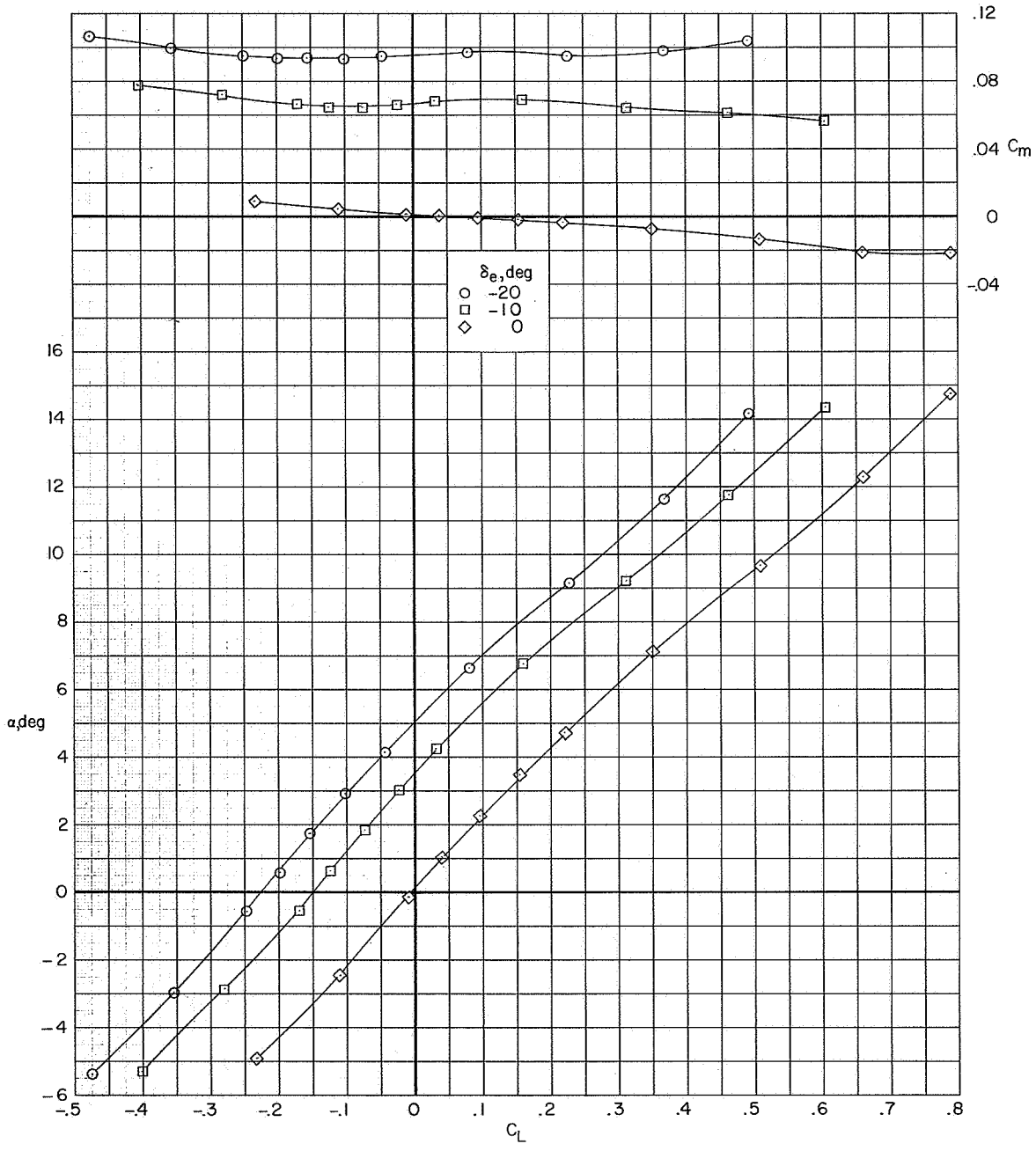

(c) M = 0.93.

Figure 8.- Continued.

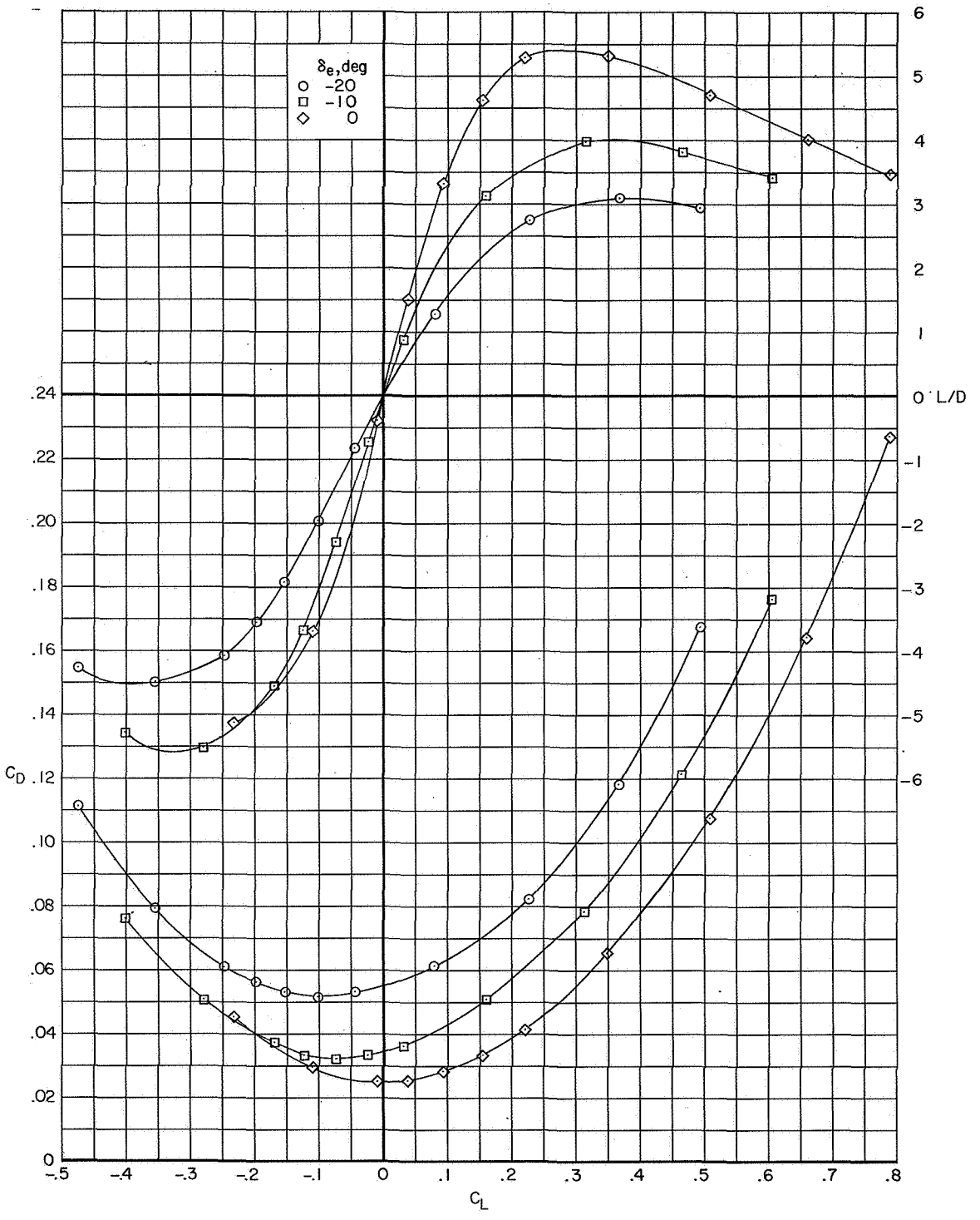

(c) Concluded.

Figure 8.- Continued.

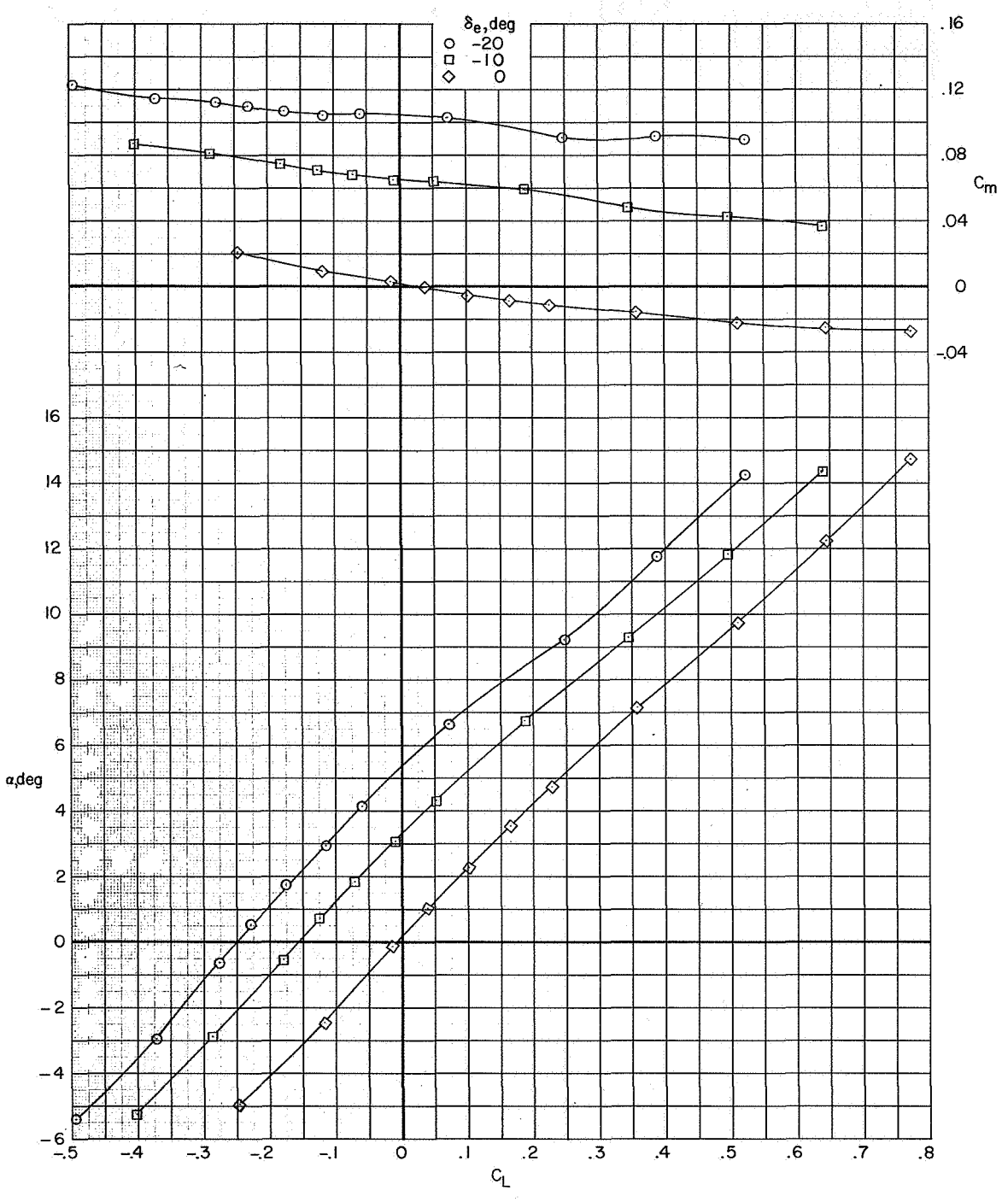

(d) M = 0.96.

Figure 8.- Continued.

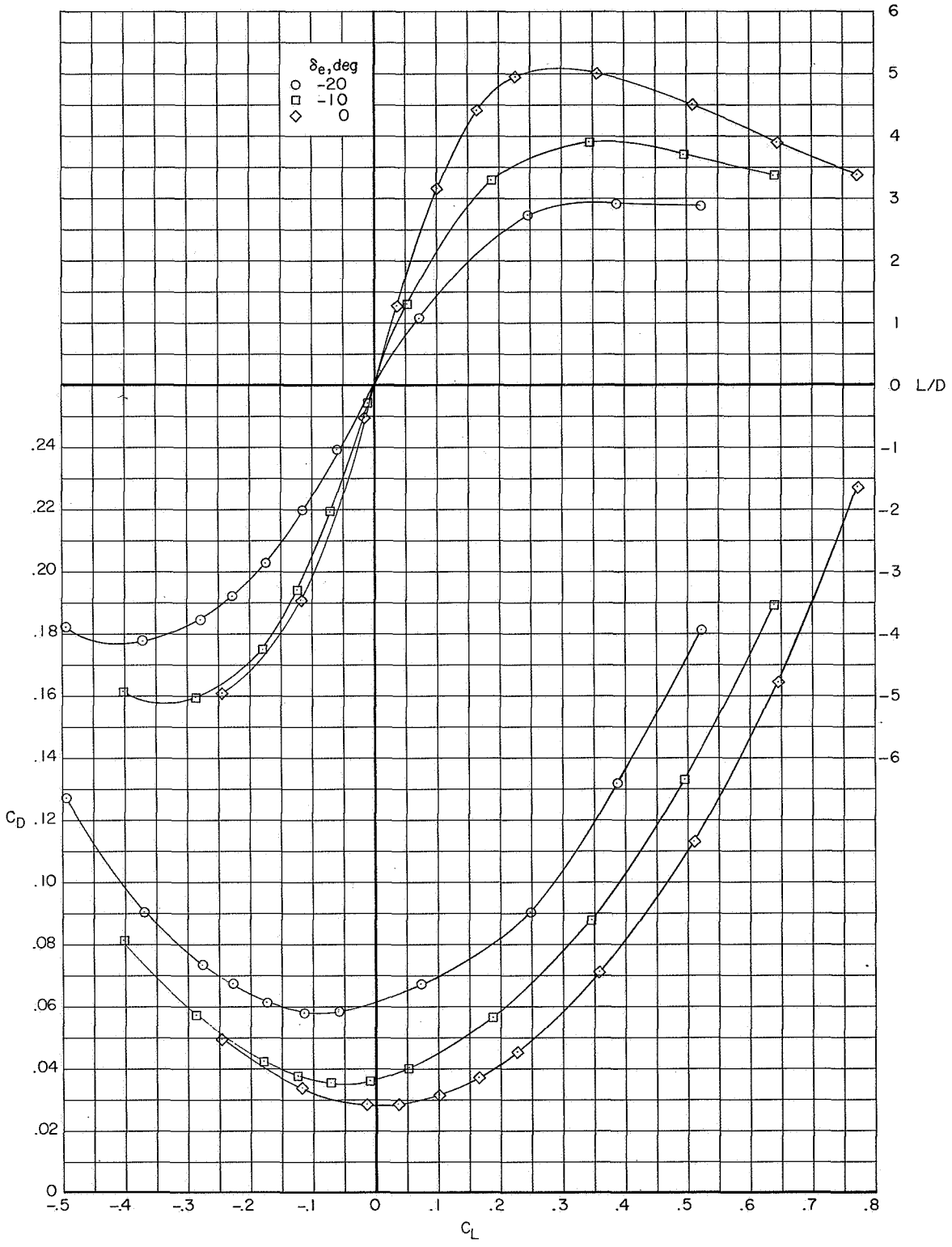

(d) Concluded.

Figure 8.- Continued.

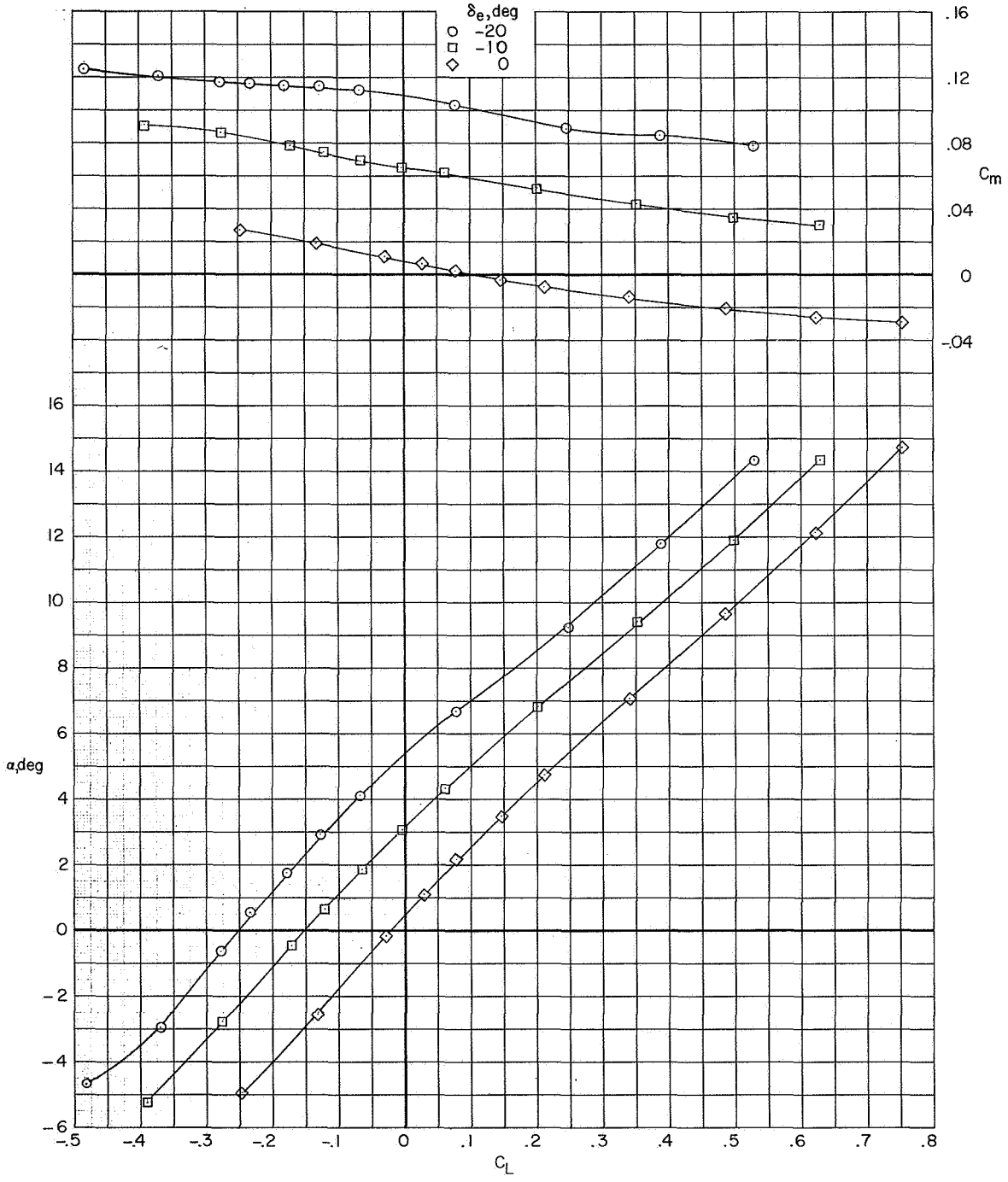

(e) M = 1.00.

Figure 8.- Continued.

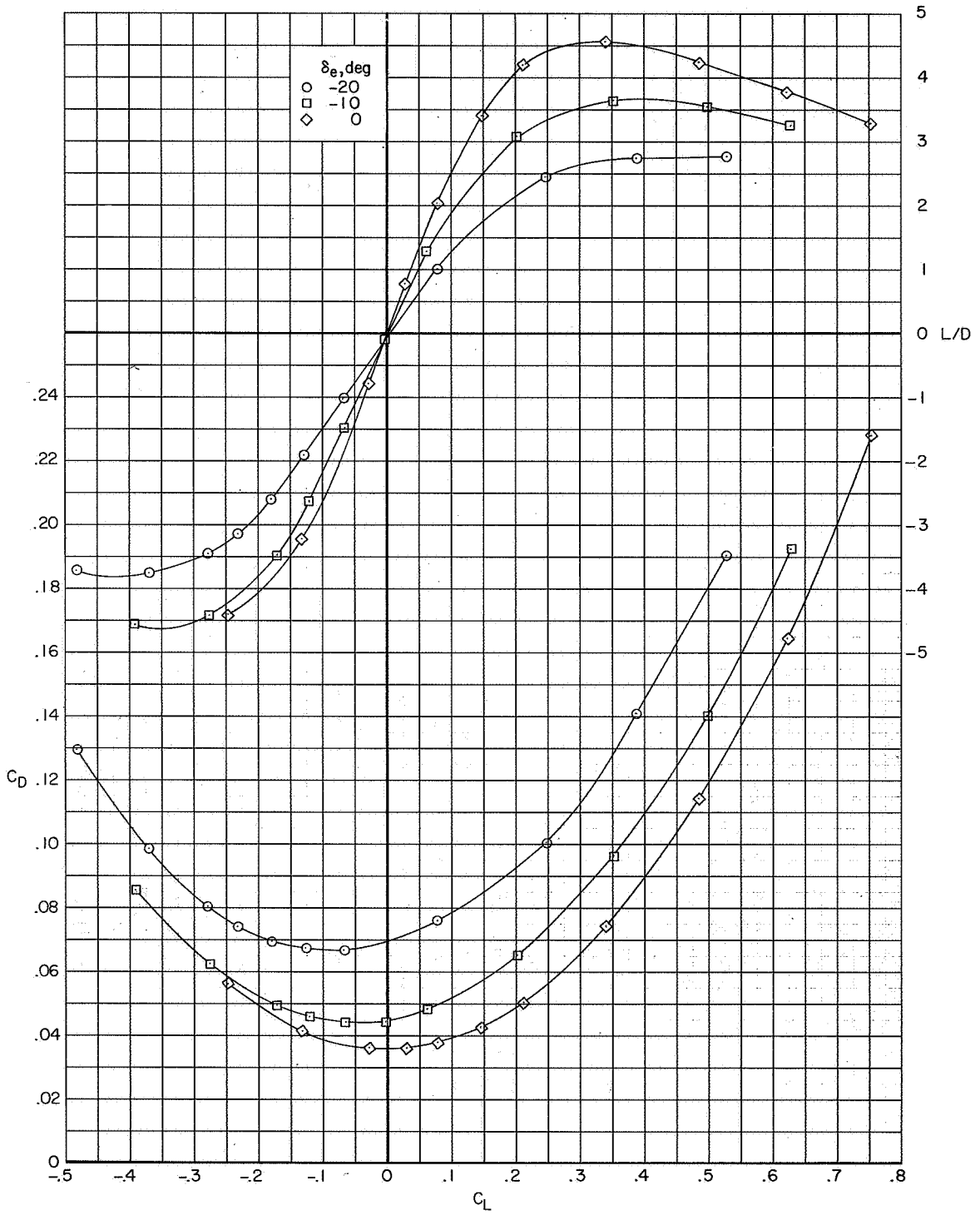

(e) Concluded.

Figure 8.- Continued.

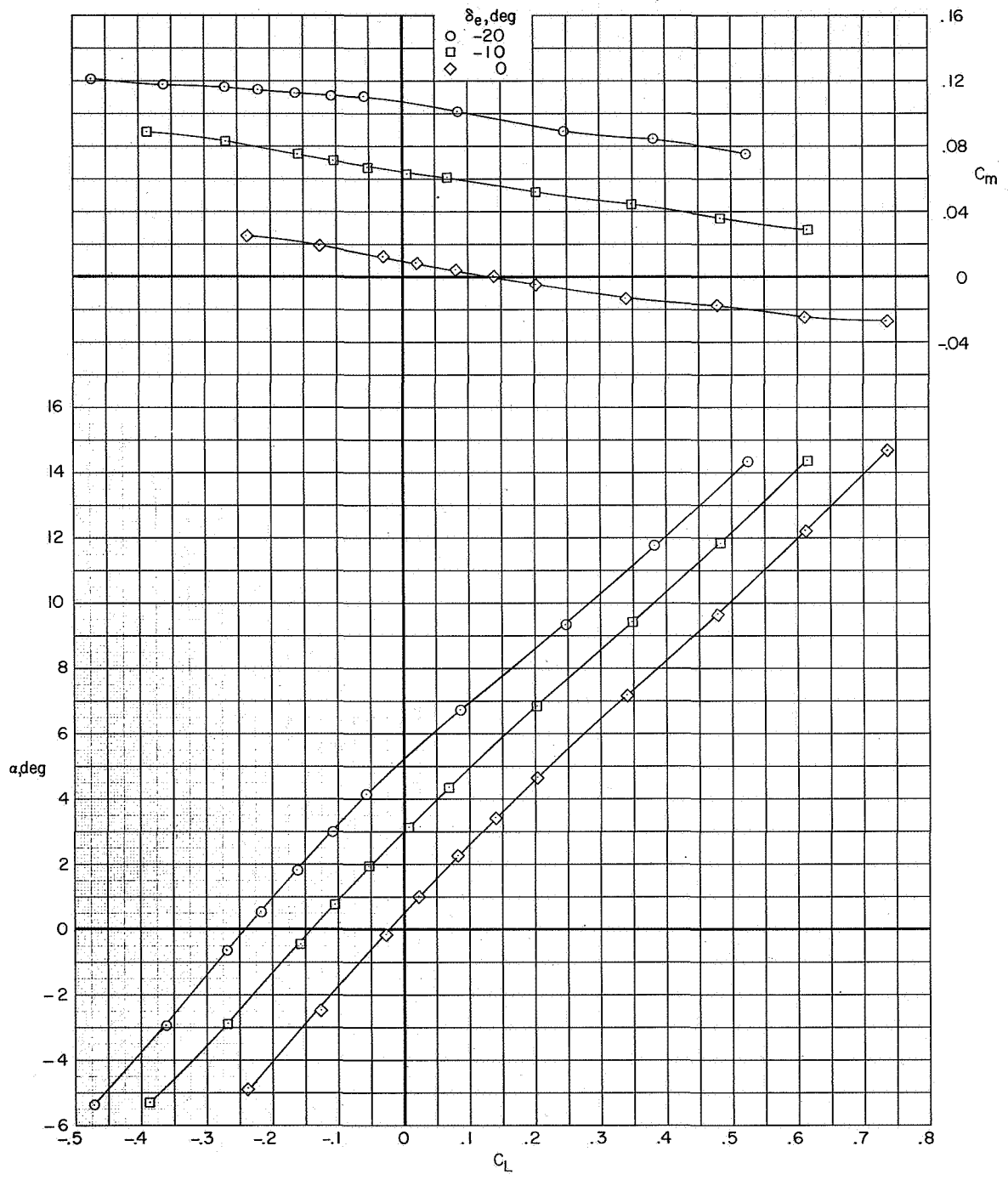

(f) M = 1.03.

Figure 8.- Continued.

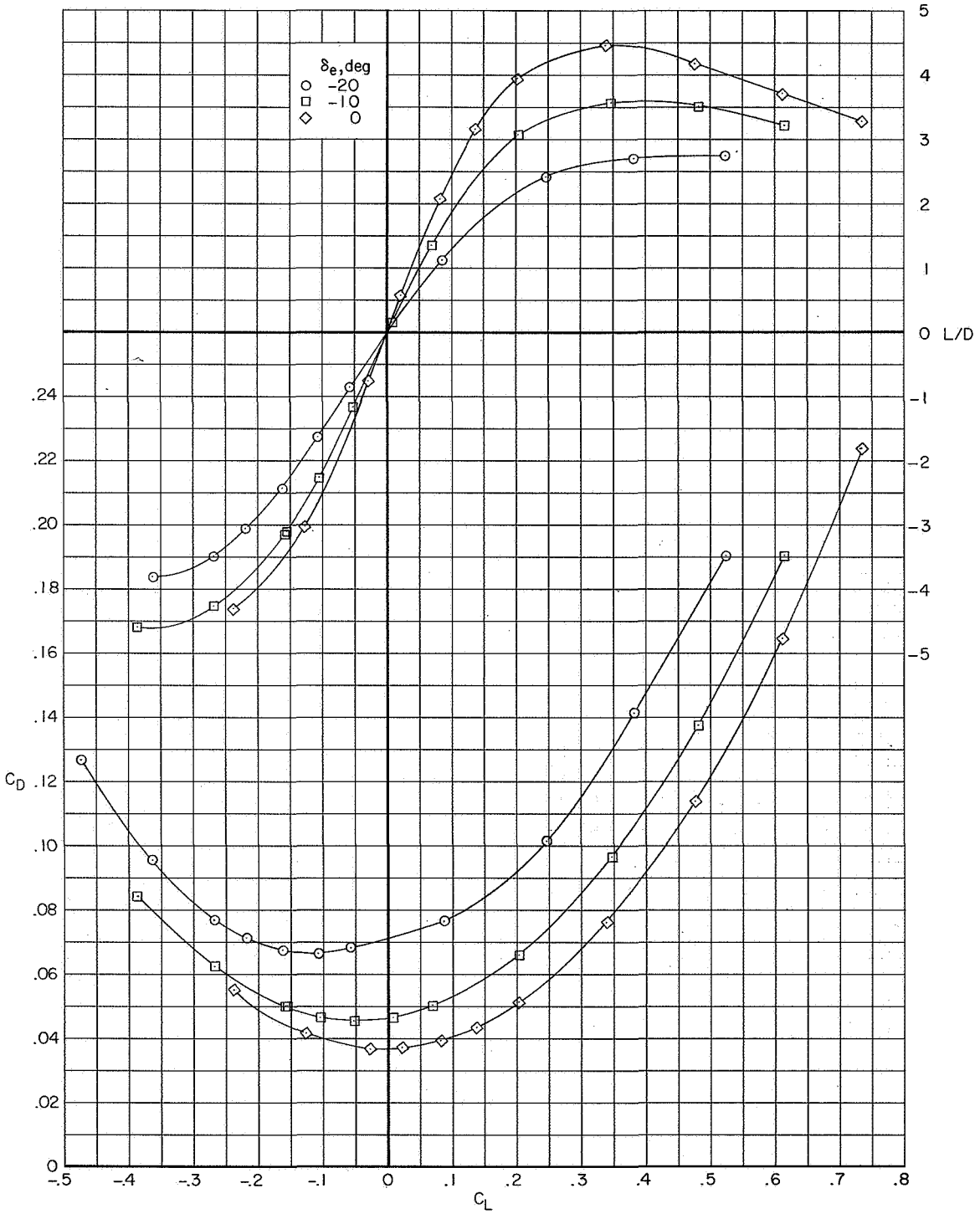

(f) Concluded.

Figure 8.- Continued.

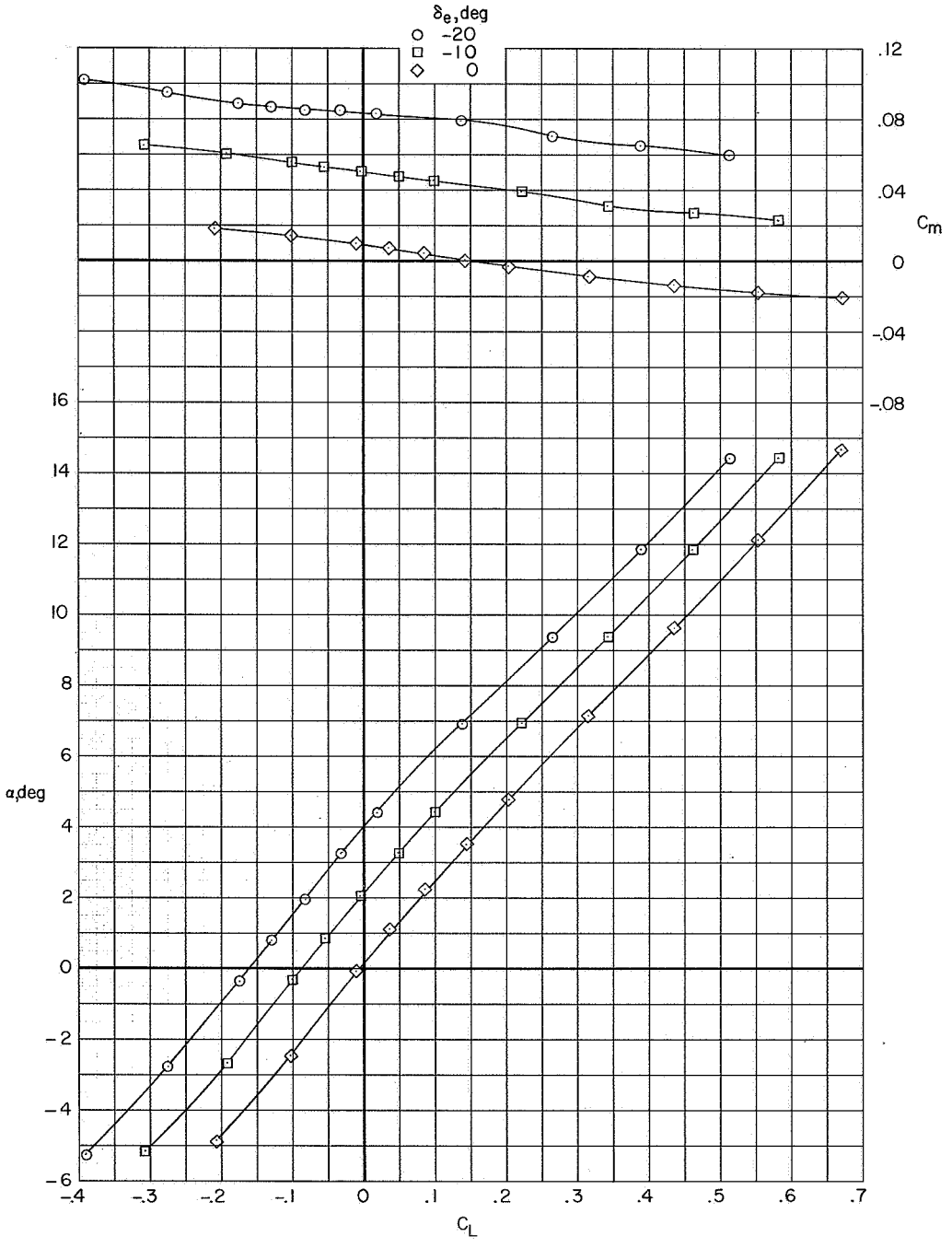

(g) M = 1.20.

Figure 8.- Continued.

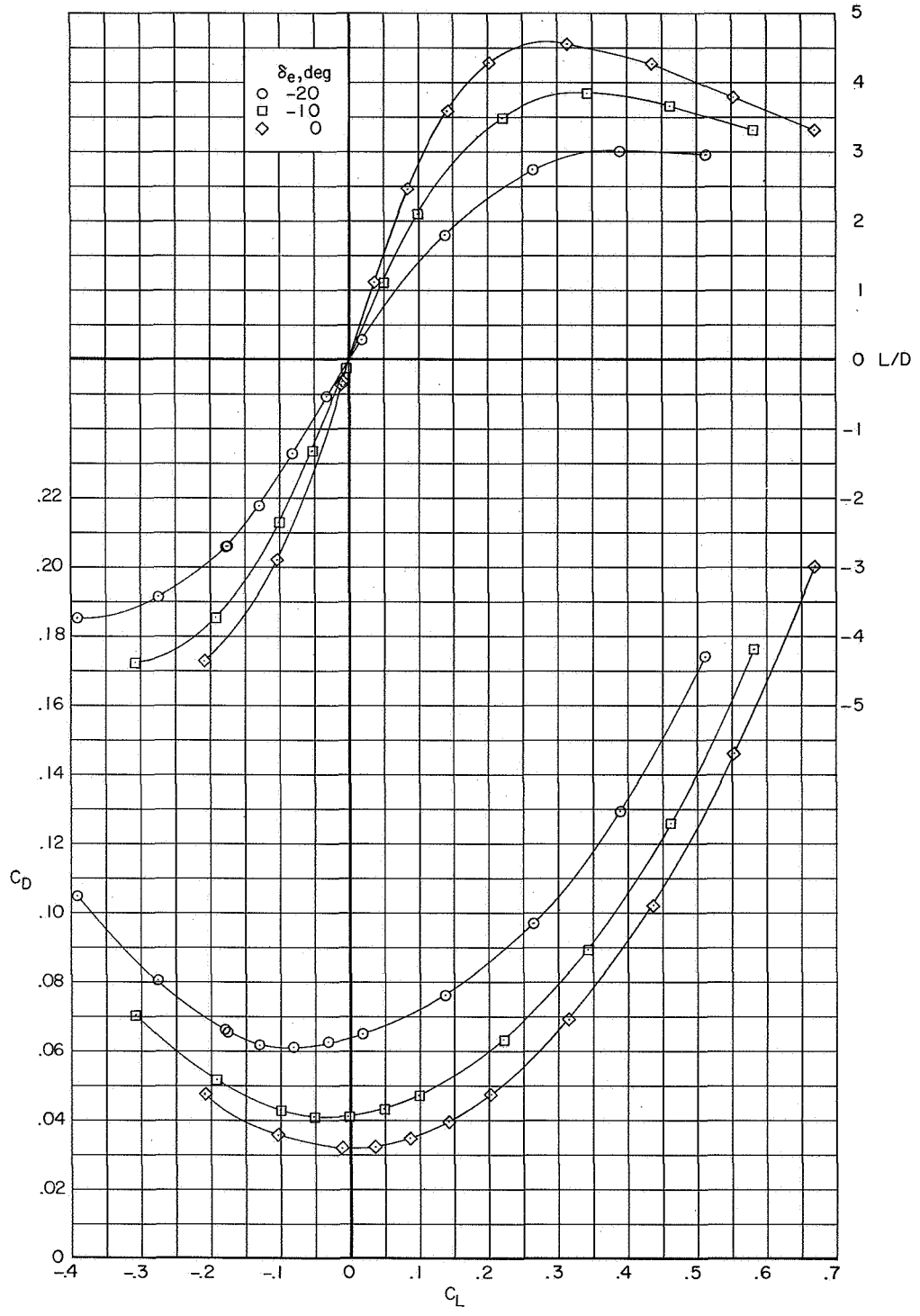

(g) Concluded.

Figure 8.- Concluded.

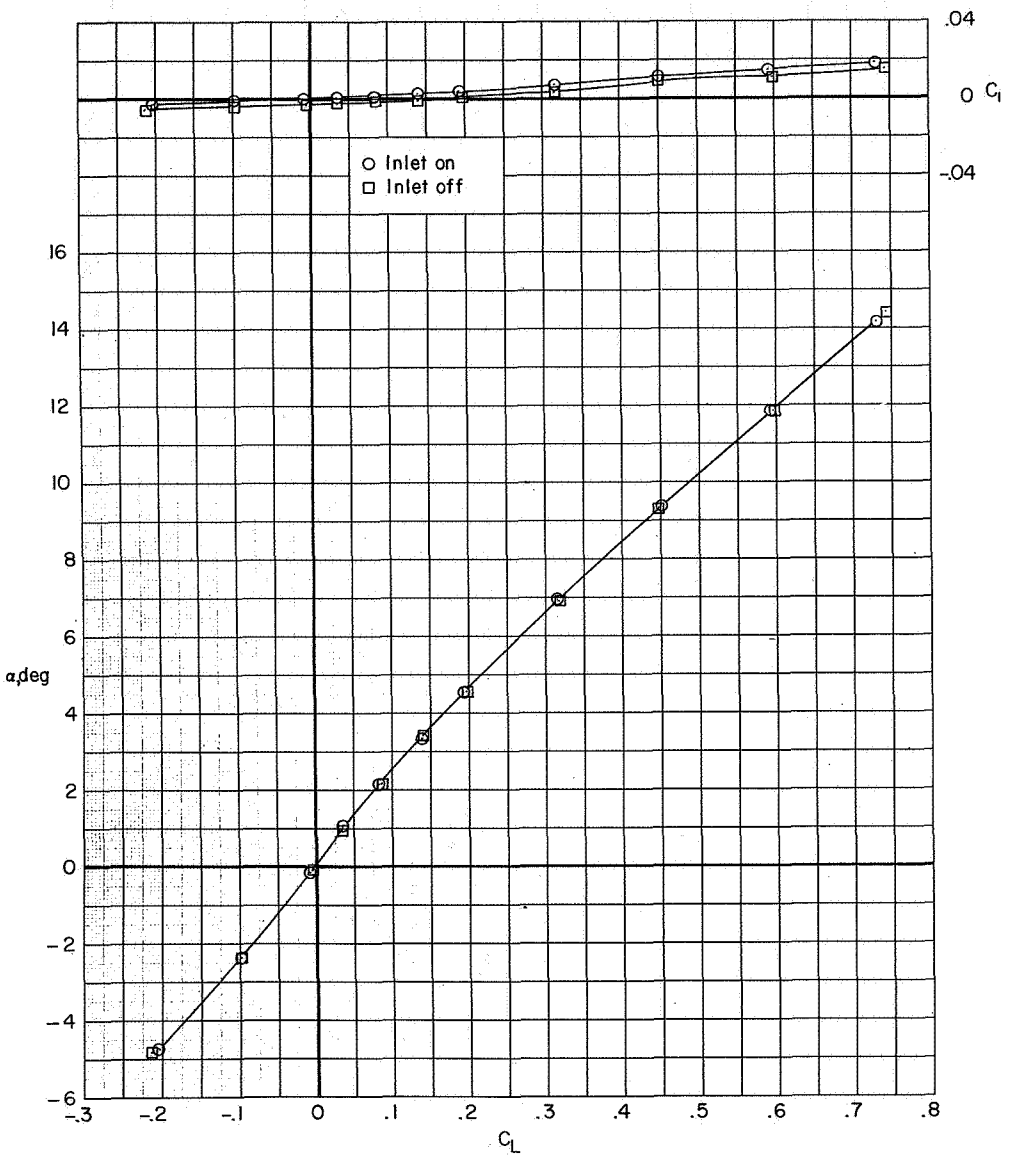

(a) M = 0.80.

Figure 9.- Inlet effects on the longitudinal aerodynamic characteristics of configuration BWB. $\delta_e = 0^0$.

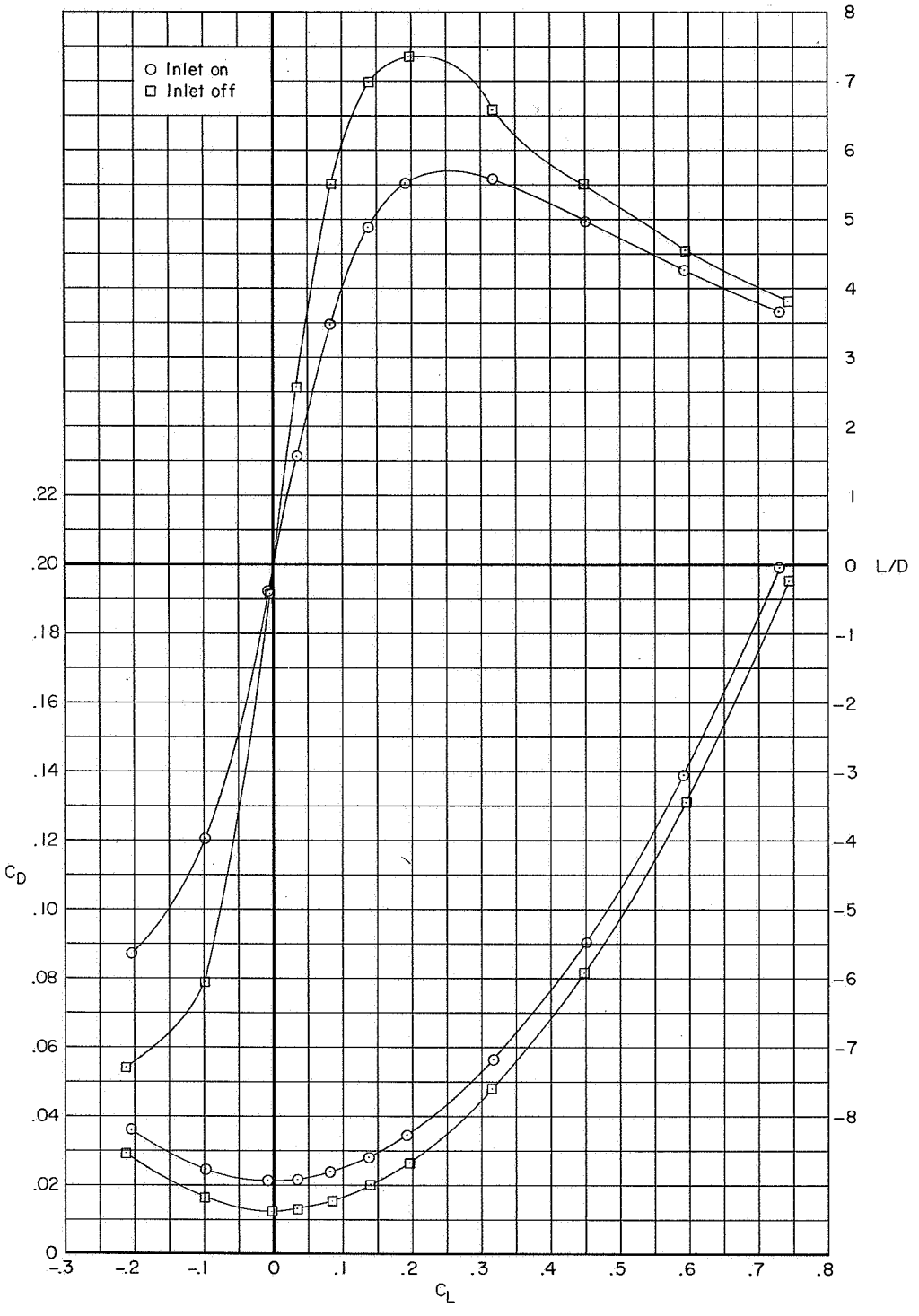

(a) Concluded.

Figure 9.- Continued.

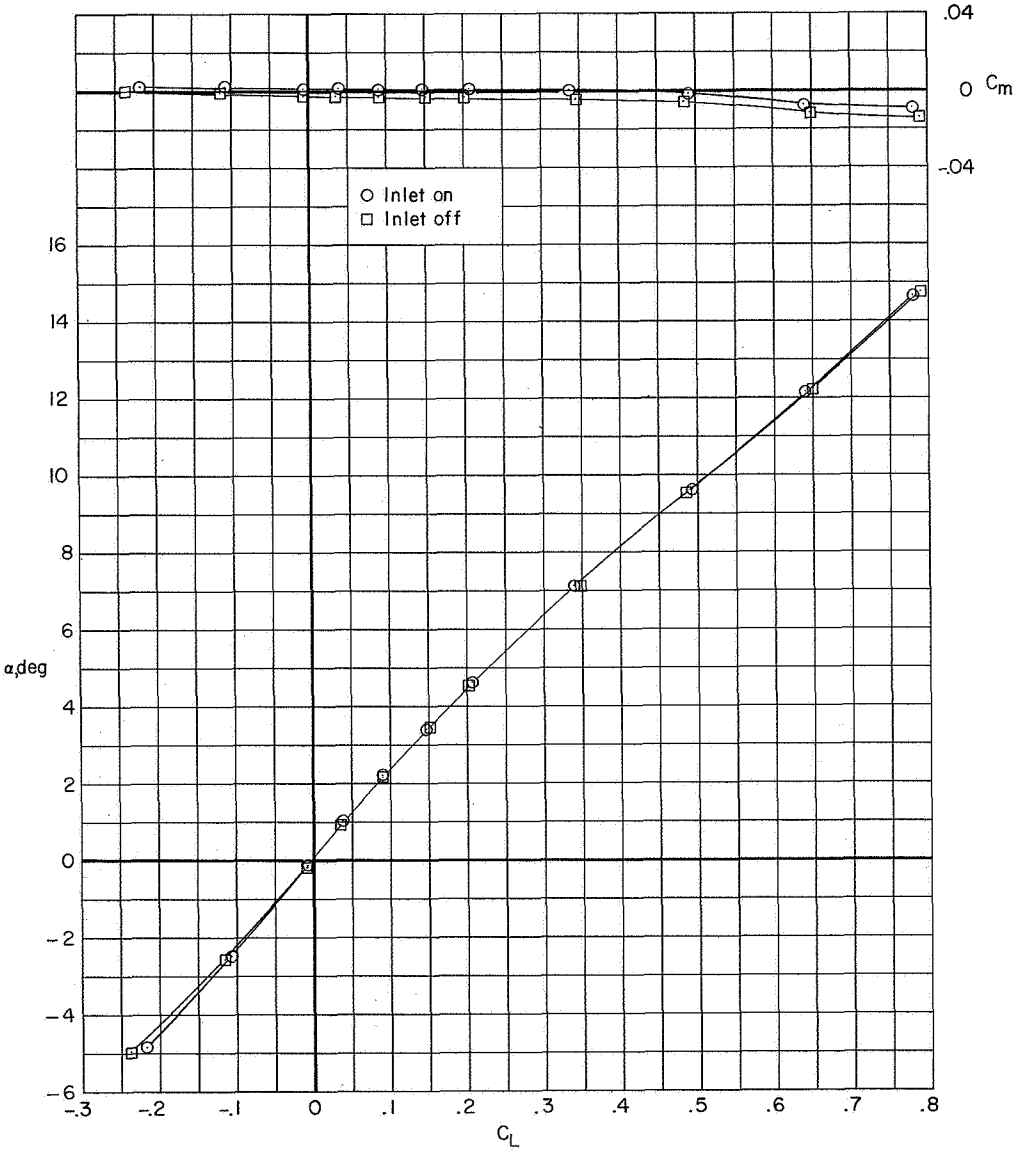

(b) M = 0.90.

Figure 9.- Continued.

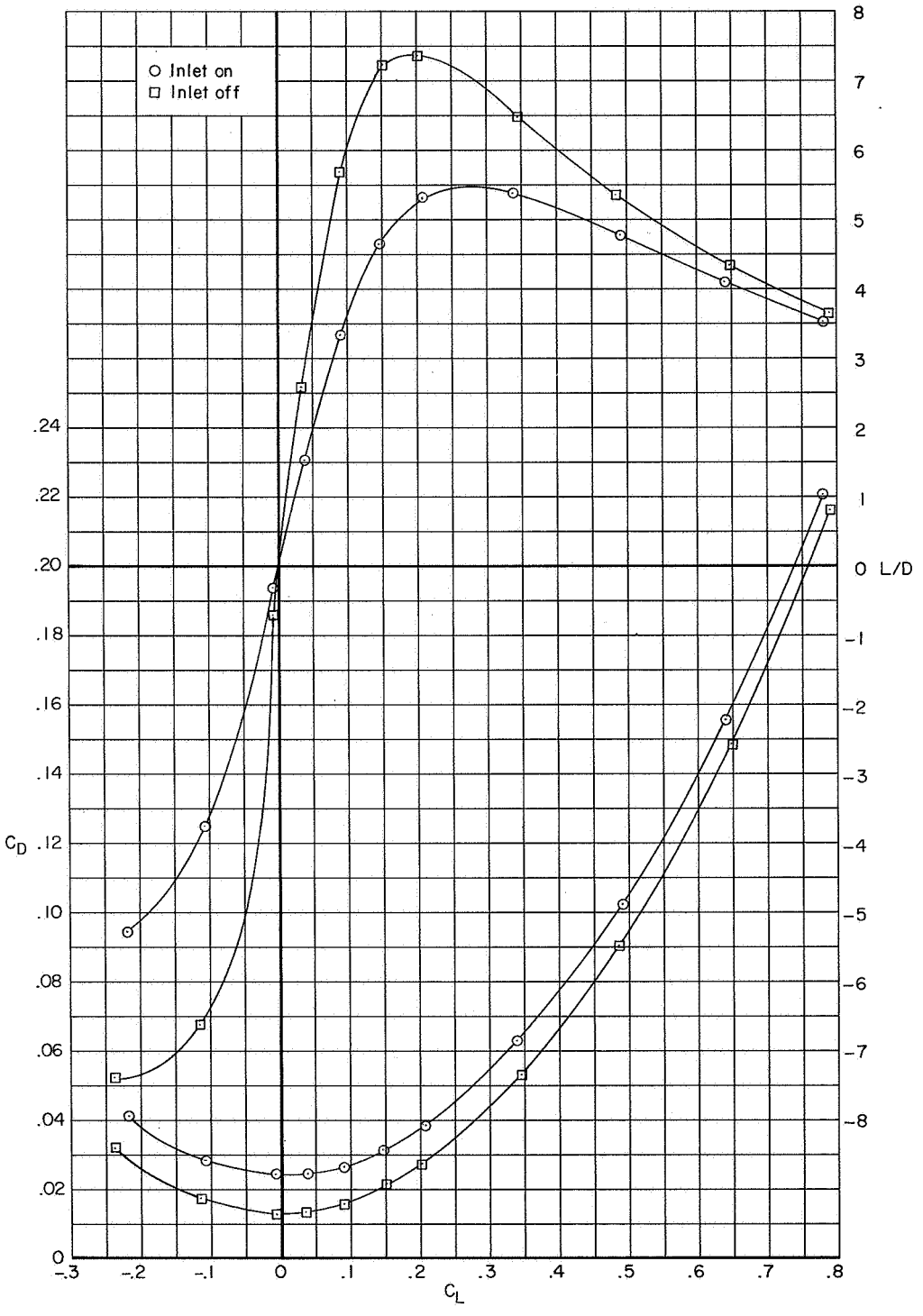

(b) Concluded.

Figure 9.- Continued.

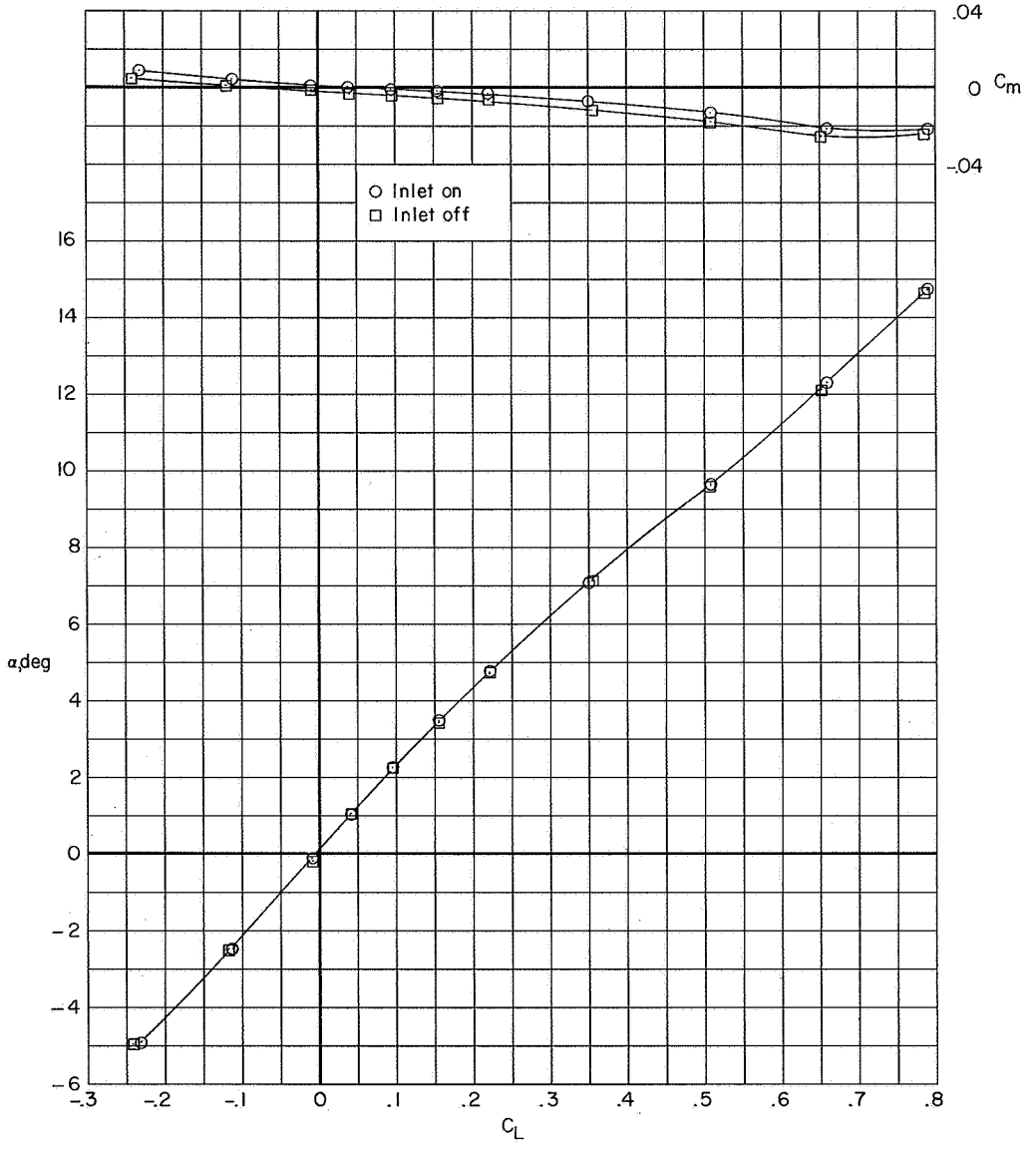

(c) M = 0.93.

Figure 9.- Continued.

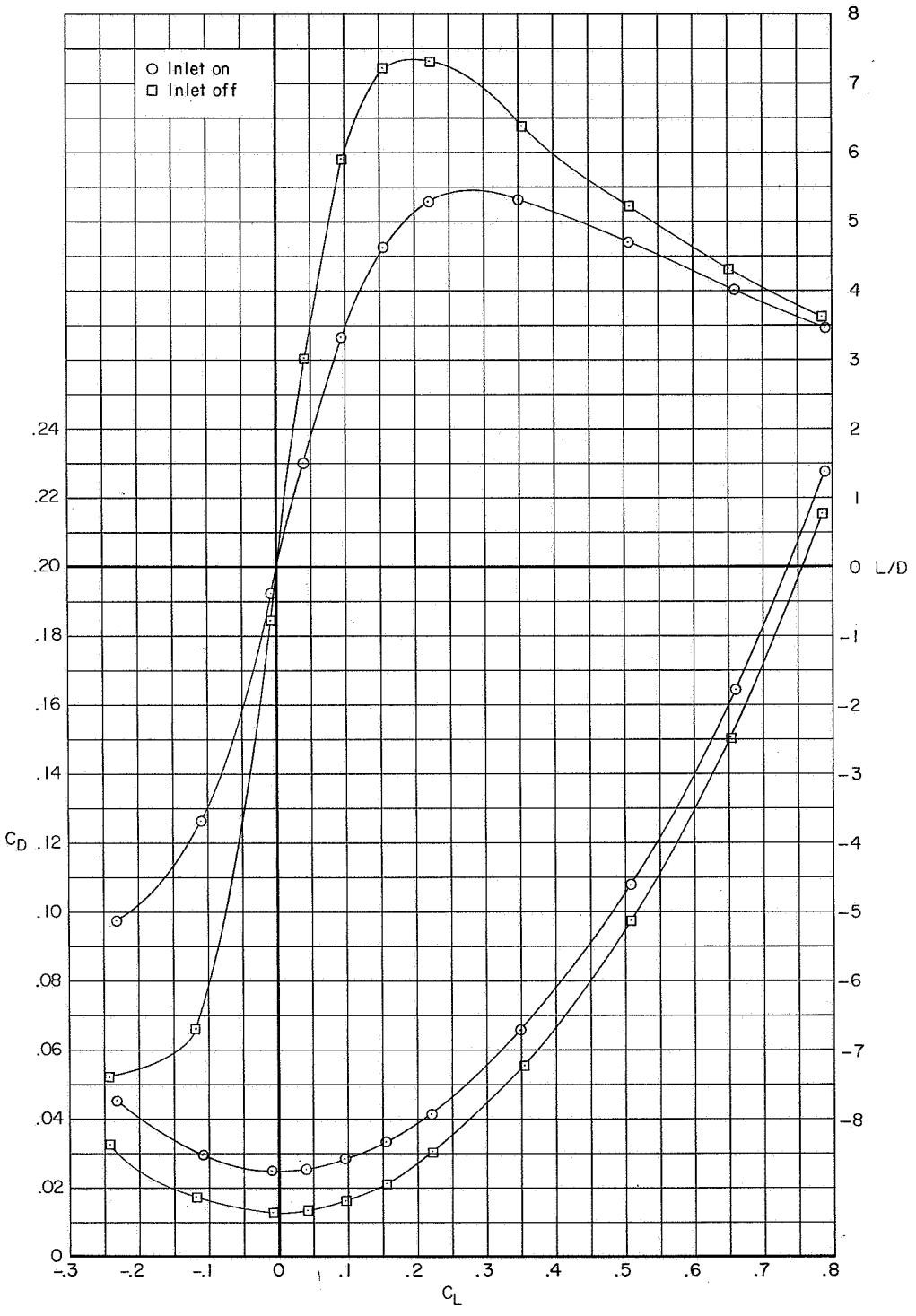

(c) Concluded.

Figure 9.- Continued.

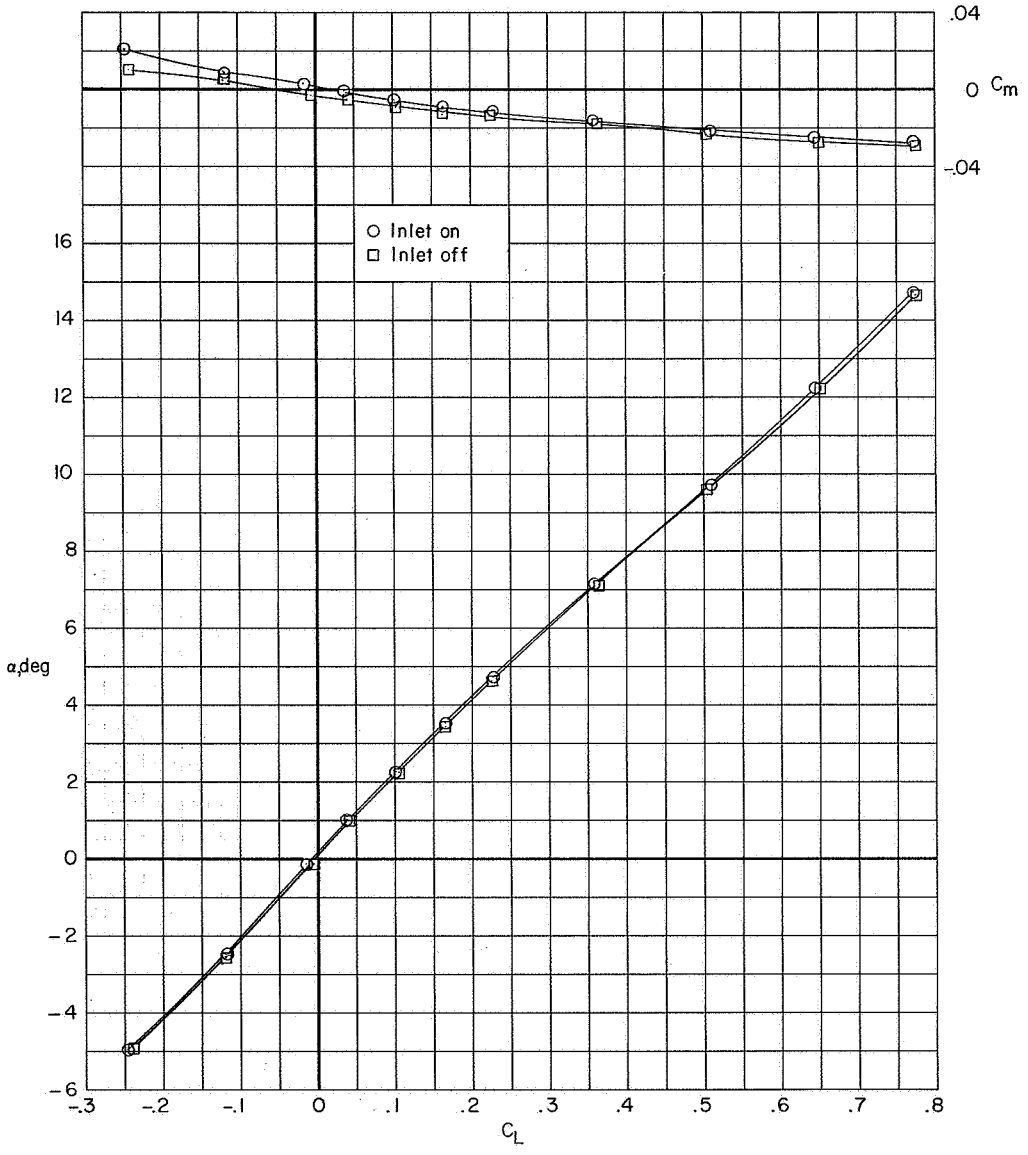

(d) M = 0.96.

Figure 9.- Continued.

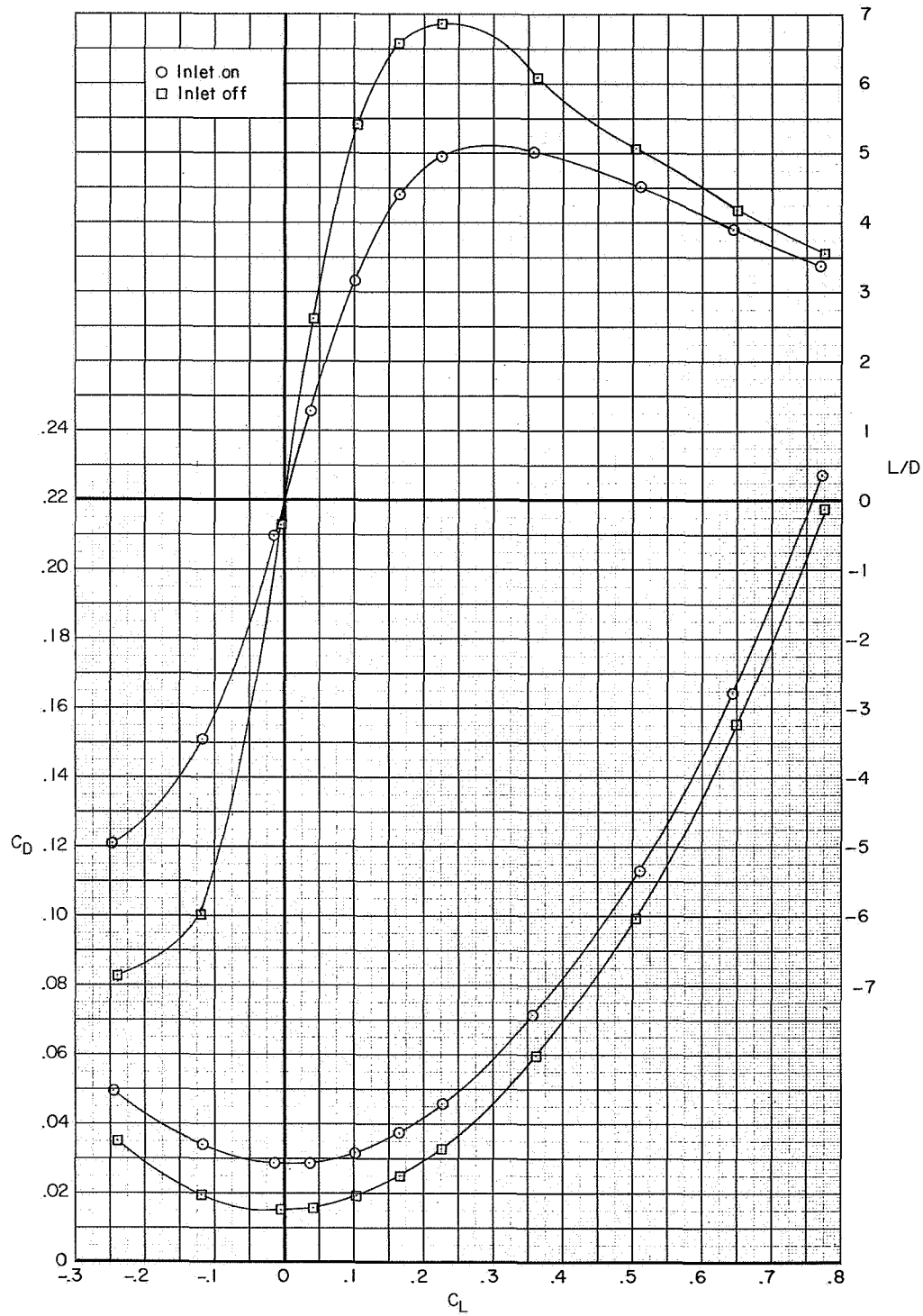

(d) Concluded.

Figure 9.- Continued.

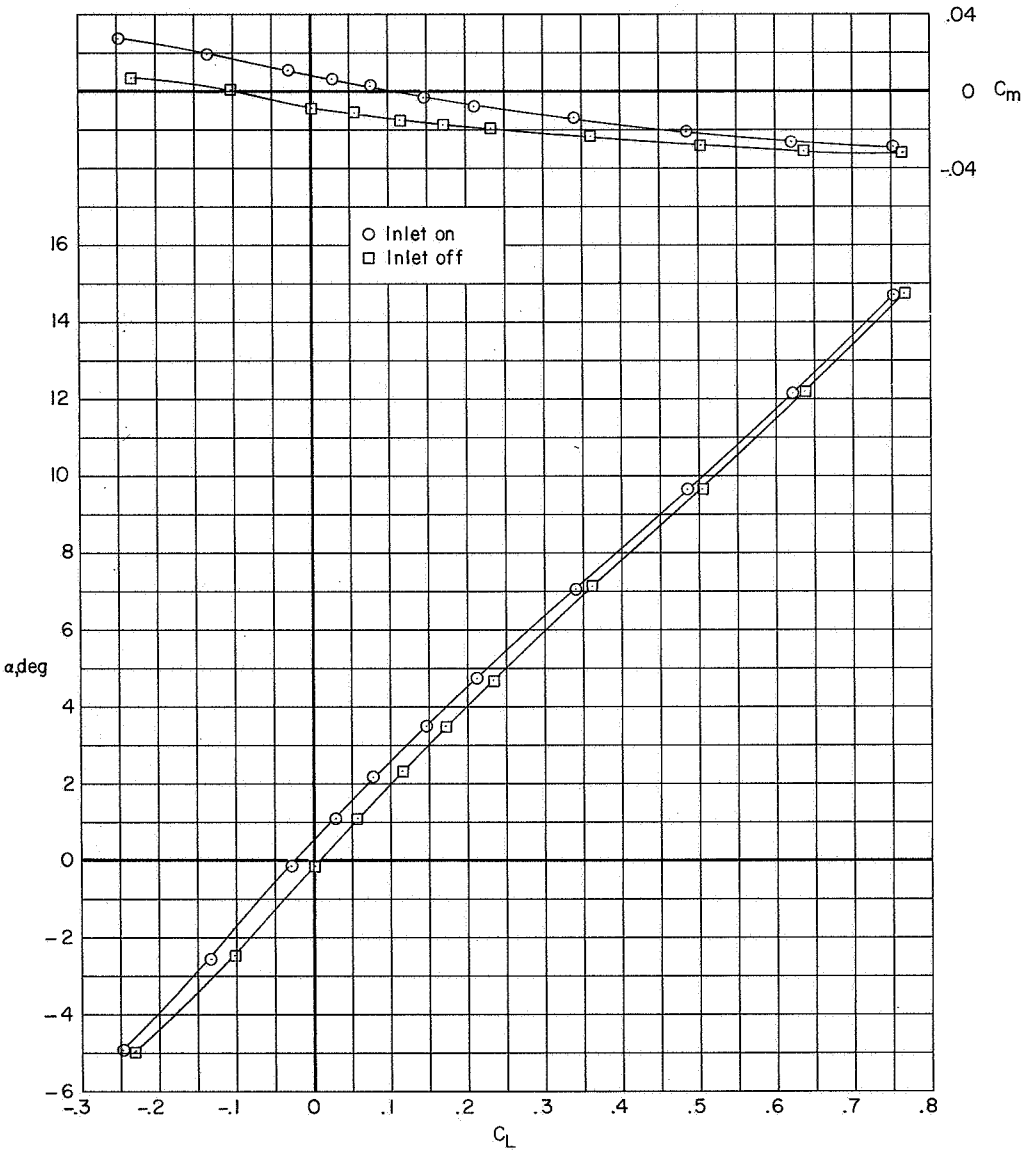

(e) M = 1.00.

Figure 9.- Continued.

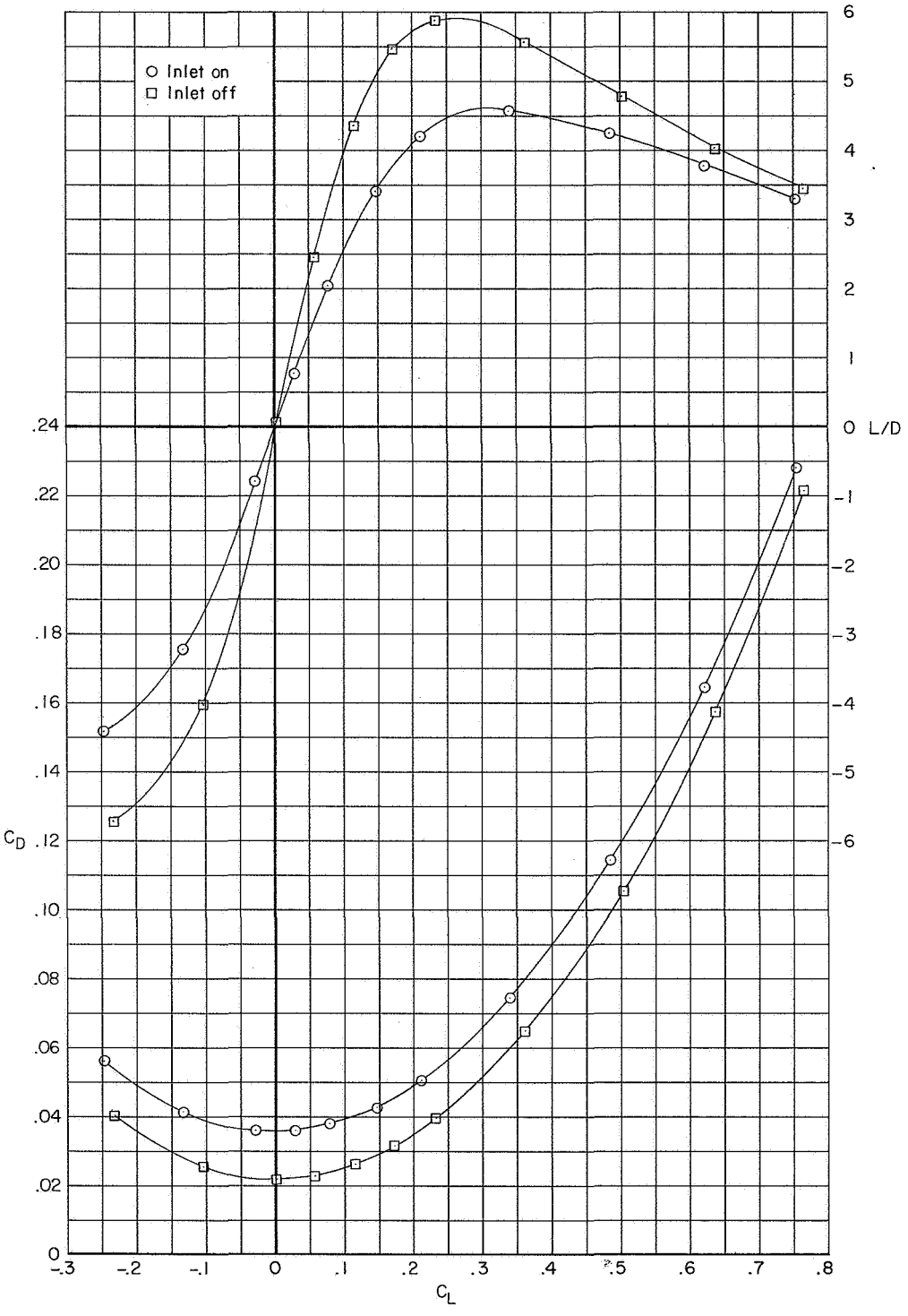

(e) Concluded.

Figure 9.- Continued.

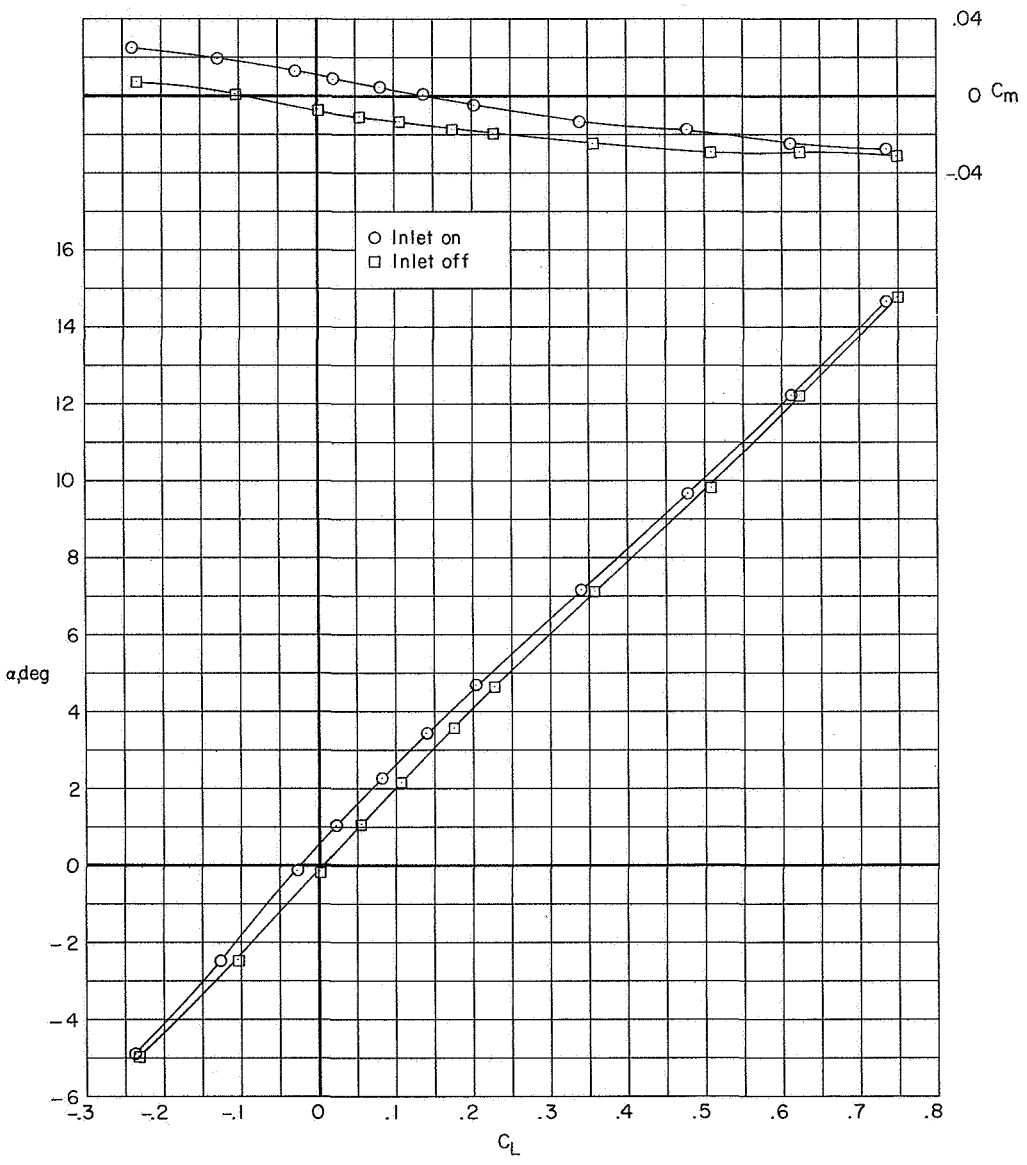

(f) M = 1.03.

Figure 9.- Continued.

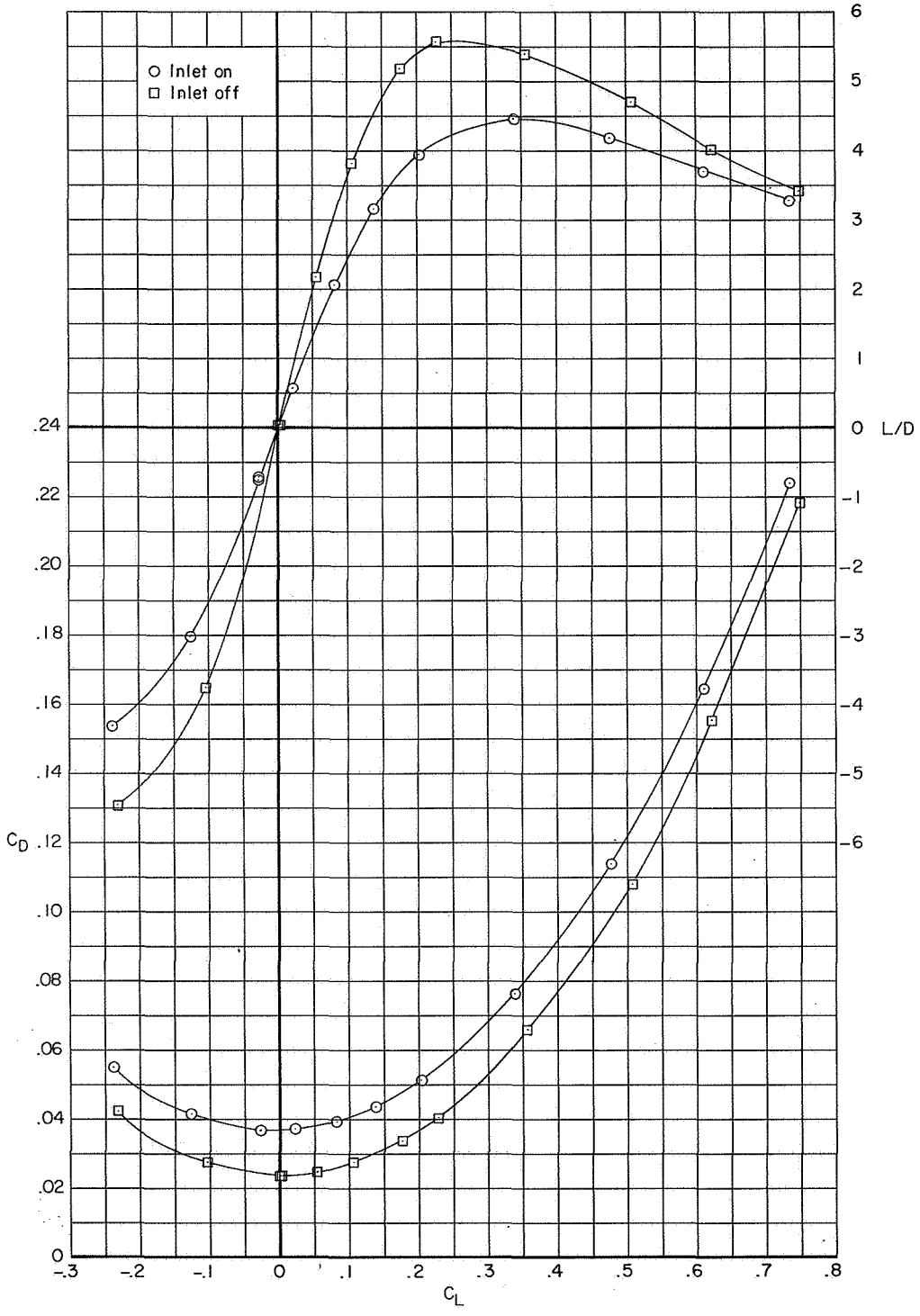

(f) Concluded.

Figure 9.- Continued.

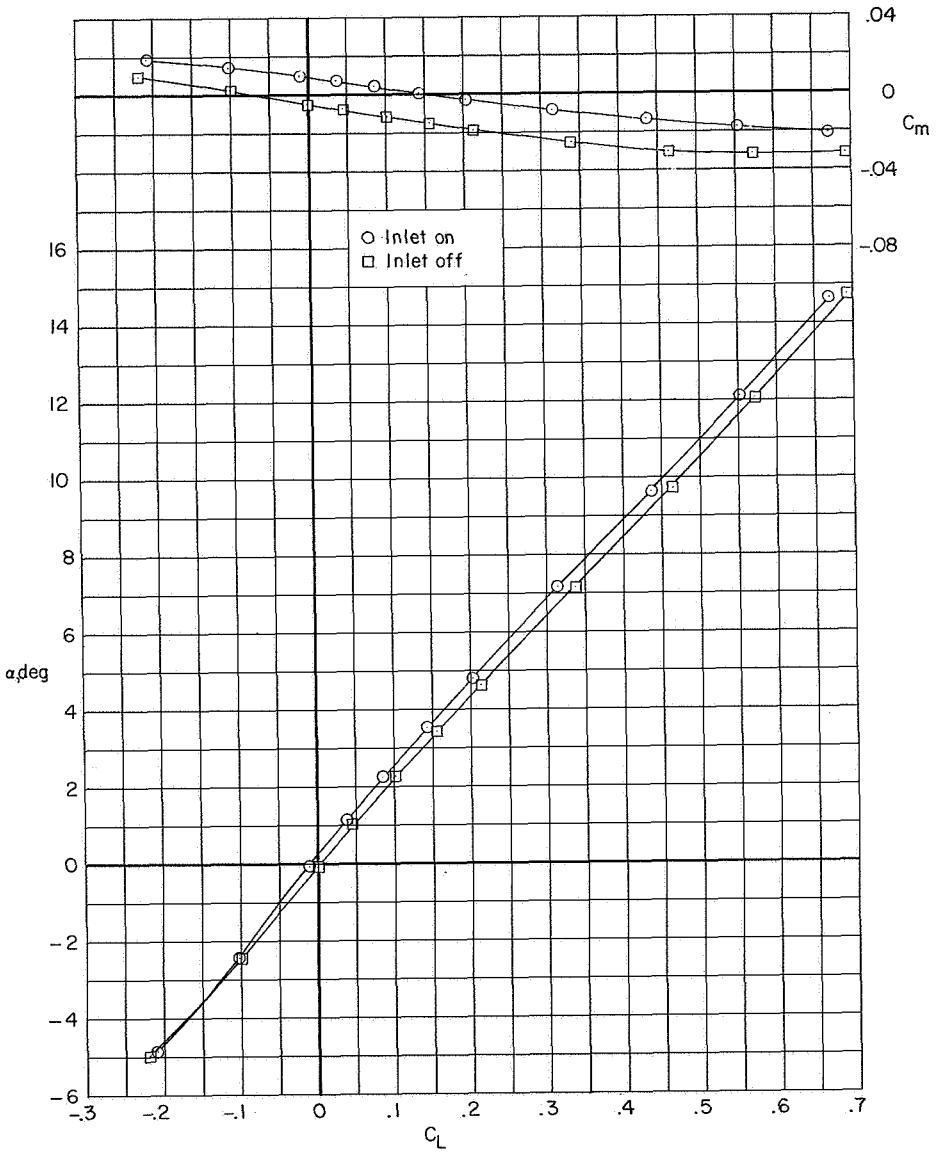

(g) M = 1.20.

Figure 9.- Continued.

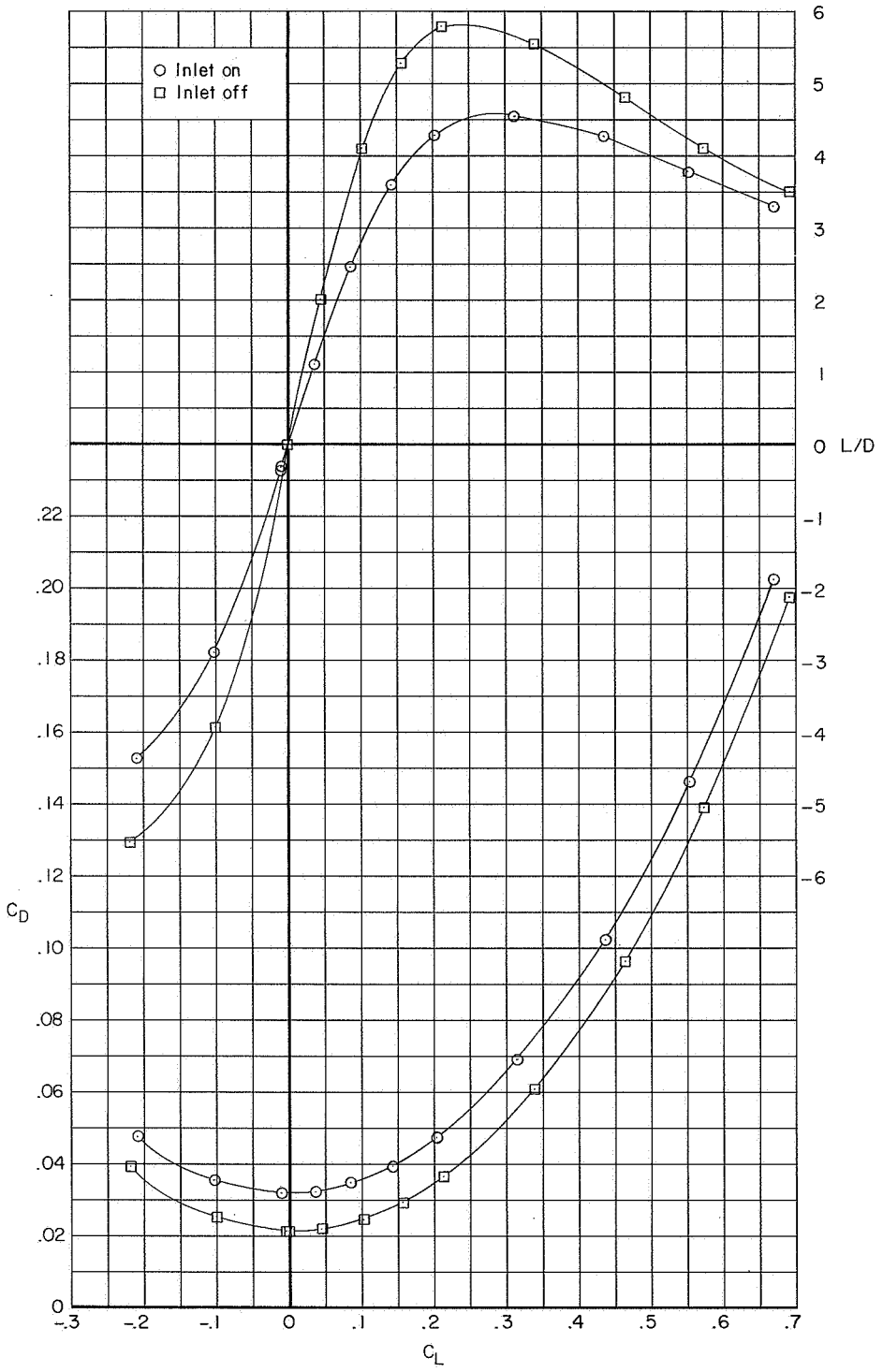

(g) Concluded.

Figure 9.- Concluded.

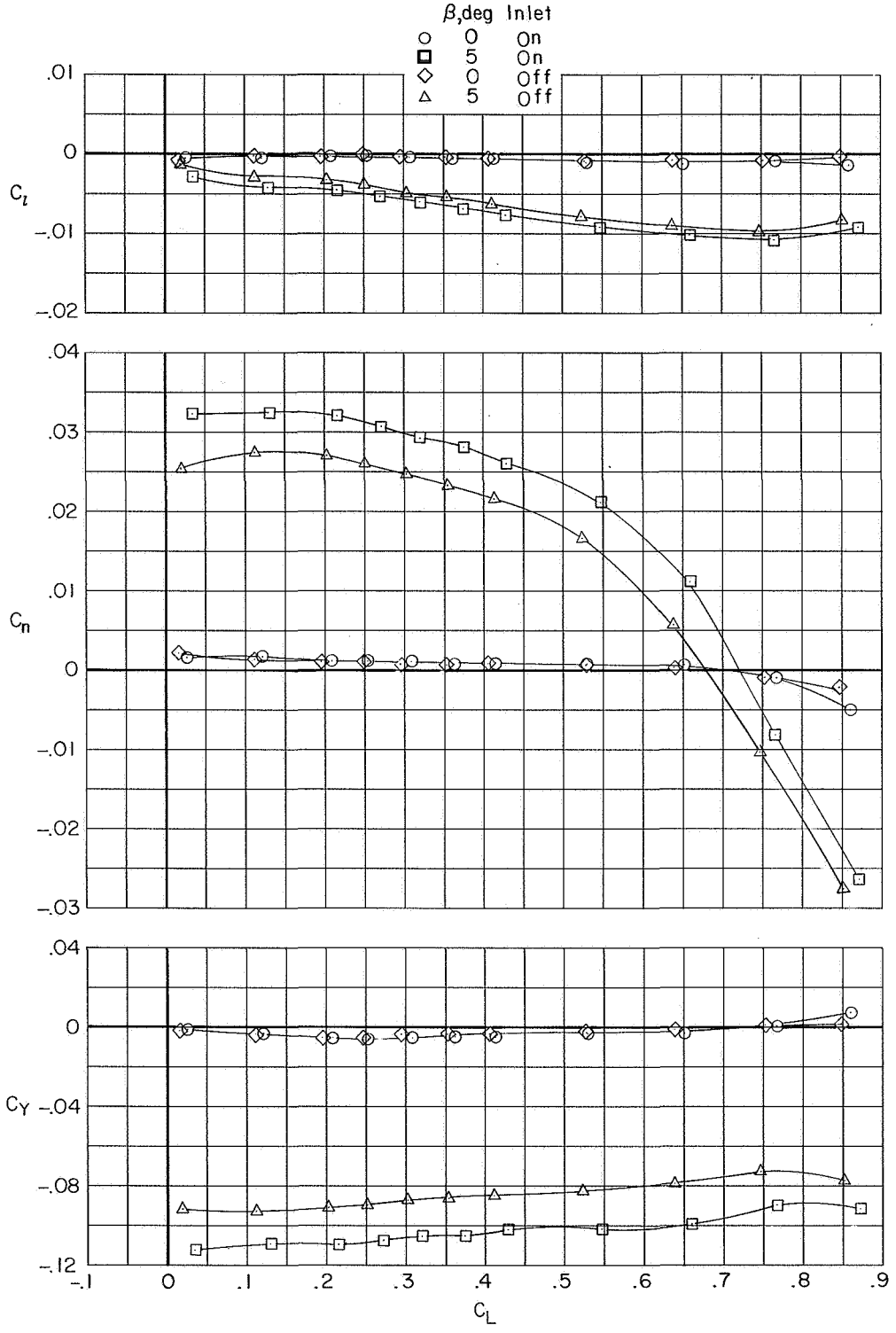

(a) M = 0.80.

Figure 10.- Inlet effects on the lateral aerodynamic characteristics of configuration DWB. Horizontal tail off.

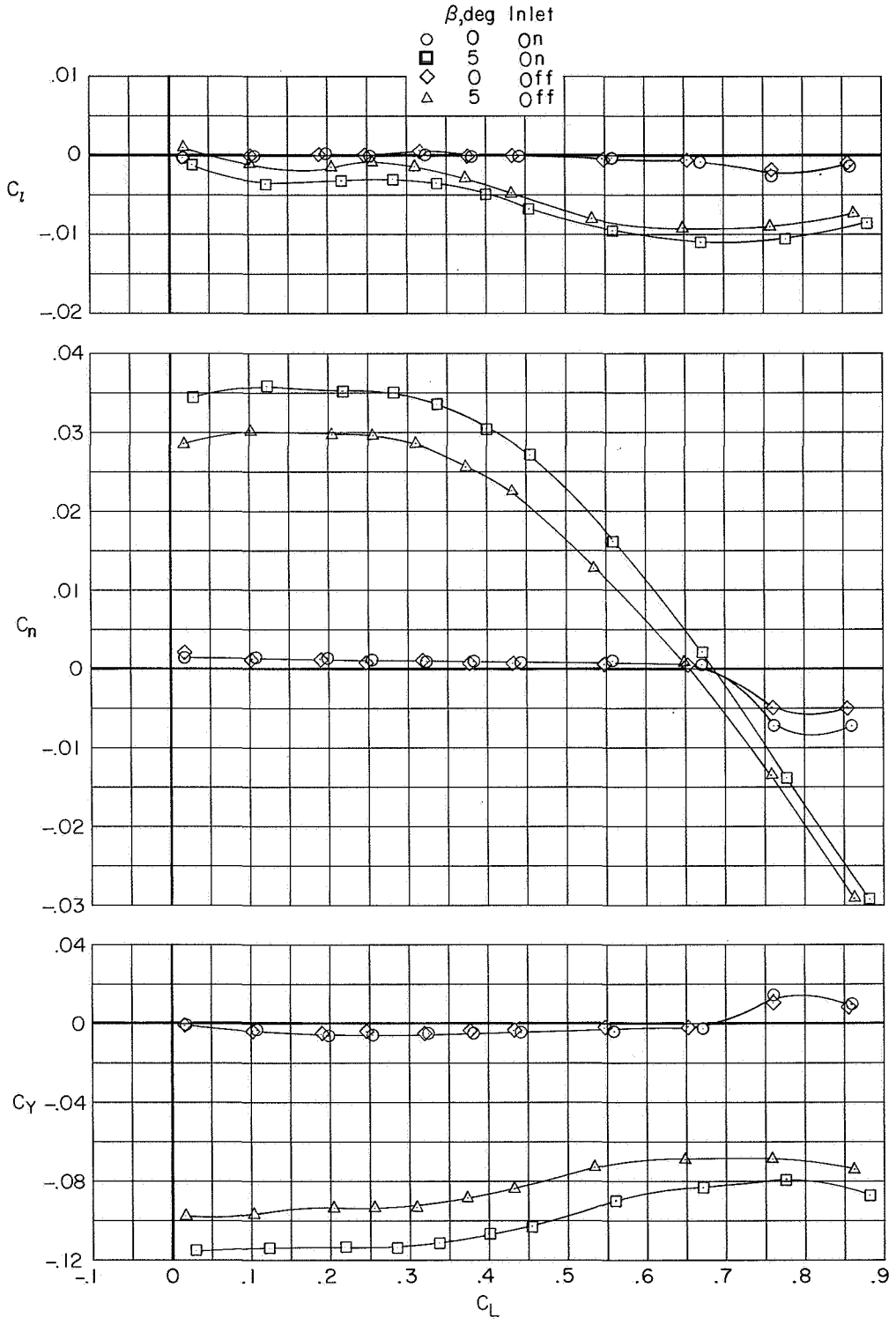

(b) M = 0.90.

Figure 10.- Continued.

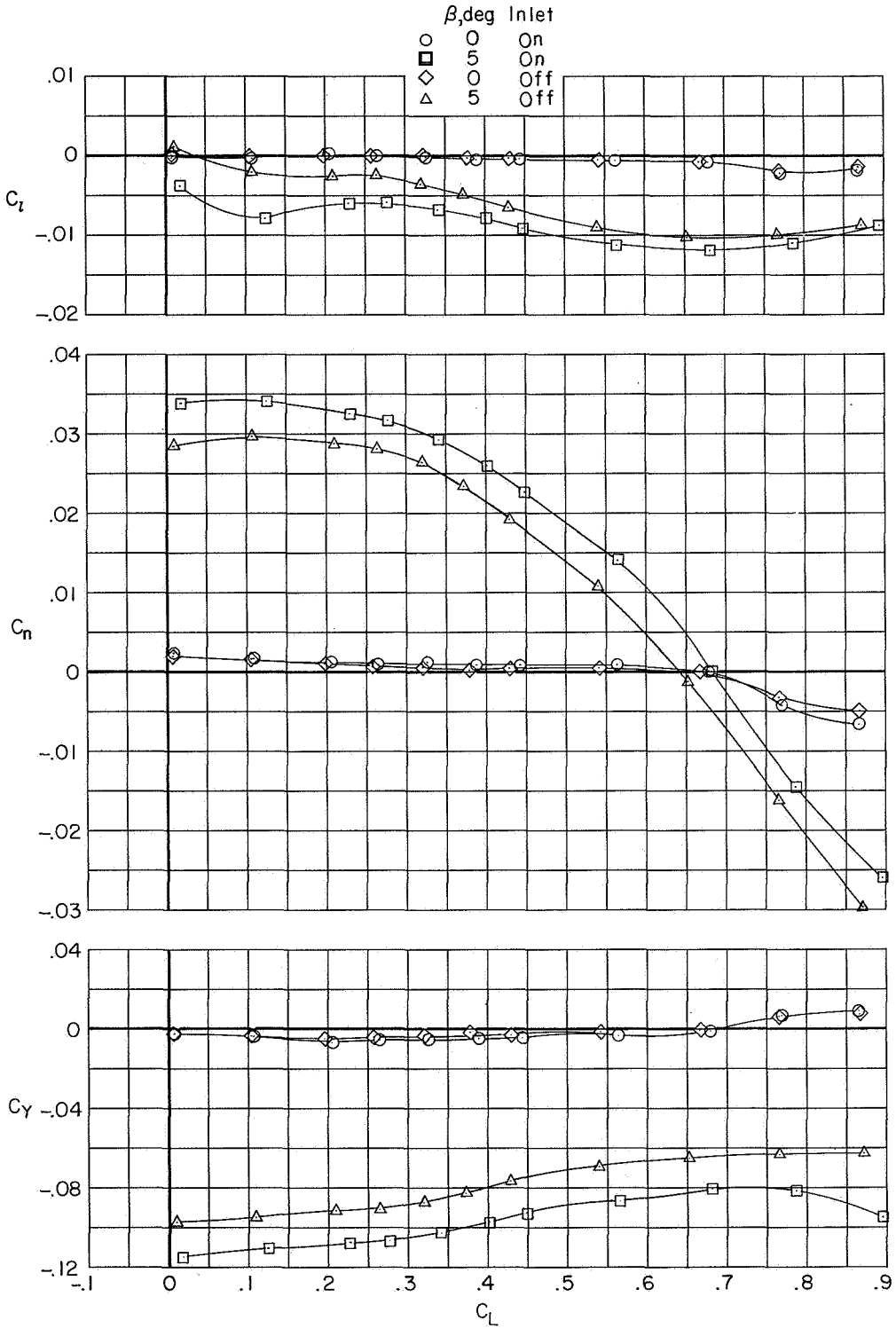

(c) M = 0.93.

Figure 10.- Continued.

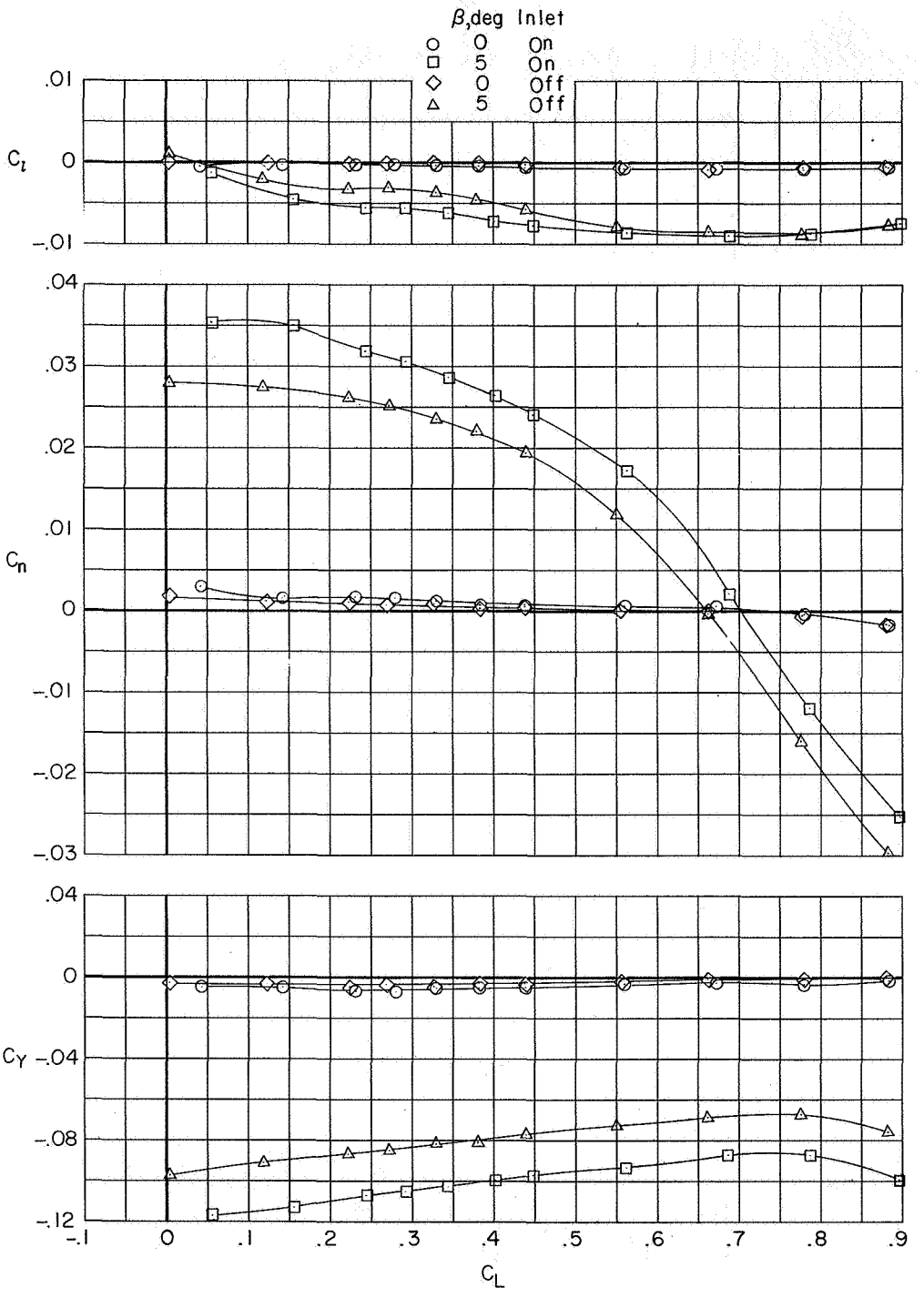

(d) M = 0.96.

Figure 10.- Continued.

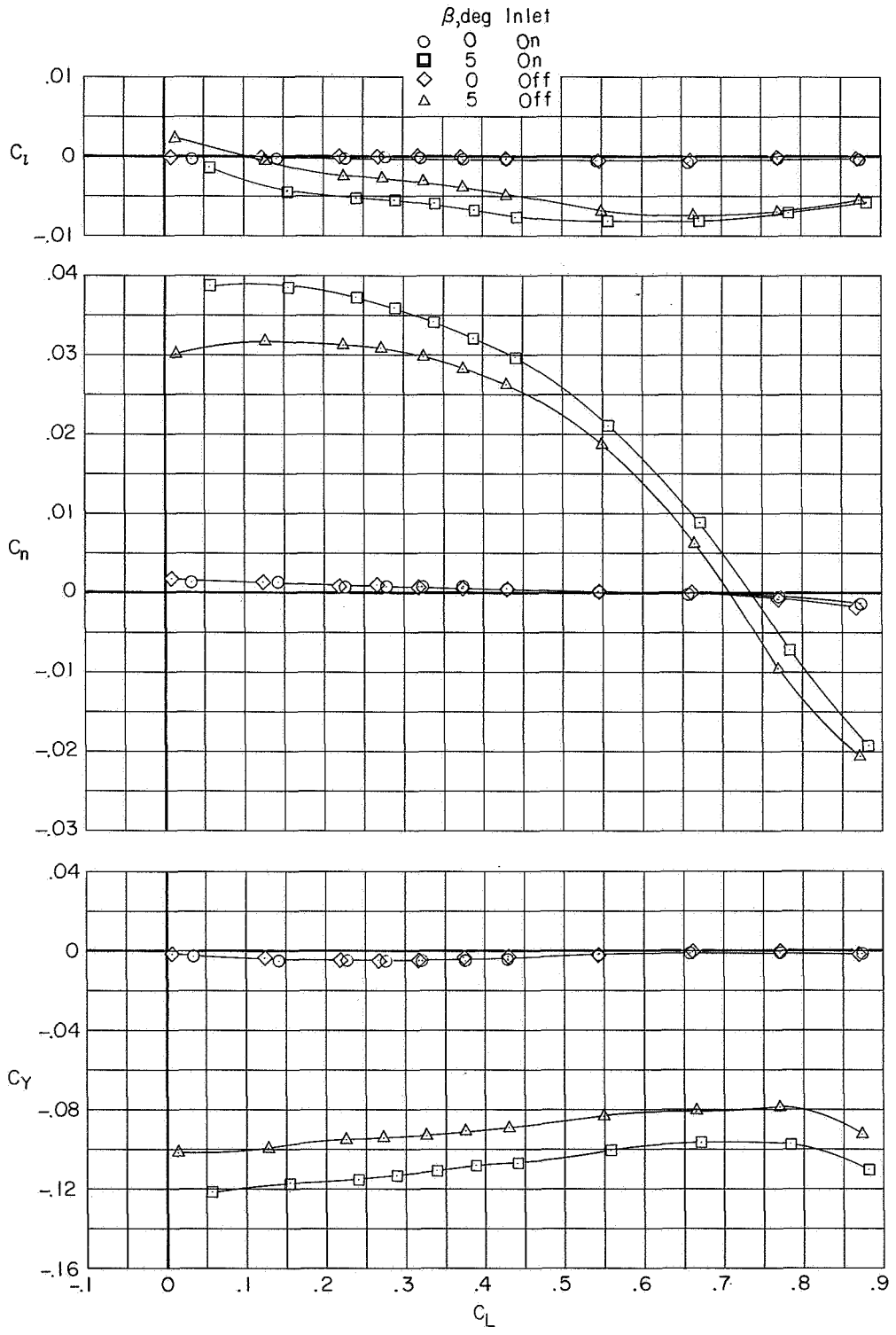

(e) M = 1.00.

Figure 10.- Continued.

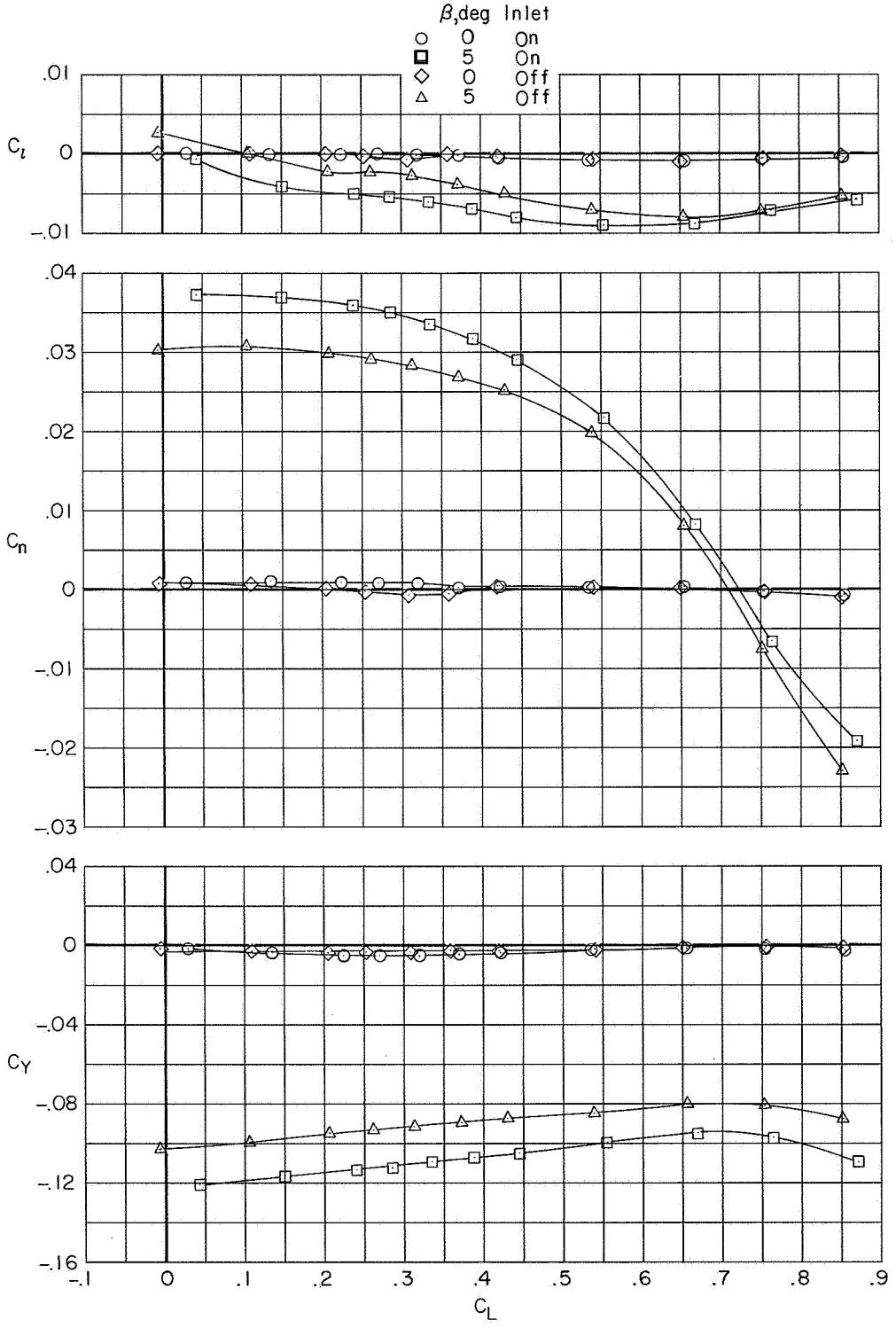

(f) M = 1.03:

Figure 10.- Continued.

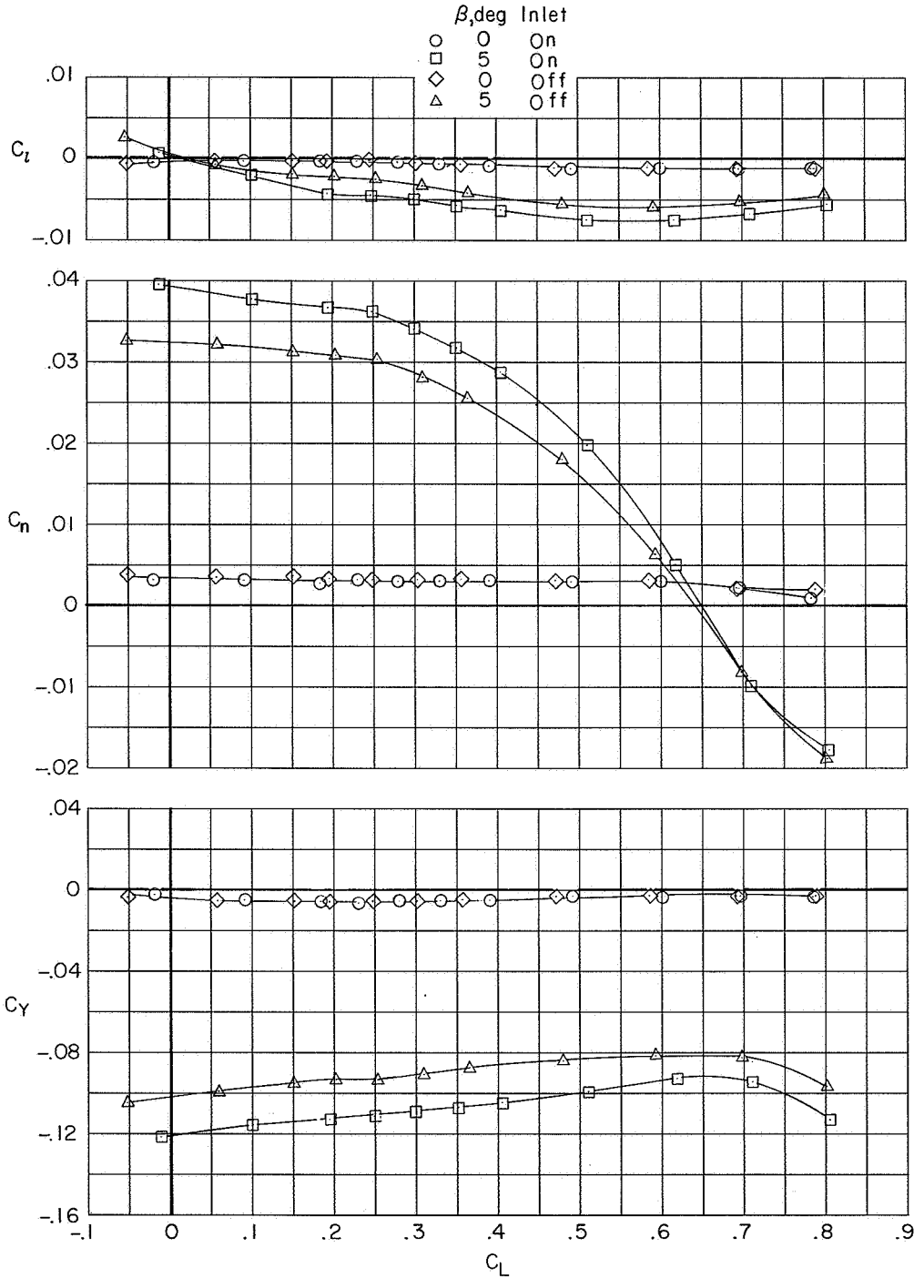

(g)--M = 1.20.

Figure 10.- Concluded.

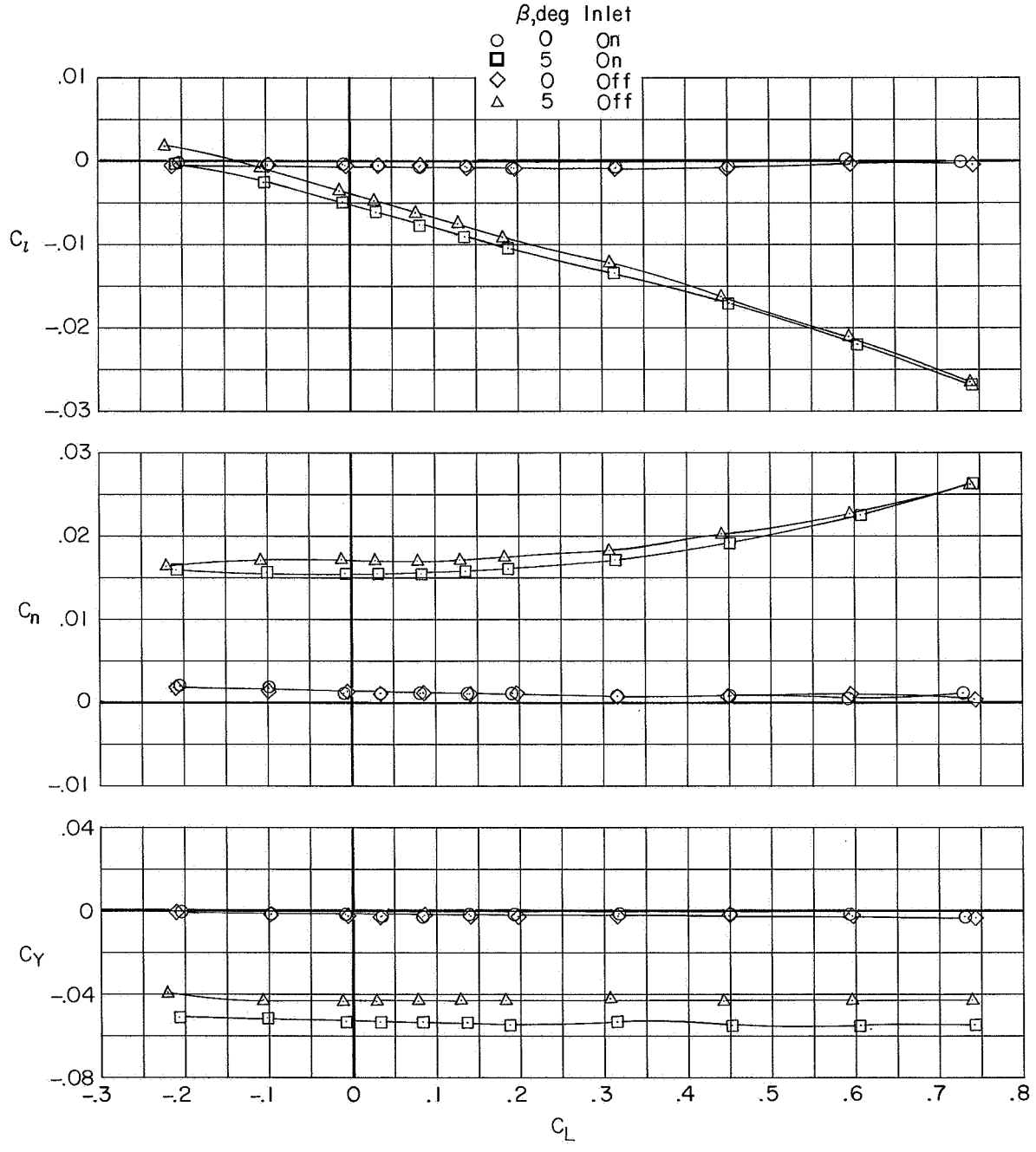

(a) M = 0.80.

Figure 11.- Inlet effects on the lateral aerodynamic characteristics of configuration BWB. $\delta_e = 0^0$.

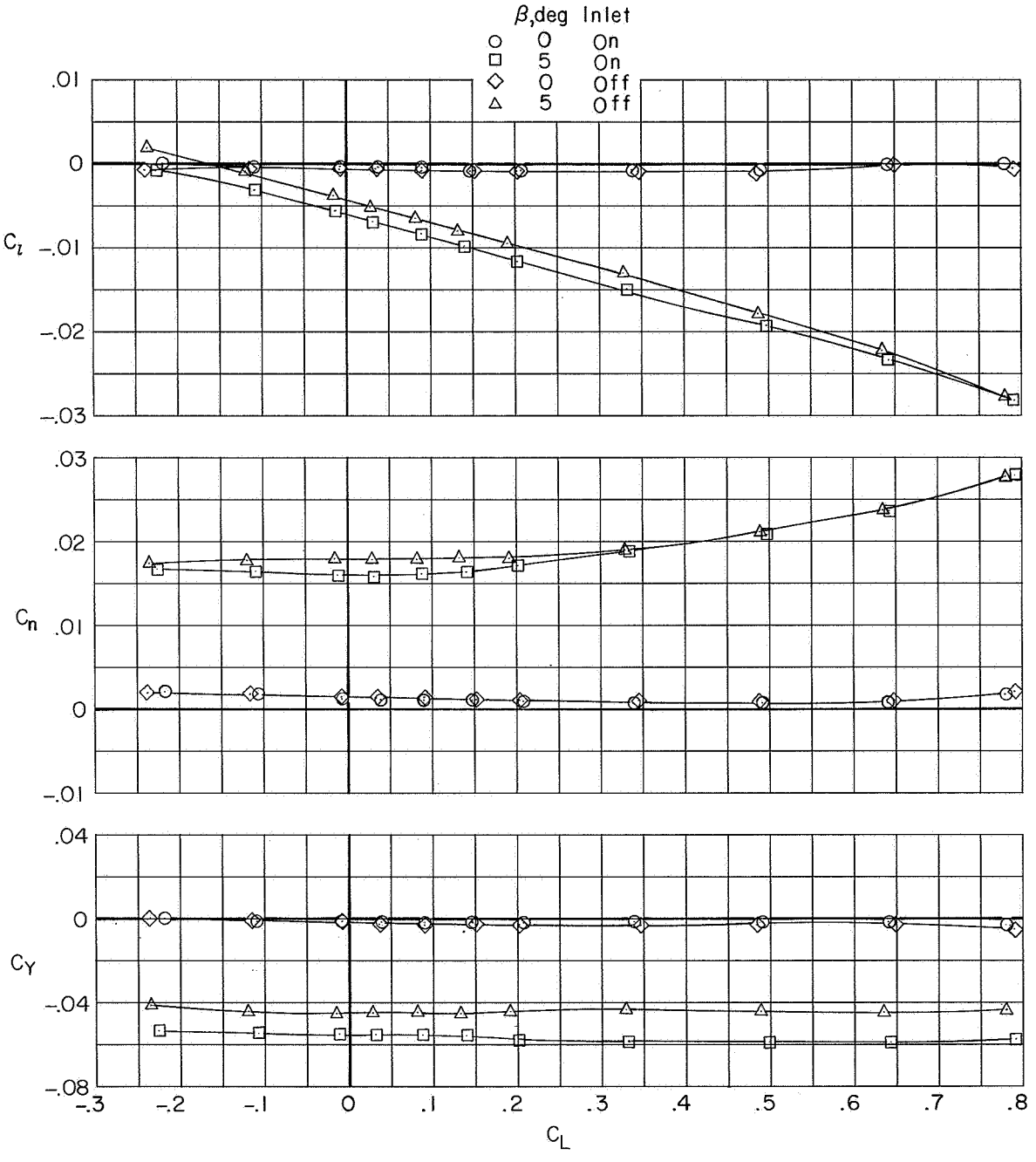

(b) M = 0.90.

Figure 11.- Continued.

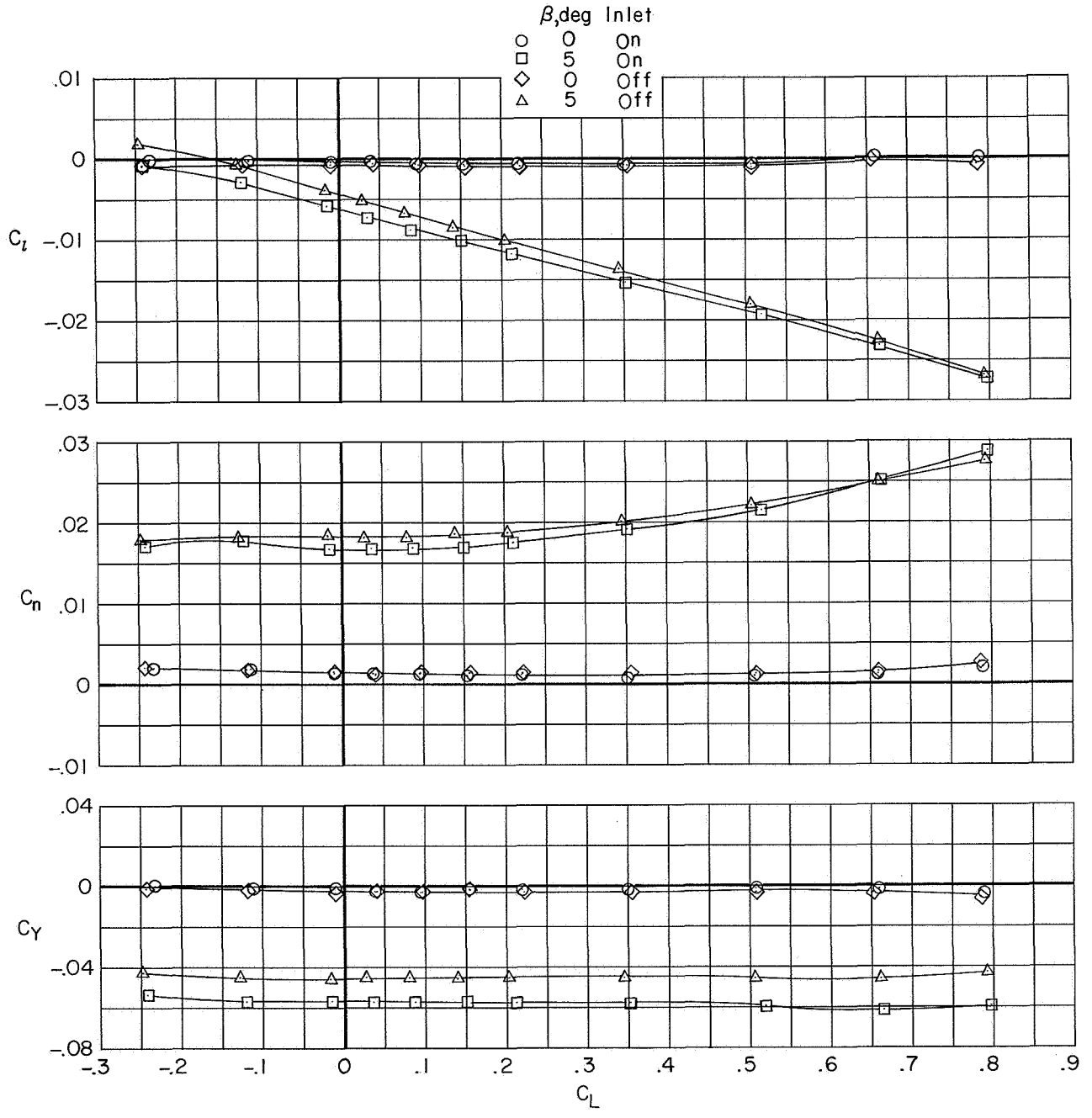

(c) M = 0.93.

Figure 11.- Continued.

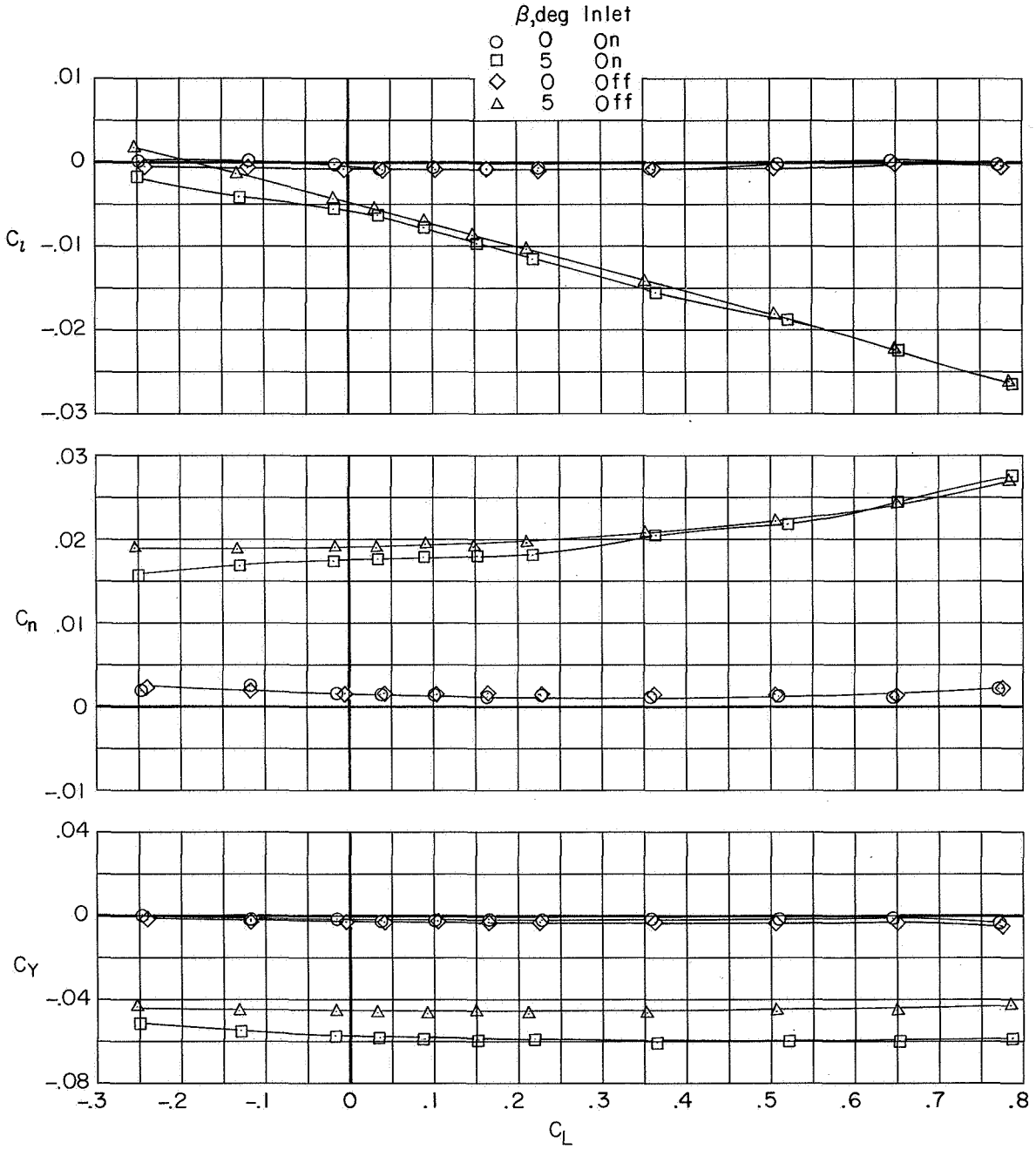

(d) M = 0.96.

Figure 11.- Continued.

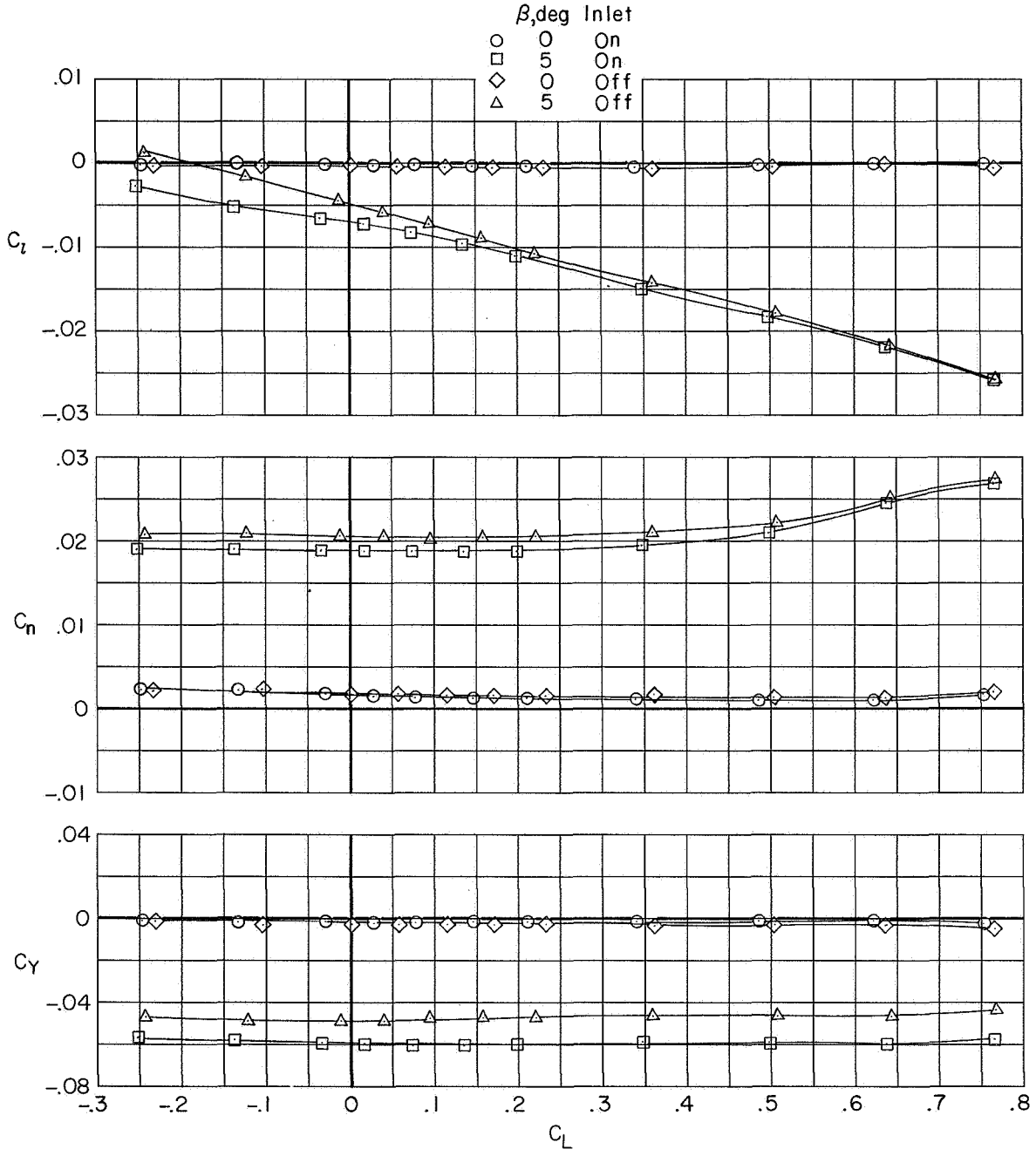

(e) M = 1.00.

Figure 11.- Continued.

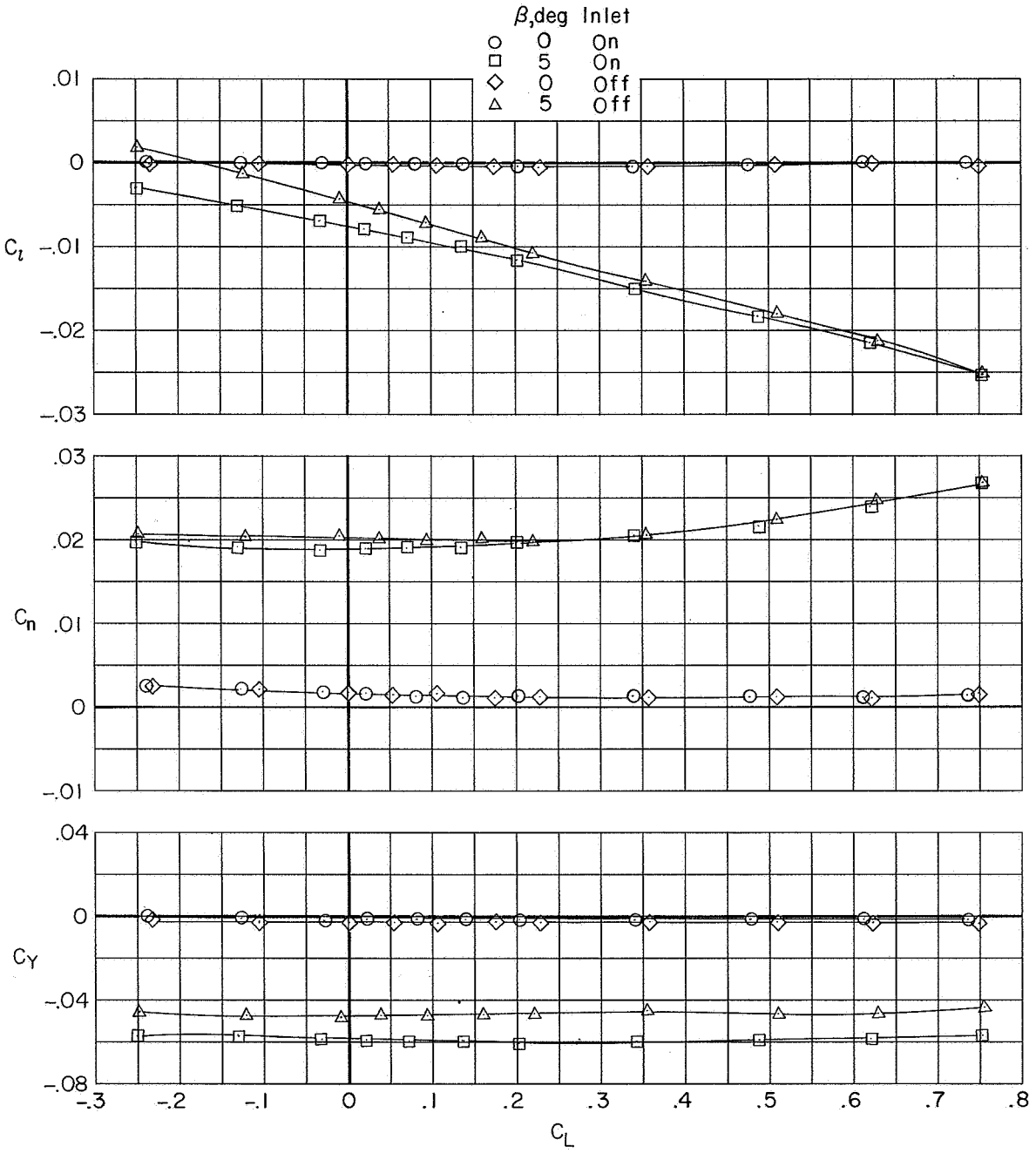

(f) M = 1.03.

Figure 11.- Continued.

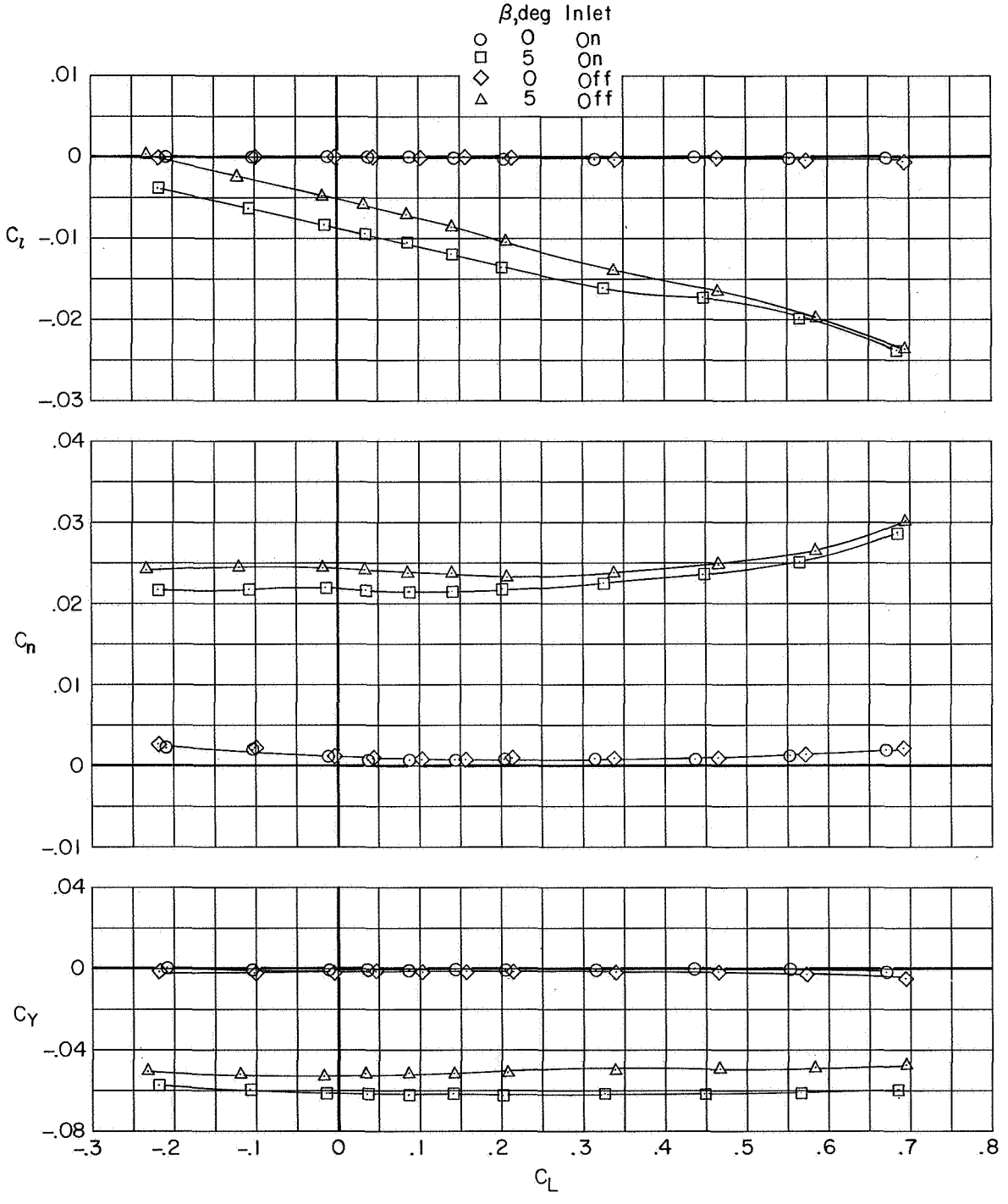

(g) M = 1.20.

Figure 11.- Concluded.

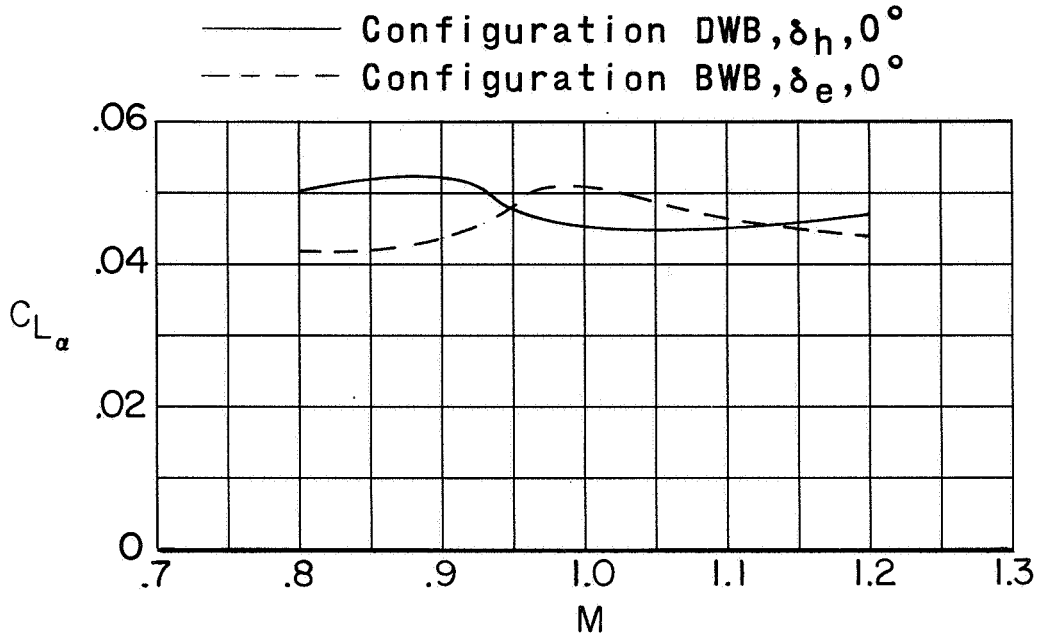

Figure 12.- Variation of C_{L_α} with Mach number for configurations DWB and BWB. $C_L \approx 0.3$.

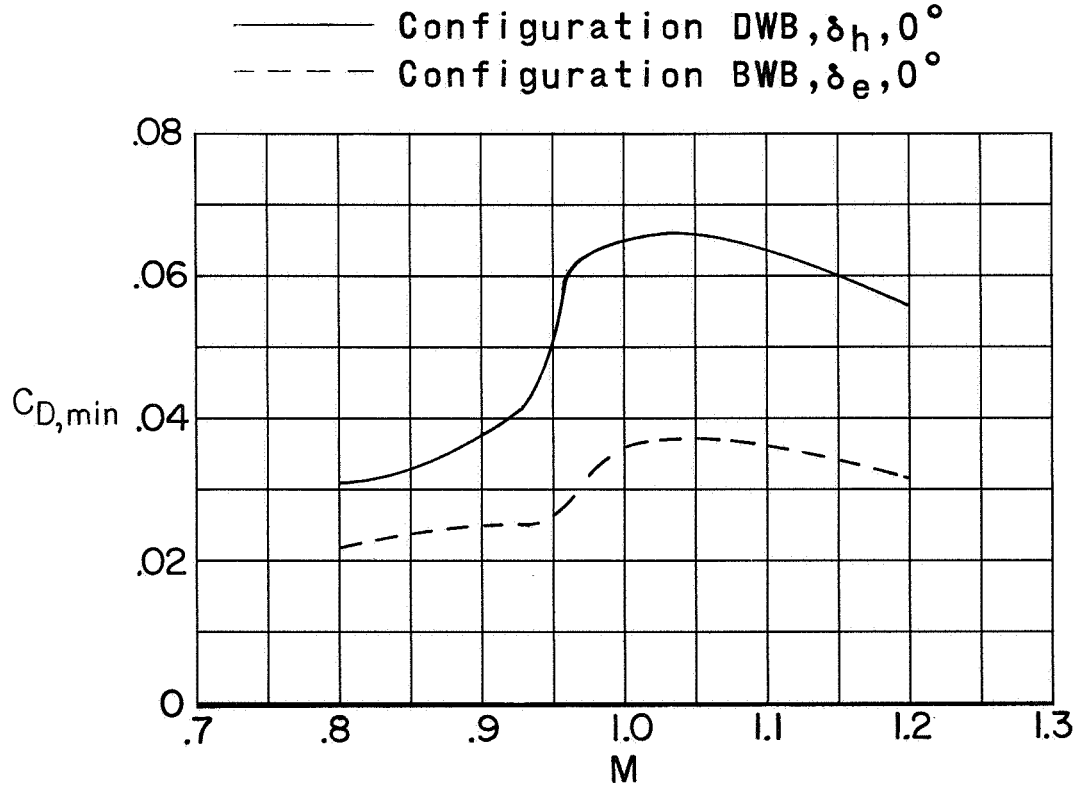

Figure 13.- Variation of $C_{D,min}$ with Mach number for configurations DWB and BWB.

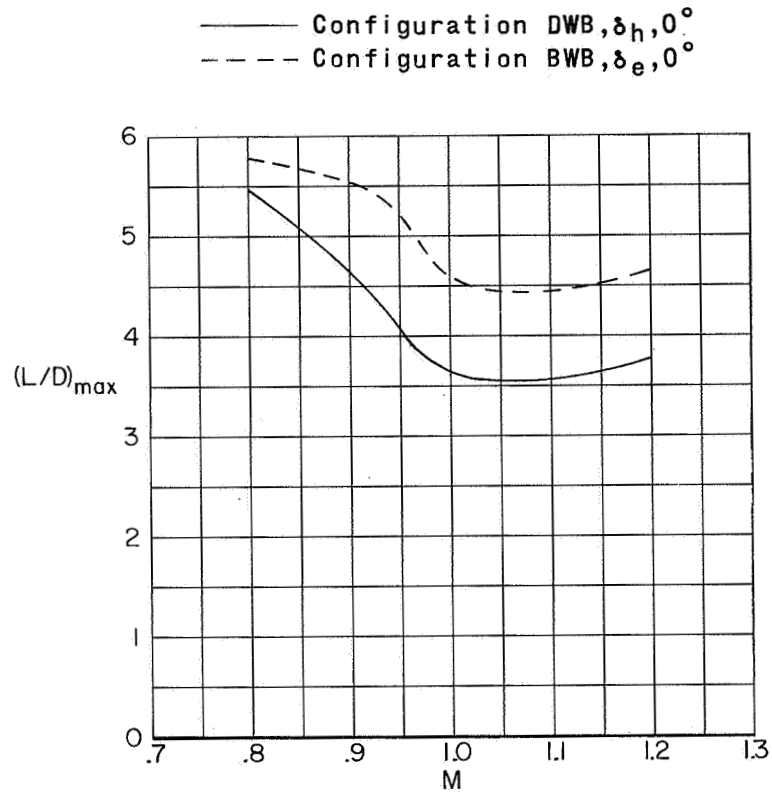

Figure 14.- Variation of $(L/D)_{max}$ with Mach number for configurations DWB and BWB.

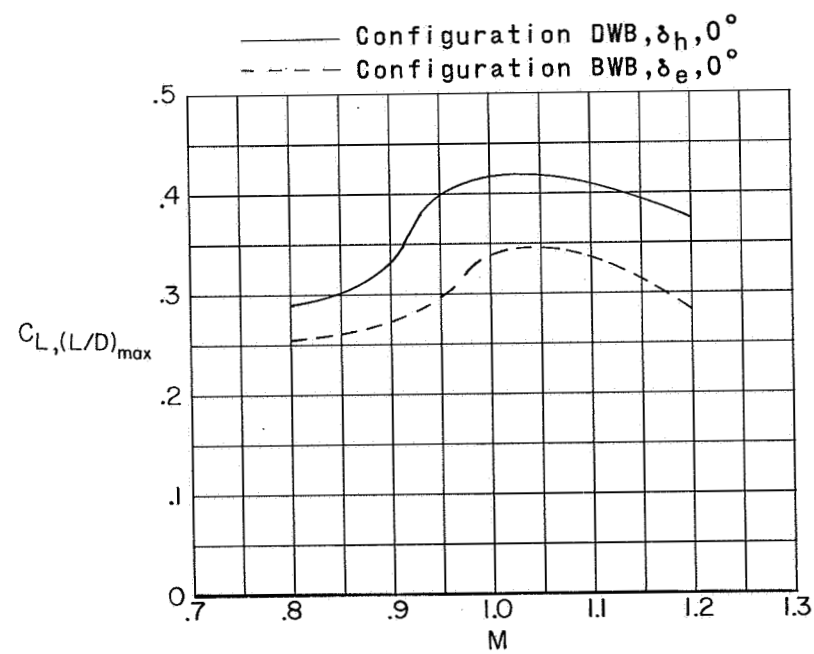

Figure 15.- Variation of $C_{L,(L/D)_{max}}$ with Mach number for configurations DWB and BWB.

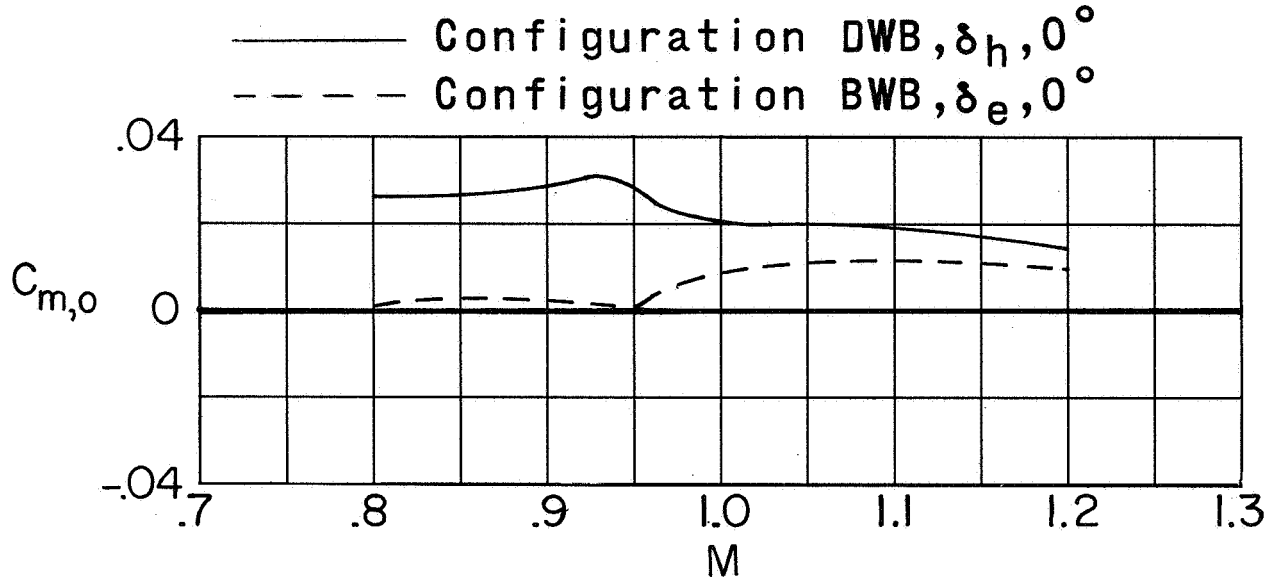

Figure 16.- Variation of $C_{m,o}$ with Mach number for configurations DWB and BWB.

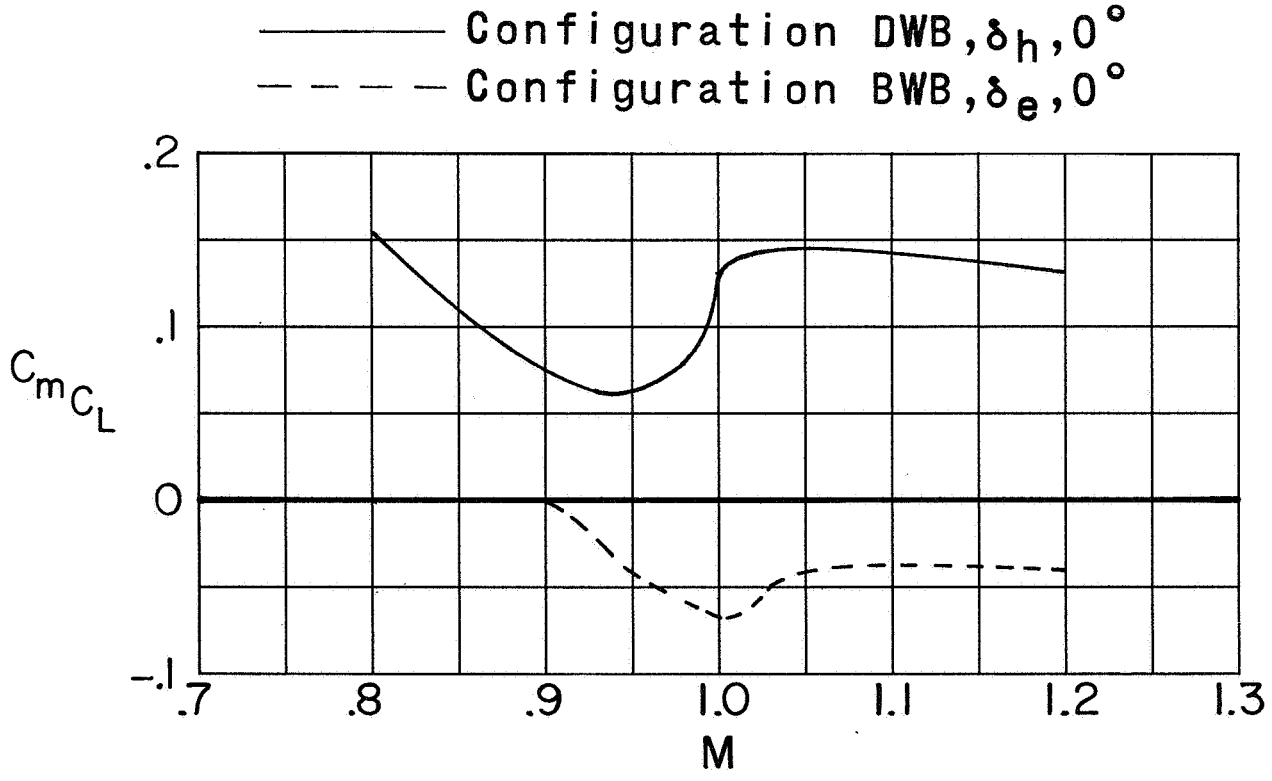

Figure 17.- Variation of $C_{m_{C_L}}$ with Mach number for configurations DWB and BWB. $C_L \approx 0.3$.

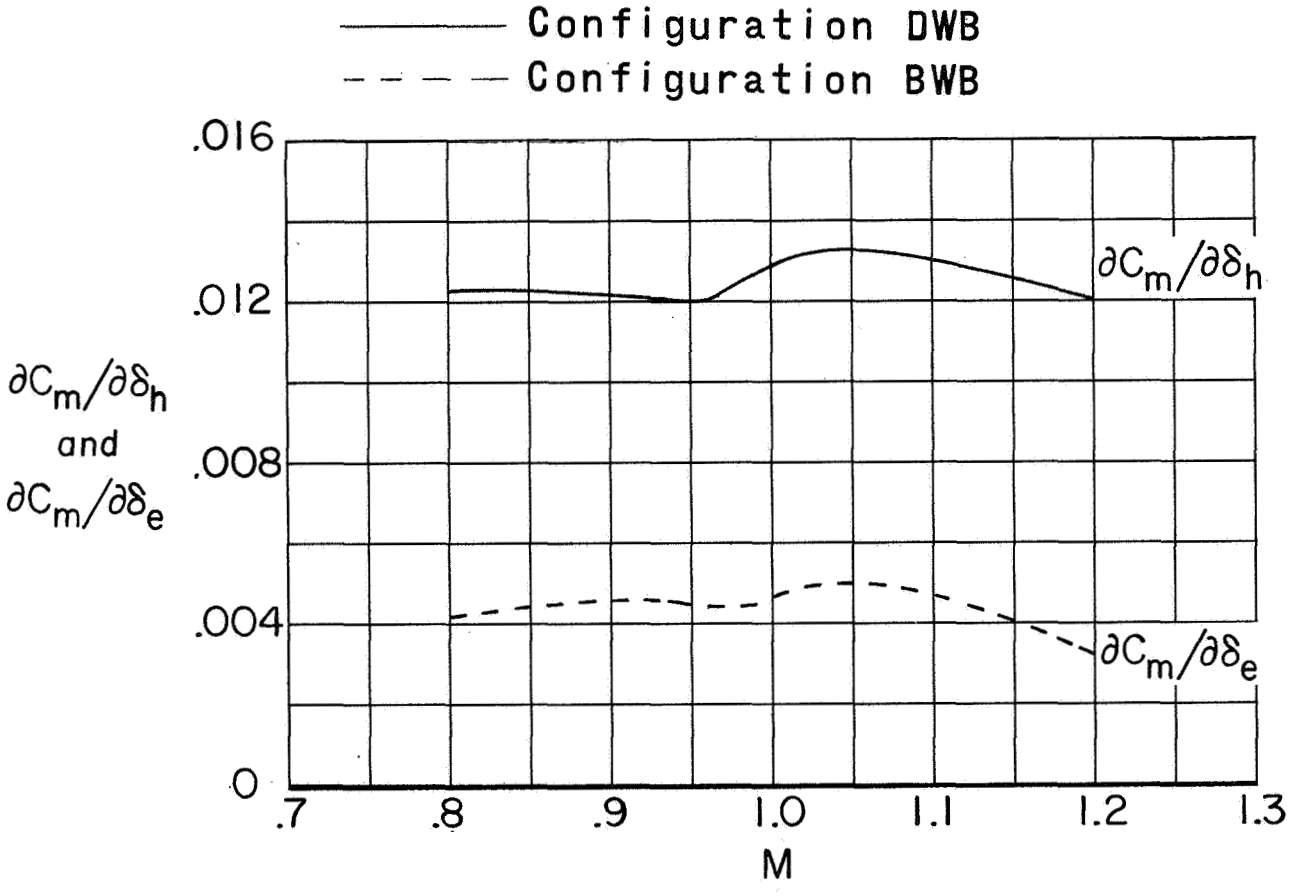

Figure 18.- Variation of $\partial C_m/\partial \delta_h$ for configuration DWB and $\partial C_m/\partial \delta_e$ for configuration BWB with Mach number.

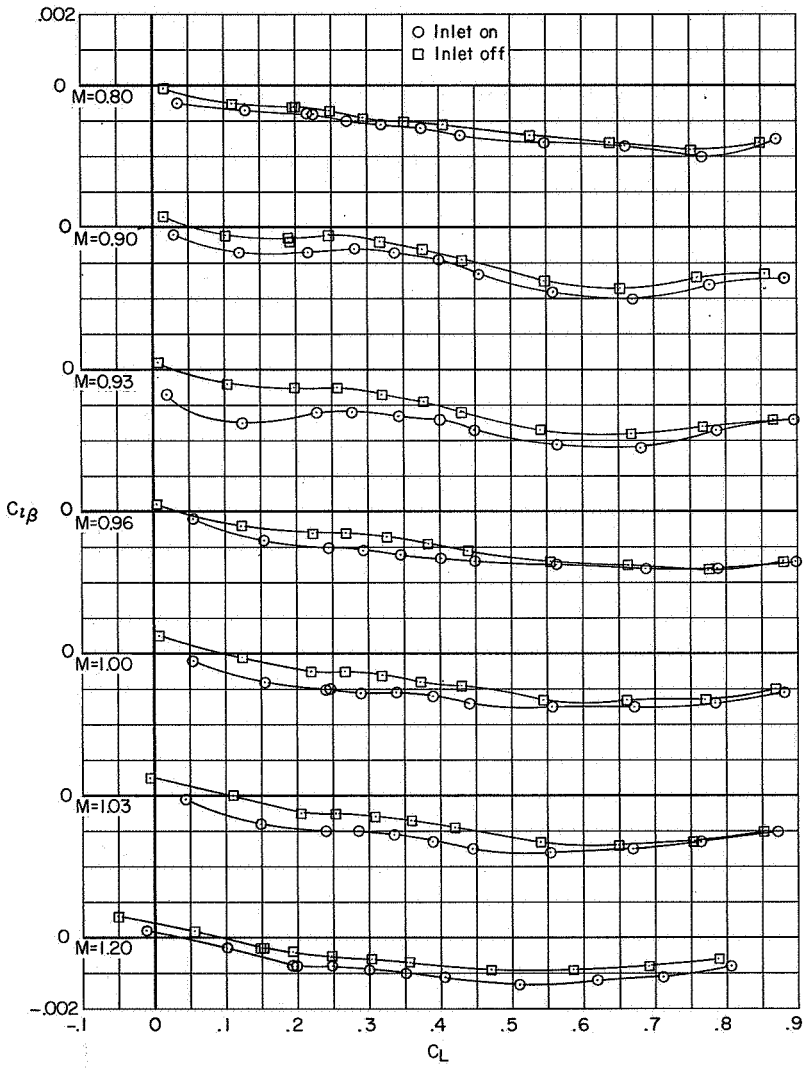

(a) C_{l_β}.

Figure 19.- Inlet effects on the variation of lateral stability derivatives with lift coefficient of configuration DWB. Horizontal tails off.

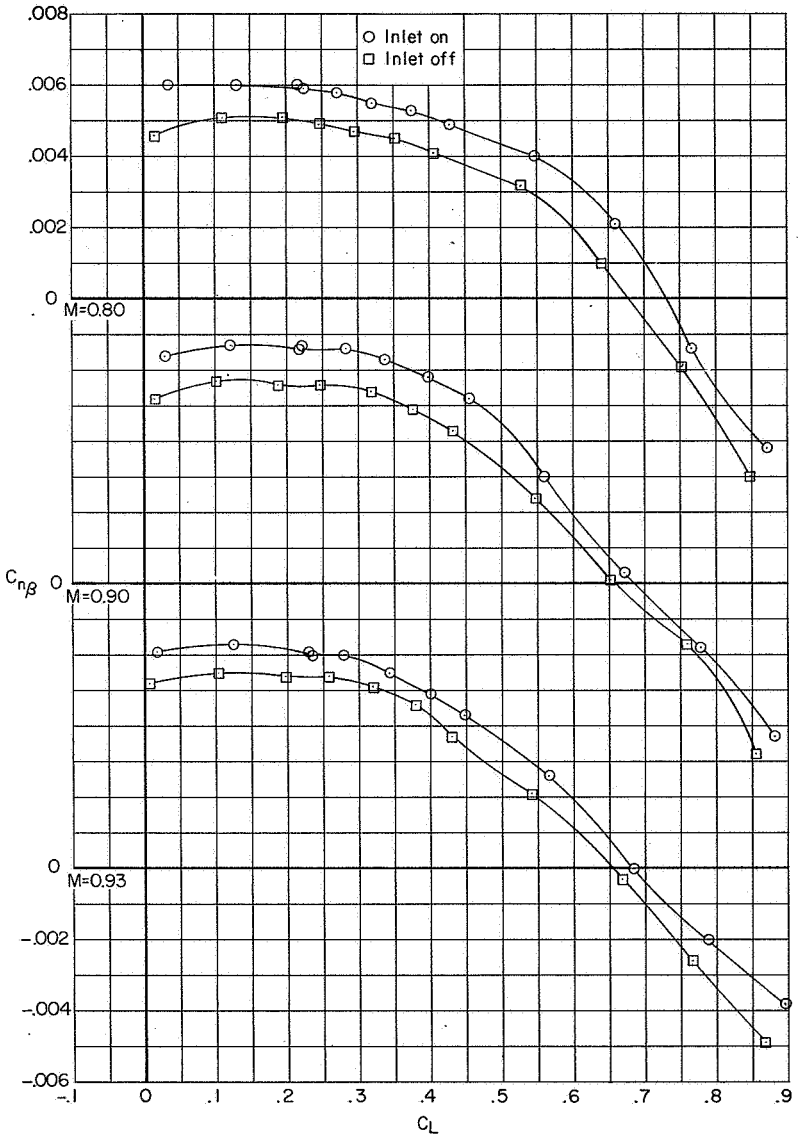

(b) C_{n_β}.

Figure 19.- Continued.

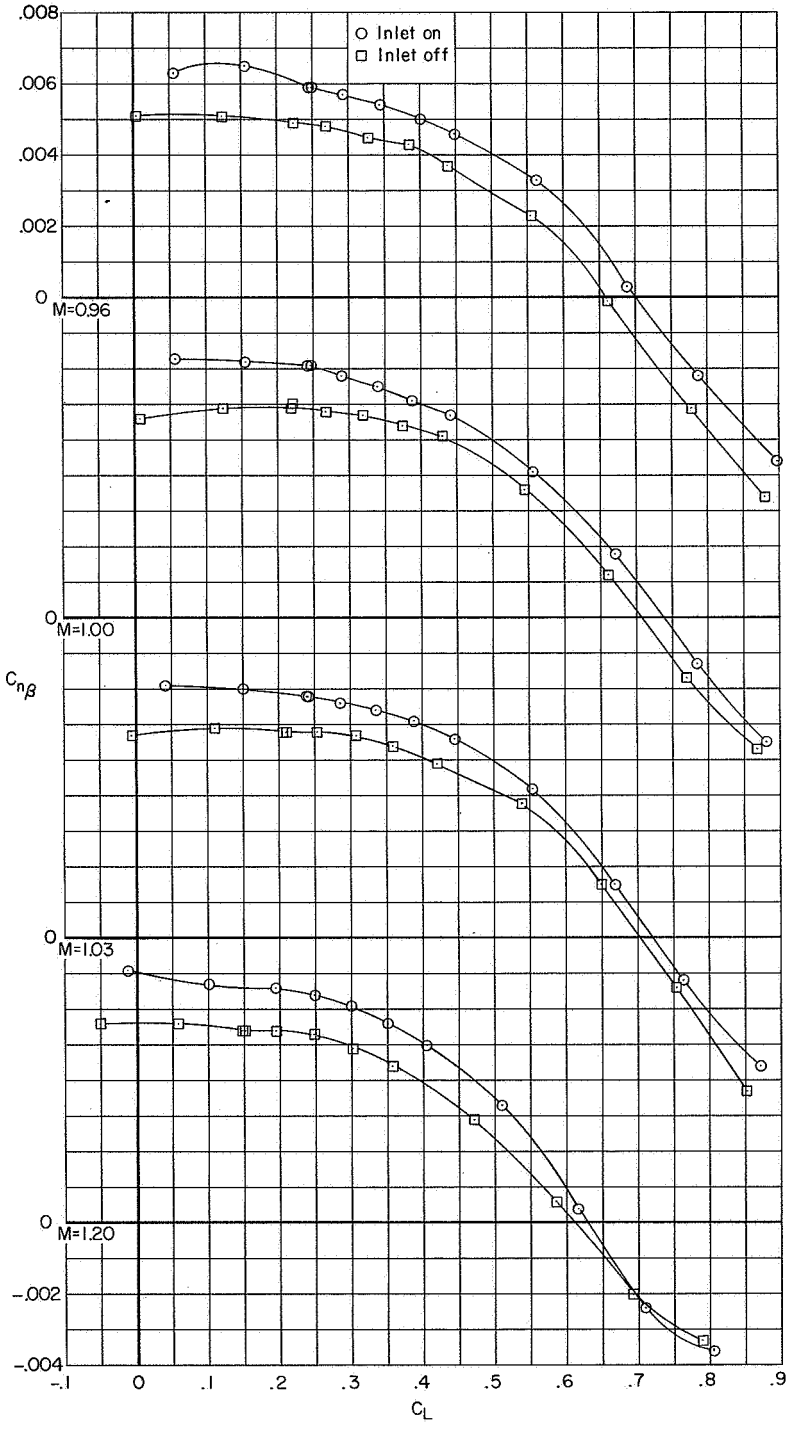

(b) Concluded.

Figure 19.- Continued.

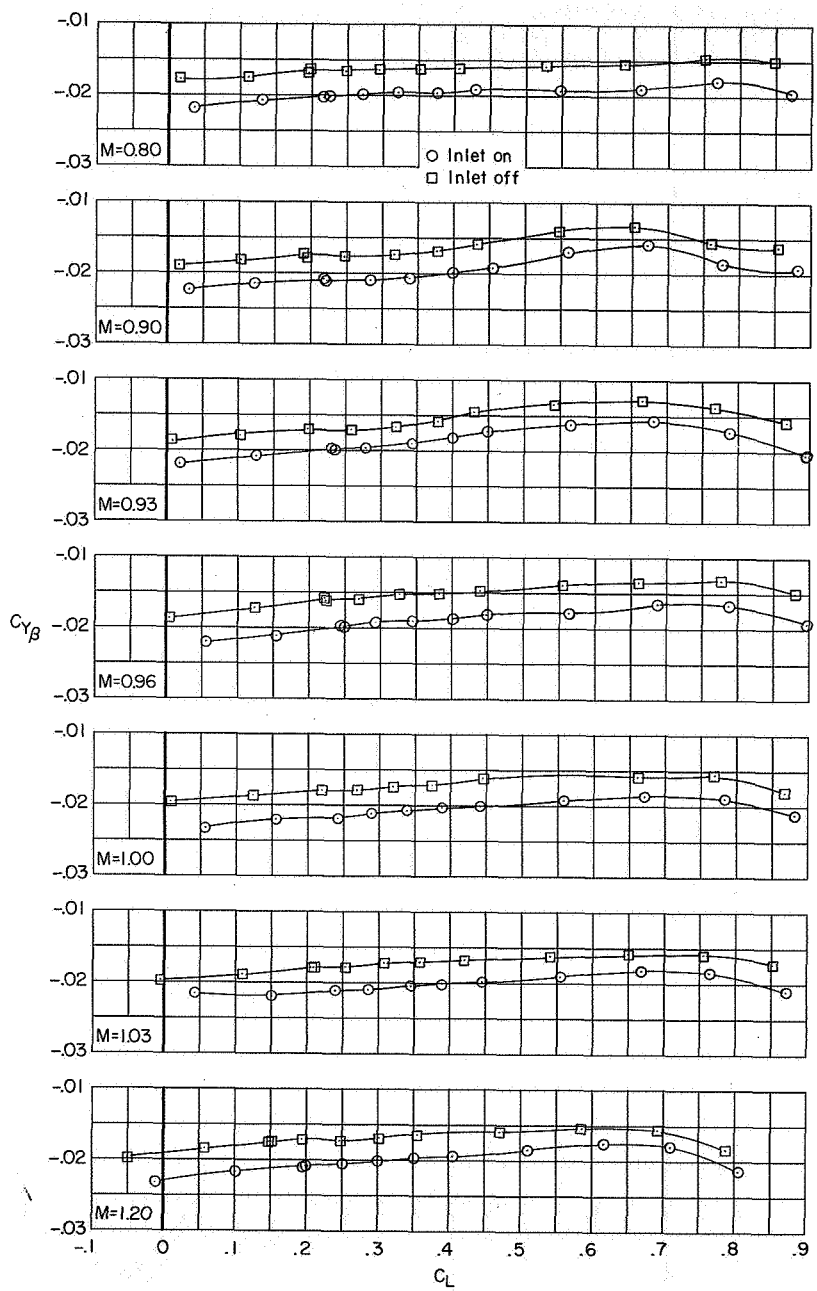

(c) C_{Y_β}.

Figure 19.- Concluded.

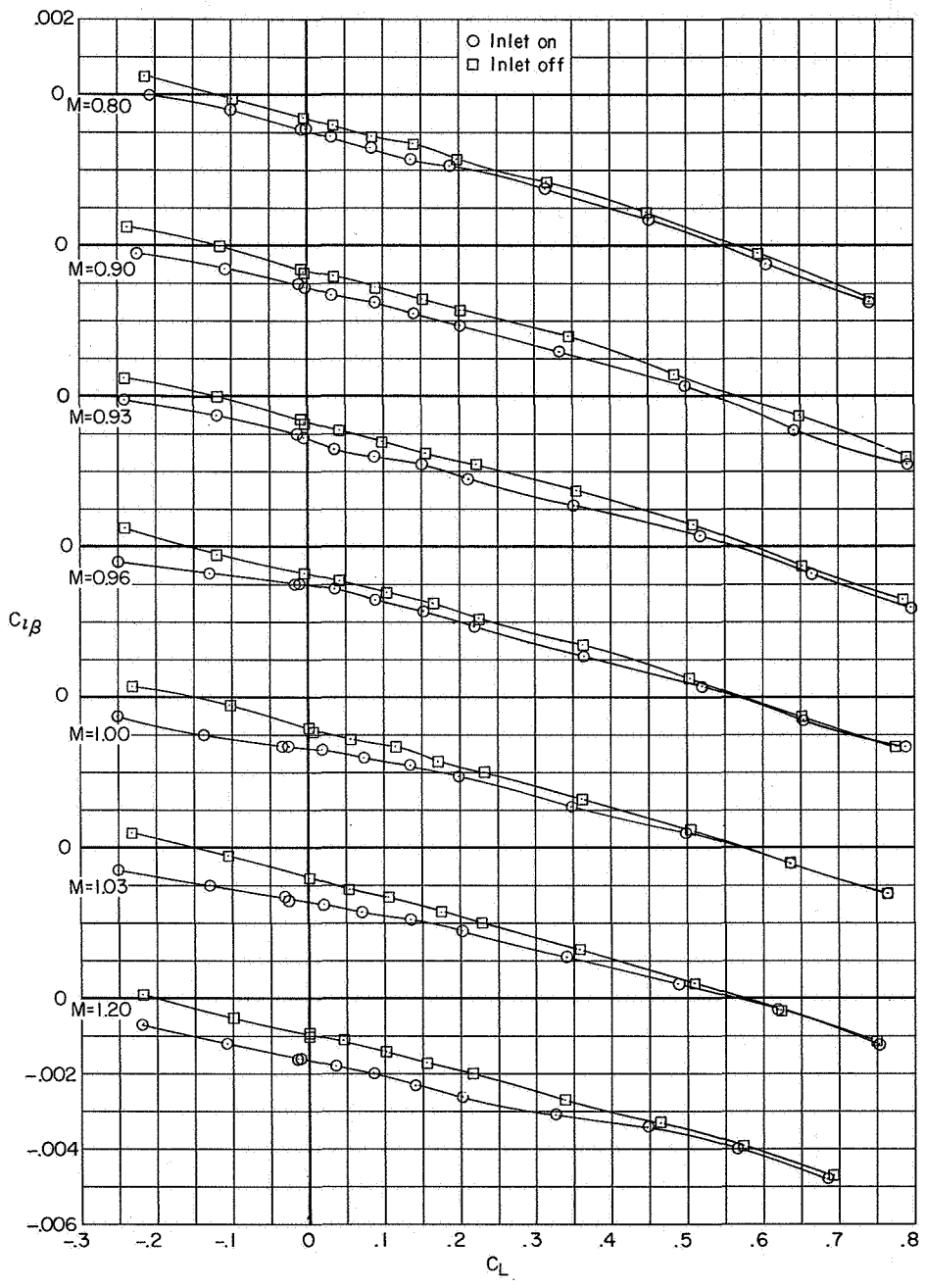

(a) C_{l_β}.

Figure 20.- Inlet effects on the variation of lateral stability derivatives with lift coefficient of configuration BWB. $\delta_e = 0^o$.

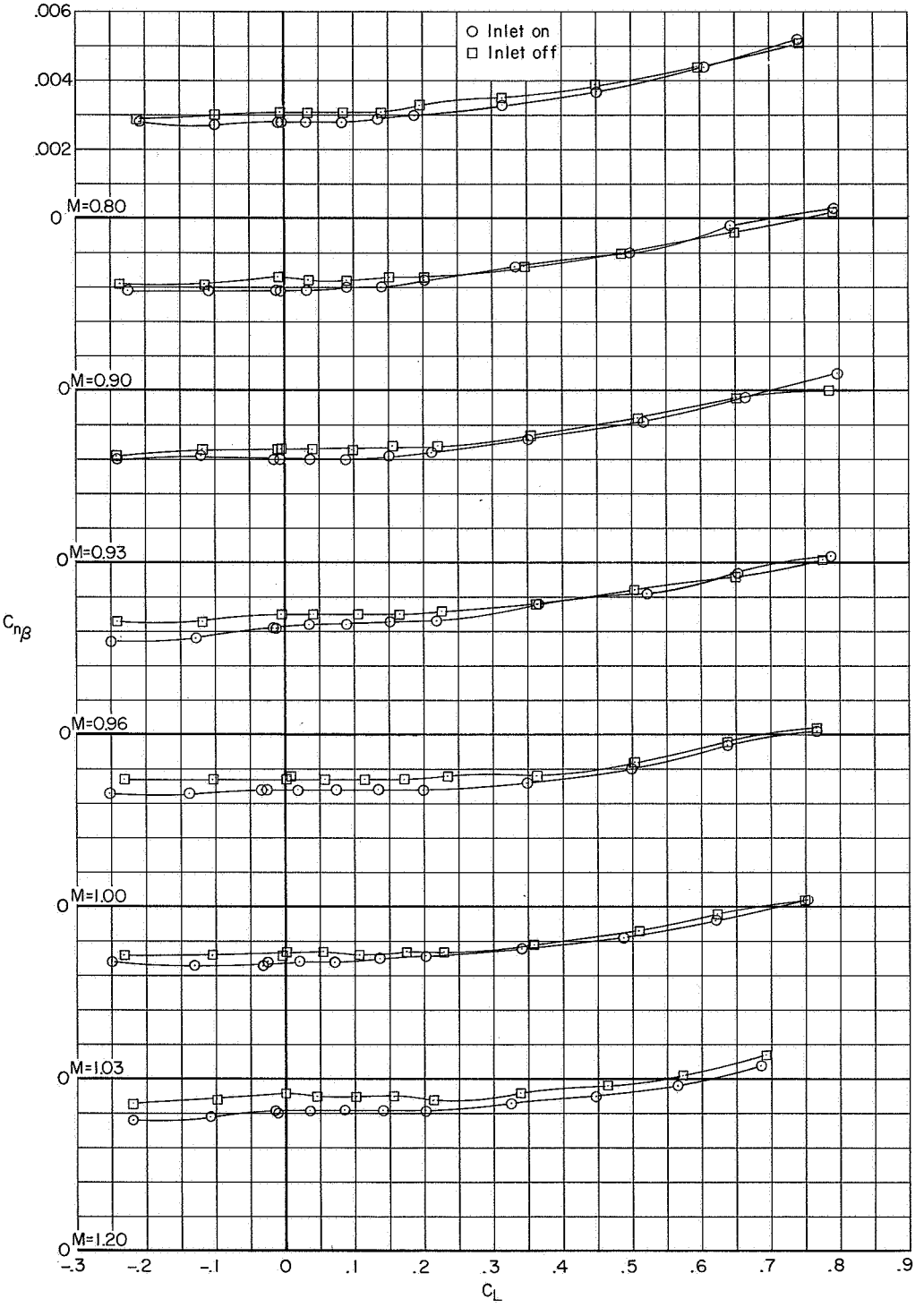

(b) C_{n_β}.

Figure 20.- Continued.

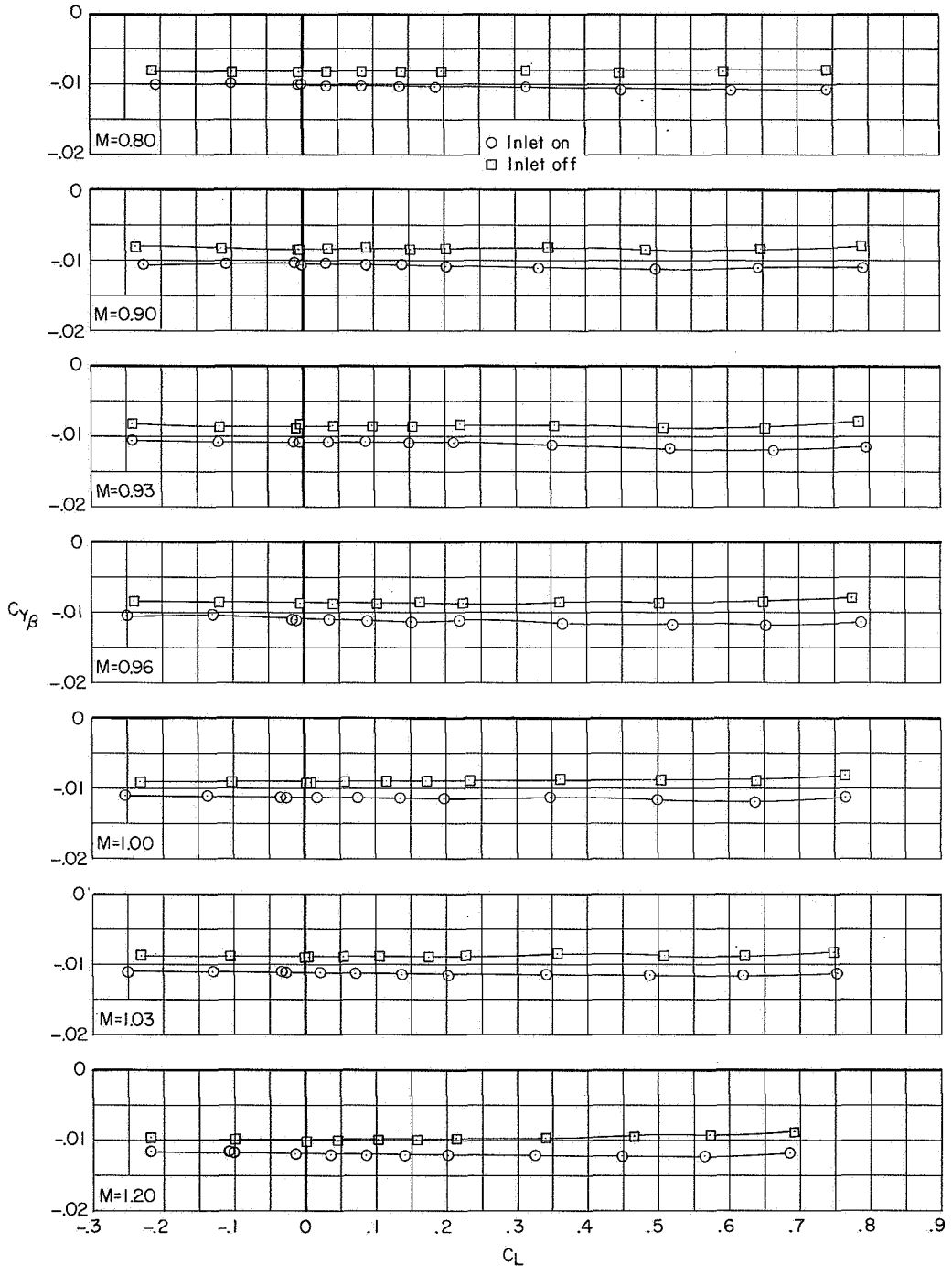

(c) C_{Y_β}.

Figure 20.- Concluded.

NATIONAL AERONAUTICS AND SPACE ADMINISTRATION
WASHINGTON, D.C. 20546

OFFICIAL BUSINESS

FIRST CLASS MAIL

POSTAGE AND FEES PAID
NATIONAL AERONAUTICS A
SPACE ADMINISTRATION

POSTMASTER: If Undeliverable (Section 15
Postal Manual) Do Not Retu

"The aeronautical and space activities of the United States shall be conducted so as to contribute . . . to the expansion of human knowledge of phenomena in the atmosphere and space. The Administration shall provide for the widest practicable and appropriate dissemination of information concerning its activities and the results thereof."

—NATIONAL AERONAUTICS AND SPACE ACT OF 1958

NASA SCIENTIFIC AND TECHNICAL PUBLICATIONS

TECHNICAL REPORTS: Scientific and technical information considered important, complete, and a lasting contribution to existing knowledge.

TECHNICAL NOTES: Information less broad in scope but nevertheless of importance as a contribution to existing knowledge.

TECHNICAL MEMORANDUMS: Information receiving limited distribution because of preliminary data, security classification, or other reasons.

CONTRACTOR REPORTS: Scientific and technical information generated under a NASA contract or grant and considered an important contribution to existing knowledge.

TECHNICAL TRANSLATIONS: Information published in a foreign language considered to merit NASA distribution in English.

SPECIAL PUBLICATIONS: Information derived from or of value to NASA activities. Publications include conference proceedings, monographs, data compilations, handbooks, sourcebooks, and special bibliographies.

TECHNOLOGY UTILIZATION PUBLICATIONS: Information on technology used by NASA that may be of particular interest in commercial and other non-aerospace applications. Publications include Tech Briefs, Technology Utilization Reports and Notes, and Technology Surveys.

Details on the availability of these publications may be obtained from:

SCIENTIFIC AND TECHNICAL INFORMATION DIVISION

NATIONAL AERONAUTICS AND SPACE ADMINISTRATION

Washington, D.C. 20546